THE UNIVERSITY OF CHICAGO

EVALUATION OF NOVEL ENGINEERED STRATEGIES FOR THERAPEUTIC ANTIGEN IMMUNOTHERAPY

A DISSERTATION SUBMITTED TO
THE FACULTY OF THE DIVISION OF THE BIOLOGICAL SCIENCES
AND THE PRITZKER SCHOOL OF MEDICINE
IN CANDIDACY FOR THE DEGREE OF
DOCTOR OF PHILOSOPHY

COMMITTEE ON IMMUNOLOGY

BY
ANDREW CARL-JOSLIN TREMAIN

CHICAGO, ILLINOIS
JUNE 2021

TABLE OF CONTENTS

LIST OF FIGURES

CHAPTER 1

CHAPTER 2

CHAPTER 3

CHAPTER 4

LIST OF TABLES

ACKNOWLEDGEMENTS

First, I want to acknowledge my thesis advisor, Professor Jeffrey Hubbell, for welcoming me into his lab with open arms and an open mind. I'm grateful for the trust and independence I was given in lab. Second, without Scott Wilson and his creation pGal, my main project (Chapter 2) would not have been possible. Similarly, without Alizée Grimm and her start on MFGE8, my second project (Chapter 3) would not have been possible. Finally, I want to acknowledge Stephan Kontos for his initial work into engineering AIT and his collaboration on our future pGal publication.

I've been incredibly fortunate to have a group of lab mates who have supported me through exceedingly difficult times and helped make work fun, despite the stress and chaos. Many gave hours of their time towards the work presented here: Elyse, Jenni, Tiffany, Michal, Rachel, Joe, Mindy, Ani, and Suzana.

The Committee on Immunology is an amazing academic community. The education I received in immunology was rigorous and thorough, and prepared me to tackle the challenges of interdisciplinary science. What amazes me the most about this community is that we all can play as hard as we can work, and the debauchery of our holiday cocktail parties and cluster retreats did well to balance the academic rigor. I want to acknowledge my classmates Ryan, Steven, Chris, and Jaime who strove to do their best for scholastic as well as community engagement, and whom I deeply relied upon during our first year here. The environment which UChicago fosters of my fellow graduate

students, post docs, and scientists of all ages and nationalities creates an incredibly rich experience.

It's almost every day that I reflect on why I've pursued this degree and feel gratitude for the many people who have influenced my life in a positive way, from family members to high school science teachers. I'm not sure how much control we have over what fascinates us, but I often joke that our fields of study choose us more than we choose them. Growing up with a mother who was teacher and a father who was a clinician, biology has always seemed to be in focus. My sisters were immensely inspirational in directly showing me the steps to achieving educational, career, and familial success down a route oriented towards community service through biological science. These childhood pillars constructed a clear path for my passion to follow.

Lastly, I want to acknowledge the impact my wife Amelia has made on my graduate education. There have been so many long days, late nights, stressful experiments that pushed me past my limits. Amelia gave me the strength and love I needed on a daily basis to keep me going and believe in myself. Above all else our partnership has allowed me to find peace during tough times, and to make it through this formidable experience with a brimming heart and bright spirit.

DISSERTATION ABSTRACT

Autoimmunity, allergy, and drug hypersensitivity are largely facilitated by undesirable T cell responses against inappropriate protein antigen targets. The continued rise in such immune disorders accelerates the need for innovative approaches capable of efficiently inducing robust antigen-specific T cell tolerance. Our lab has established strategies for co-opting endogenous immune surveillance networks for prophylactic tolerance induction, involving deletion, suppression, and regulatory T cell programming. Here, I advance the evaluation of these strategies for use in therapeutic settings, after T cell immunity has been established. First, using a carbohydrate polymer (pGlu) that targets antigen to hepatic APCs, I demonstrate induction of therapeutic T cell tolerance in proof-of-principle antigen models, as well as curative efficacy in a murine model of relapsing-remitting multiple sclerosis. Second, I explore a novel soluble apoptotic mediator (MFGE8) using in vitro and in vivo assays for its capacity to direct protein antigen into tolerogenic immune surveillance machinery. Through cellular and molecular-based investigations with the model antigen ovalbumin, along with a murine model of autoimmune disease, we demonstrate improvements with our engineered approaches against the unmodified protein antigens. Signatures of peripheral tolerance induction are revealed to rely on co-inhibitory ligand interaction such as PD-1. This thesis aims to further the development of two novel immunotherapies, as well as help elucidate the molecular mechanisms responsible for their effects.

CHAPTER 1: INTRODUCTION

1.1 The immunological challenge of knowing oneself

The adaptive immune system possesses a vast repertoire of T and B lymphocytes capable of defending the body against virtually any protein target. There are estimated to be over a hundred billion unique T cell receptor (TCR) specificities, each derived from a random genetic V(D)J recombination event at the variable, joining, and diversity gene segments.[1,2] From this potentially unlimited range of attack must be carved a blind spot for our own tissues, the foods we eat, and environments we live in. Within the delicate balance of distinguishing self versus non-self, a fundamental evolutionary pressure of survival exerts itself and manifests in a myriad of fascinating biological phenomena involving innate and adaptive immunity.[3,4] However, the complexities of such a system lend themselves to errors, and herein lie the causes of many diseases.

Autoimmunity, allergy, and drug hypersensitivity can generally be reduced to the same essential fault: adaptive lymphocytes incorrectly judging friend to be foe. Missteps in T cell education, cellular abnormalities such as receptor over activation, or off-target attack during pathogen defense are all theorized to contribute to aberrant immune behavior that can harm our own bodies. Evolution seems to have erred on the side of caution with regards to how our immune system deals with the outside world, granting it the ability destroy itself for a better chance at protection against virtually any possible microbial threat.

The limited treatments that are available for inflammatory conditions generally involve lifelong avoidance of the trigger or global immunosuppression. Some emerging antibody therapeutics can help eliminate etiological agents with great specificity, for example in the case of cytokine or allergic antigen depletion strategies.[5,6] Furthermore, thanks to our growing understanding of the immune system and biology in general, we are beginning to see a new dawn of potentially curative interventions for autoimmunity being carried out in clinical trials. Examples include new approaches to T cell depletion for halting onset of juvenile diabetes, novel cell engineering therapies for regulatory T cell employment, and improved strategies for antigen-mediated immunotherapy (AIT), such as our glycopolymer approach detailed in Chapter 1 below.[7,8,9] As the introduction of smallpox vaccination transformed the landscape of human health hundreds of years ago (**Figure 1.1**), and as cancer immunotherapy has recently reshaped healthcare over the last decade, there is a dawning possibility that unavoidable life burdens of inflammatory diseases such as type 1 diabetes (T1D) may soon be a problem of the past.

Figure 1.1 | 1661 Royal Support of Vaccination. After the death of Chinese Emperor Fu-lin at the hands of smallpox, his third son became Emperor K'ang (left). Having himself survived smallpox in childhood, he supported preventative inoculation and wrote: "The method of inoculation having been brought to light during my reign, I had it used upon you, my sons and daughters, and my descendants, and you all passed through the smallpox in the happiest possible manner… In the beginning, when I had it tested on one or two people, some old women taxed me with extravagance, and spoke very strongly against inoculation. The courage which I summoned up to insist on its practice has saved the lives and health of millions of men. This is an extremely important thing, of which I am very proud." — Ian and Jenifer Glynn, The Life and Death of Smallpox[10]

1.2 Preventing aberrant T cell immunity

The first step in T cell education is central tolerance. Hematopoietic precursors migrate to the thymus and undergo T cell receptor (TCR) rearrangement to generate their unique TCR.[11] Yet, the awe-inspiring diversity of protein structures that arise from V(D)J recombination is random and must be curated for use in a given individual's genetic background. Immature T cells must test their affinity to protein peptides presented by class I or class II Major histocompatibility complexes (MHC-I, MHC-II). A minimal level of signaling instructs the cells to survive, while those that cannot find any productive signal whatsoever, or those that signal too strongly, are eliminated. Selecting for a low yet detectable range of responsiveness ensures that each T cell can accurately scan MHC for its matching peptide, built on the premise that its matching peptide is not a ubiquitous self antigen. As Cluster of differentiation 8-positive ($CD8^+$) T cells survey intracellular proteins via MHC-I, and $CD4^+$ T cells survey extracellular proteins via MHC-II, there must be comprehensive education of the adaptive compartment in self versus non-self. Yet the thymus is incapable of accomplishing this task alone.

Peripheral tolerance is an essential precaution against the incompleteness of central tolerance. Despite fascinating mechanisms to express peripheral tissue antigens (PTAs) in the thymus by transcription factors such as Autoimmune regulator (AIRE) or FEZ family zinc finger 2 (FEZF2), it is a seemingly insurmountable logistical hurdle to test each T cell against every self protein.[12,13] Furthermore, as the thymic medullary epithelial cells (mTECs) responsible for expressing PTAs cannot express foreign proteins, education must continue in the periphery.

The basic tenet of peripheral tolerance is that any mature naïve T cell which meets its cognate antigen under homeostatic conditions is prevented from activating a pro-inflammatory response.[14] This rule grants our bodies the ability to maintain stability in new environments and situations, even when encountering things our evolutionary ancestors never did. Peripheral tolerance is reliant upon the underlying immune hierarchy, which places the innate immune system as the primary interpreter of environmental stimuli and adaptive lymphocytes as the secondary responders. Structuring of immunological powers grants our bodies the ability to defend against previously unmet pathogens with our adaptive lymphocytes, while avoiding adjacent healthy tissues as instructed by innate immune cells. Whereas T cells are randomly generated with potentially dangerous autoreactive receptors, innate immune cells rely strictly on evolutionarily ancient cues such as pathogen- or damage-associated molecular patterns (PAMPs, DAMPs) that instruct the adaptive immune system when and how to respond.[15,16]

In a typical infection, our bodies will detect PAMPs and DAMPs via innate sensors such as Toll-like receptors (TLR), along with pathogen-associated protein antigens by adaptive cells. The ensuing encounter of naïve T cells with cognate peptide-MHC (p:MHC) would thus result in expansion and establishment of proinflammatory cell programs capable of carrying out effector functions. $CD8^+$ T cells are referred to as killer T cells, or cytotoxic T lymphocytes (CTL, T_C), due to their ability to kill infected cells presenting foreign antigen on MHC-I via secretion of cytolytic factors such as perforin or granzyme. $CD4^+$ T cells are called helper T cells (T_H) because while they do not kill

infected cells, they orchestrate immune responses by fueling the activation of other lymphocytes, such as T follicular helpers (T_{FH}) that aid the production of antibodies by B cells. CD4 fate decisions involve transcriptional regulation that drives the canonical helper programs: type 1 immunity with T_H1 (via T-box transcription factor 21, T-bet), type 2 immunity with T_H2 (via GATA binding protein 3, GATA3), or type 3 immunity with T_H17 (via RAR-related orphan receptor gamma t-isoform, RORγt). Each of these programs is tasked with a specific subset of pathogens: type 1 for intracellular viruses or bacteria, type 2 for helminths, and type 3 for mucosal barrier protection. Furthermore, each subset produces corresponding effector cytokines that help protect the host given their specified responsibilities, for example: T_H1 produce interleukin 12 (IL-12); T_H2 produce IL-4, 5, and 13; T_H17 produce IL-17. Depending on the contextual cues present when a naïve T cell encounters p:MHC, it will be directed down the necessary lineage.

Contrastingly, as Bonifaz showed in 2002, efficient delivery of foreign protein to antigen presenting cells (APCs) without adjuvant induces abortive proliferation and ultimately deletion of the corresponding T cell population of interest.[17] The vast and dynamic power of the adaptive immune system is critically held in check by the innate immune system (**Figure 1.2**).

Specialized networks for peripheral tolerance have been identified, such as the systemic clearance of apoptotic debris (efferocytosis), hepatic blood filtration, and the upper region of the small intestine.[18,19,20] Each of these biological systems are under evolutionary pressures that necessitate immunological regulation. Efferocytosis is a

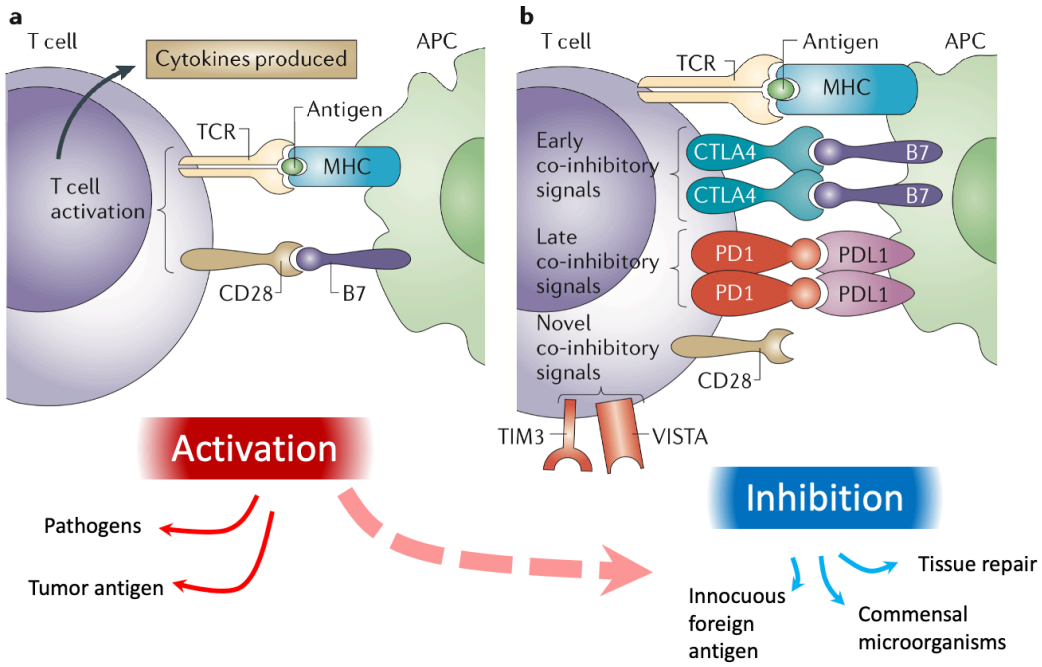

Figure 1.2 | Activating versus inhibitory T cell education. T cells constantly survey the body for their matching antigen presented by MHC. If a cognate antigen is encountered along with co-activating ligands such as B7.1/.2, a productive outcome will ensue that drives production of proinflammatory cytokines and clonal T cell expansion required for protection against pathogens. On the other hand, if antigen is encountered in the presence of co-inhibitory ligands such as PD-1 or CTLA4 (which can outcompete CD28 for B7 binding), cognate T cells will be prevented from carrying out further attack against the target antigen. An inhibitory immune context is required for appropriate T cell education against self and foreign proteins necessary for healthy tissue functionality. Inappropriate context can drive aberrant activation that leads to autoimmunity and allergy. Adapted from Sharma 2011 *NatRevCancer*.[21]

delicate process whereby danger signals from dying cells must be sequestered and silenced in order to prevent activation against self protein debris. Similarly, the liver must avoid aberrant activation despite its constant filtering of toxins from the gut. The draining lymph nodes (dLNs) of the upper small intestine have recently been shown to favor tolerogenic outcomes, which, situated adjacent to the acidic gut and far from the colon, is interpreted to be a safe haven for tolerance induction to food antigens where pathogens cannot reach. Yet even with the aid of central and peripheral deletion, our

adaptive immune system is insufficiently capable of staving off autoimmunity and clearing our bodies of potentially dangerous clonotypes.[22]

1.3 Modes of T cell tolerance

When a naïve T cell undergoes peripheral tolerance, it can result in a variety of possible fate decisions; namely, death, quiescence, or induction of a dominant regulatory program.[23,24] Because the first essential signal of activation (signal 1) is perceived by the T cell receptor (TCR) as it encounters its cognate antigen presented by MHC, there is an initial phase of proliferation as the downstream signaling machinery involving nuclear factor of activated T-cells (NFAT) is induced. However, without stimulation of the innate antigen presenting cell (APC) via PAMP or DAMP, secondary inputs of co-TCR ligands (signal 2) or tertiary soluble factors (signal 3) are not imparted in a pro-inflammatory manner by the APC. The T cell thereby does not receive essential pro-survival support from transcription factors such as Nuclear factor kappa-light-chain-enhancer of activated B cells (NFKB) or Activator protein 1 (AP1) downstream of CD28 engagement. This partnerless NFAT signaling drives tolerance induction in cognate T cells through abortive proliferation, observed as a short burst of replication followed by collapse of the population shortly thereafter.[25] T cells can also undergo deletion even in the face of signal 2 via pro-apoptotic factors such as Fas.

Partnerless NFAT signaling has also been shown to lead to states of anergy and exhaustion.[26,27] While exhaustion refers to suppression after repeated encounters with antigen, for example in the context of chronic viral infection, anergy typically refers to

induction of a hyporesponsive state upon initial antigen encounter. Both share the same essential feature of reduced effector functionality, as observed by the increased expression of co-inhibitory surface markers including Programmed death ligand 1 (PD-1) and reduction of proinflammatory cytokines such as interferon gamma (IFNγ) or IL-2.

Thymic and peripheral induction of dominant regulators such as Forkhead box P3-postive ($FOXP3^+$) CD4+ T regulatory cells (Treg) that can suppress autoreactive escapees are appreciated to be an essential safeguard on the regulation of immunity. Treg importance is evidenced by the surprising extent of lethal background autoimmunity that is unleashed upon their ablation using αCD25 depletion antibodies.[28] Importantly, a proportion of mature naïve T cells that recognize proteins affiliated with our own bodies or environmental antigens such as commensal microbiota are granted immunoregulatory faculties such as FOXP3 expression.[29] Peripheral Treg induction ensures that any dangerous escapees from the inevitably incomplete deletion or suppression of central and peripheral tolerance can be prevented from becoming activated.

Other examples of dominant regulatory immune cell programs that have been more recently identified include the so called T regulatory type 1 (Tr1) FOXP3-CD4+ which produce the suppressive cytokine IL-10, as well as various reports of immunosuppressive CD8+ and B cell phenotypes.[30,31,32] There has been some controversy regarding adaptive suppressor cells, and the precise biology of CD8 and B regulatory cells are yet to be clearly elucidated.

Upon encounter of cognate antigen in the periphery, we can expect a given T cell population to respond according to receptor-based or soluble contextual. In the absence

of proinflammatory signals, TCR engagement will lead to a diminution in population size and effector functionality, as well as involve some degree of dominant regulatory program induction. Each of the three layers of T cell control – central deletion, peripheral deletion, and dominant regulation – contribute to our ability to distinguish self from non-self and avoid aberrant immune responses. Nevertheless, hundreds of millions of people around the globe today face health issues related to autoimmunity and allergy.[33,34]

1.4 Insidious outcomes of miseducation

Breakdowns in immune tolerance allow potentially dangerous lymphocytes to carry out their programs. Autoimmune diseases affect millions of people around the globe, and incidences are rising for unknown reasons. There are many Mendelian disorders that can result in autoimmunity, for example Autoimmune polyendocrinopathy candidiasis ectodermal dystrophy (APECED) is a polyglandular autoimmune disease caused by mutations in the Aire gene that decreases the effectiveness of central tolerance.[35] Diseases such as arthritis, lupus, T1D, multiple sclerosis (MS), and celiac disease instead correlate with the genetics of Human leukocyte antigen (HLA, aka MHC) haplotype, particularly class II.[36] Congruently, each of these different types of HLA-associated autoimmune diseases is associated with undesirable adaptive lymphocytes targeting a discrete set of self antigens.

T1D and MS both involve autoantibody targeting and T cell mediated destruction of pancreatic islets or myelin sheaths, respectively. Although T1D occurs primarily in pre-pubescence, MS does not onset until late adulthood. Nevertheless, the destruction of

these essential tissues leads to lasting impairments in physiology and require lifelong treatment. Several autoantigens responsible for driving these aberrant T cell responses have been identified, but the initial sources of pro-inflammatory signaling that unleash the adaptive immune response is unclear.

Three key antigen targets that have been found to drive T1D are insulin, Glutamic acid decarboxylase 65-kDa isoform (GAD65), and Islet antigen 2 (IA-2).[37] In the case of juvenile onset T1D, pancreatic restructuring during infancy may provide the endogenous antigenic stimulus that ultimately drives autoantibody induction and T cell infiltration.[38] Some reports have suggested exogenous inducers of autoimmunity, such as viral mimetic epitopes, but the frequency of diabetes in germ free non-obese diabetic (NOD) mice reveal the sufficiency of endogenous triggers in the case of T cell-mediated pancreatic destruction.[39,40] There are currently no approved interventions for T1D – patients are required to inject recombinant insulin throughout life.

MS involves adaptive lymphocyte targeting of myelin-associated proteins such as Myelin basic protein (MBP), Myelin oligodendrocyte glycoprotein (MOG), and Proteolipid protein (PLP).[41] There is a combination of attacks mediated by innate and adaptive immune cells on the central nervous system (CNS) that results in destruction of the neural sheath along with cellular oxidative stress, eventually leading to loss of motor function. The initial trigger that activates the immune system against myelin is yet to be identified, although many environmental triggers have been hypothesized. Treatments for MS involve global immunosuppressants such as fingolimod or blocking antibodies

against Very late antigen-4 (VLA-4) which can prevent T cell invasion in the CNS and delay progression of symptoms while treatment is given.

Celiac disease is an interesting condition whereby a harmless food antigen causes autoimmune attack of intestinal epithelia. The gluten-associated antigen gliadin activates autoreactive T cells in people with the HLA haplotypes DQ2 or DQ8 via presentation of gliadin peptides that have been deamidated by transglutaminase.[42] This reaction drives autoantibody production and downstream villus atrophy. There are no treatments for celiac disease – patients must avoid gluten.

Allergy and drug hypersensitivity are similar to autoimmunity with regards to detrimental activation of adaptive lymphocytes. The cause for initiation against innocuous foreign antigen is unclear, but again likely involves some environmental trigger in genetically susceptible individuals.[43] Both disorders are primarily mediated by antibodies of the immunoglobulin G and E isotypes (IgG, IgE), which require T cell help to class switch. Alternatively, delayed type hypersensitivity reactions are directly mediated by T cell activity. The targeted antigen is usually readily identifiable with testing, such as skin pricks in the case of IgE-mediated allergy, while drug hypersensitivity flare ups are detected upon intravenous injection of a given pharmaceutical. Symptoms of either condition generally involve anaphylaxis mediated by mast cell degranulation. While avoidance of the allergic trigger is essential to mitigating pathology, global immunosuppressants such as glucocorticoids and antihistamines are often maintained throughout life.

1.5 Antigen immunotherapy

In 1911, Leonard Noon first reported on AIT in his Lancet publication *Prophylactic Inoculation Against Hay Fever*.[44] He describes experiments performed by WP Dunbar a few years earlier in which patients suffering from hay fever were found to experience improvement in their symptoms after subcutaneous injection of the target allergen. At the time, this evidence was interpreted to indicate that injection of allergens could give rise to "active immunity against the toxin," similar to how inoculation with smallpox provided protection against its associated disease. It is now appreciated that while some measures of regulatory humoral immunity may be induced with AIT, for example the more inert antibodies of the IgG4 subclass, suppressing the reactive T cell compartment via deletion, anergy, or induction of regulatory programs such as Treg or Tr1 is likely an essential element in the treatment of harmful antigen-specific immune responses.[45,46,47]

Approaches to AIT have traditionally utilized subcutaneous, sublingual, or oral inoculation with the target protein. Upon injection, antigens drain to proximal LNs where they are then taken up by resting APCs such as dendritic cells (DC) or macrophages. In the absence of innate stimuli, presentation to T cells theoretically results in downstream tolerogenic outcomes across cellular and humoral compartments.

Complexities arise in the context of therapeutic AIT where prophylactic tolerance induction of naïve lymphocytes is no longer an option. If T cells have previously been activated against a given target, they will have memory of that reaction and upregulate survival markers such as the IL-7 receptor (IL-7R), which allow for maintenance of the memory pool in the absence of antigen and rapid reactivation upon subsequent antigen

encounter.[48] The presence of pre-existing immune memory thus requires more delicate handling of AIT as compared to prophylactic settings, since inoculation of the target antigen could result in further exacerbation of the established adverse immune response.

A key hurdle for achieving successful AIT in antibody-mediated conditions such as allergy is the elimination of plasma cells, a unique cell type rich with endoplasmic reticulum that B cells adopt in order to produce as many antibodies as possible. T-B interaction resulting from germinal center dynamics leads to selection of high-affinity B cells clones in a process called affinity maturation. The highest affinity clones are then directed to migrate from whatever lymphoid organ housed their germinal center to the bone marrow, where they remain for the duration of their lifespan (which can last 20 years or more) actively secreting antibodies into circulation for protection against future threat. While suppression of the cognate T cell repertoire can prevent further germinal center reactions from occurring, and thereby prevent further induction of antibody producing B cells, affecting the long-lived plasma cell compartment in the bone marrow is a major obstacle in achieving comprehensive therapeutic tolerance. Antibodies for B cell depletion have been successfully employed in the clinic for cancer, and are being developed for autoimmunity, but the canonical B cell markers such as CD19 or B220 are lost upon induction of plasma cell fate. Other techniques involving broad cellular toxicity may offer some promise.

Nevertheless, identification of the immunodominant antigens responsible for specific allergies has aided the development and application of AIT to a wide array of conditions, for example, the major allergens in peanuts (Ara h 2), birch pollen (Bet v 1),

cat dander (Fel d 1), and house dust mite (Der p 1).[49,50,51,52] The homeopathic practice of ingesting local honey to aid with seasonal allergies is an example of oral AIT against pollens. The route of administration may affect the outcome of peripheral tolerance against a given antigen. Along these lines, work by other members of my lab explores local s.c. pGal-antigen delivery for allergy relief.

While allergens have primarily been the focus of AIT, the use of self proteins for suppression of autoimmunity is gaining promise. Many experiments have demonstrated prophylactic efficacy in prevention of murine models of autoimmunity, but therapeutic tolerance induction is more challenging due to existing obstacles involving an activated APC network alongside pre-existing T cell memory and circulating antibodies. Yet some success has been found in clinical trials for peptide therapies in diseases such as: rheumatoid arthritis, using the chaperone DnaJ peptide dnaJP1; lupus, using the U1-70K spliceosomal protein peptide P140; T1D, using the heat shock protein 60 peptide DiaPep277; and MS, using the MBP peptide MBP8298.[53,54,55,56,57,58] In each case, researchers were able to demonstrate safety of their approach along with at least some minor improvement in symptoms. The underlying mechanisms responsible for clinical efficacy are only partially understood and include a variety of potential actors, such as PD1 and IL-10 (**Table 1.1**). Other cell types responsible for tolerance induction that have been identified include TR1 cells, CD103+ DCs, and even microbiota.[59,60] Yet, classical AIT fails to reach a sufficient level of effectiveness in many cases and new strategies are needed to fully harness endogenous networks of peripheral tolerance induction.

	Route	Disease	Antigen	Dose	Mechanism	Ref.
1	Oral	Rheumatoid arthritis	dnaJP1 + hydroxychloroquine	25mg daily	Decrease in TNFa and increase in IL10. Coexpression of PD1 prerequisite for clinical efficacy.	53
2	SC	Moderately active SLE	Spliceosomal peptide P140	200ug or 1000ug x3 (2wk interval)	Mechanism unclear (no increase in IL-10). Anti-dsDNA antibody levels decreased, disease activity decreased (in 200ug group), and abolished T cell intramolecular spreading within U1-70K and intermolecular spreading to other spliceosomal proteins such as SmD1.	54
3	SC	Recent-onset T1D	DiaPep277 (hsp60)	0.2, 1, or 2.5mg at 0, 1, 6, & 12mo	Cytokine production dominated by IL10, associated with beta-cell preservation.	58
4	IV	Progressive MS	MBP8298	500mg every 6mo	Anti-MBP autoantibody suppression was observed more generally and largely independent of HLA haplotype, but not predictive of clinical benefit.	56
5	SL	Seasonal allergic rhinitis	grass pollen	1 tablet daily	Reduced clinical score with IL10 induction in KLRG1+ ILC2s via retinol metabolic pathway, cytokine-cytokine receptor interactions, and JAK-STAT signaling.	57

Table 1.1 | AIT clinical trials. Examples of recent AIT clinical trials and their associated mechanisms in relation to clinical benefit.

Contemporary strategies to AIT often involve engineering the antigen such that it may avoid signals of innate activation and favor a tolerogenic outcome. For example, in a different AIT trial for MS than mentioned above, researchers coupled seven different disease-associated antigens to peripheral blood mononuclear cells (PBMCs) that had previously been collected from patients, and then reinfused the antigen-coupled cells back into the patients.[9] Uptake of antigen with naturally dying PBMCs leads to presentation of the antigens via efferocytotic pathways and ensuing tolerance.

A separate class of AIT therapeutics being developed involves the use of nanoparticle carriers. One approach couples MHC-peptide complexes onto nanoparticle surfaces, which can then interact with T cells as if the nanoparticles were inactivated APCs presenting antigen without signal 2 or 3.[61] Another strategy utilizes the nanoparticles as cargo vesicles into which antigen is loaded along with rapamycin.

Rapamycin inhibits cellular metabolism and thus forces a suppressive phenotype onto APCs that pick up the antigen, thereby presenting it in a tolerogenic fashion to cognate T cells.[62]

1.6 Overview of research

The research presented below aims to improve our understanding of therapeutic tolerance induction in adaptive lymphocytes through the use of novel engineered approaches to AIT. First, I demonstrate therapeutic suppression of previously established T cell immunity and disease by targeting the liver for antigen presentation. Second, I explore a new strategy for delivering antigen to systemic efferocytotic machinery. Both of these projects were built off of former research done in the lab.

The original concept of engineering antigens for AIT was motivated by the work of former grad student Stephan Kontos. In his 2012 paper, Stephan demonstrates a novel strategy for delivering protein antigen to the peripheral tolerance network responsible for clearing apoptotic erythrocytes (eryptosis).[63] By conjugating the model protein ovalbumin (chicken egg white protein, OVA) to a red blood cell-binding peptide (ERY1), upon i.v. injection the antigen will piggy-back on RBCs to their regularly scheduled turnover mediated in large part by hepatic phagocytes. The resulting T cell education leads to abortive proliferation of the antigen-specific compartment, and as shown in later studies, prevention of downstream humoral responses.[64]

Building from this idea, a recent postdoc in the lab, Scott Wilson, moved to target hepatic APCs directly. Utilizing RAFT polymerization, Scott engineered a suite of

glycopolymers capable of directing protein into lectin scavenging networks richly abundant in the liver. Poly-N-acetyl glucosamine and galactosamine (pGlu, pGal) were found to induce robust T cell tolerance.[65] Using his glycopolymers, Scott demonstrated prophylactic tolerance induction as well as suppression of adoptively transferred ex vivo activated transgenic CD4 cells. A key advantage of pGlu and pGal as compared to ERY1 is the improved efficiency with which the antigen is taken up by scavenging hepatic APCs. For application to therapeutic settings, avoiding prolonged time in the blood and off-target uptake in potentially activated APCs outside of the liver are essential features.

The pGal polymer I used was graciously synthesized and conjugated to antigen by Scott and a fellow grad student in the lab, Michal. I then purified constructs using fast performance liquid chromatography (FPLC) on a size exclusion column (SEC). We finally confirmed endotoxin-free preparation in vitro using a cell line that detects TLR4 activation. I was fortunate enough to join the lab at time when we were poised to take pGlu/pGal into therapeutic testing, which offered me the chance to apply my education in immunology with hands on translational application of a promising novel drug platform. My efforts to evaluate the clinical potential for therapeutic intervention with pGal-antigen immunotherapy are illustrated in Chapter 2 below.

Our lab is now developing pGal in collaboration with the startup biotech company Anokion, due to its promising results in prophylactic scenarios and its translatability to humans. Anokion has begun clinical trials for celiac disease and has plans to begin with MS and T1D soon. The primary receptor we hypothesize to be responsible for scavenging pGal in humans is the Asialoglycoprotein receptor (ASGR1), which has a homologous

carbohydrate recognition domain (CRD) as the C-type lectin 10 alpha (CLEC10A) or Macrophage galactose-type lectin (MGL) in mice.[66,67] Uptake of constructs is detectable in a variety of hepatic phagocytes including liver sinusoidal endothelial cells (LSEC), hepatocytes, Kupffer cells, and dendritic cells, in order of decreasing relative uptake magnitude.

A further evolution in platform design occurred in the lab when recent grad student Alizée Grimm conceived the idea to directly target systemic efferocytotic networks. By fusing OVA to the soluble efferocytotic mediator Milk fat globule epidermal growth factor 8 protein (MFGE8, MFGE8-OVA), she imagined that we can achieve tolerogenic antigen presentation anywhere in the body. This approach builds off the earlier strategies of ERY1 and pGal/Glu by combining the elements of apoptotic piggybacking with direct, efficient uptake. Furthermore, MFGE8 itself can drive inhibitory signaling in APCs. The work detailed in Chapter 3 captures my efforts at furthering the development of this strategy in vitro and in vivo. This project has turned into a collaboration with a younger student in the lab, which will see a combined effort of investigation into utilizing soluble efferocytotic mediators MFGE8 and Growth arrest-specific 6 protein (GAS6), alone and in combination, towards the application of therapeutic AIT.

The majority of experiments discussed below were performed in inbred mice housed in a specific-pathogen free (SPF) facility. Transgenic mice were used in many experiments, which allows us to artificially increase the size of a given clonotype within a mouse's T cell repertoire by transplanting lymphocytes from a transgenic donor into a

wild-type (WT) recipient. These transgenic mice have unique protein isoforms that allow us to track them in the recipient, which grants us the opportunity to measure effects in antigen-specific cells.

The use of mice is unfortunately essential in immunology research due to the immeasurable complexities of multi-organ interactions that play out in a given immune response. In vitro experiments were used wherever possible. Ethical treatment of animals is of utmost importance in our experimental considerations. Due to limited numbers of animals used, many experiments are statistically underpowered.

CHAPTER 2: SUPPRESSION OF ESTABLISHED T CELL IMMUNITY AND DISEASE VIA GLYCOSYLATED ANTIGEN IMMUNOTHERAPY

2.1 Abstract

Current treatments for autoimmunity, allergy, and drug hypersensitivity generate global immune suppression, resulting in an increased risk of infection and malignancy. A therapy that leverages the body's inherent mechanisms for the induction of antigen-specific immune tolerance would represent a major step forward in the treatment of numerous diseases. One such mechanism is the presentation of antigen in the immunosuppressive environment of the liver. By targeting antigen to scavenging receptors specifically expressed on hepatic antigen presenting cells, presentation of the antigen can be restricted to the liver and result in T cell tolerance. Carbohydrate scavenging receptors are abundant in the liver, allowing for highly efficient uptake of glycosylated proteins from the blood. In previous work, our lab synthesized an N-acetyl galactosamine polymer (pGal) that is conjugated to protein antigen via a self-immolative linker, allowing for dissociation of antigen from the targeting polymer upon endocytosis. Here, we show therapeutic i.v. treatment with pGal conjugated to ovalbumin (pGal-OVA) results in suppression of previously activated T cell responses in antigen-specific T cells. Using in vivo and ex vivo molecular-based investigations of antigen-specific murine lymphocytes in experimental murine models, we probe underlying signatures of tolerance induction in cognate T cells and elucidate the role of co-inhibitory ligands in therapeutic

tolerance induction. Ultimately, we demonstrate lasting protection from relapse with pGal-antigen therapy in a murine model of relapsing-remitting of multiple sclerosis.

2.2 Introduction

Peripheral tolerance ensures the adaptive immune system does not inappropriately mount a response against innocuous foreign antigen, commensal microbes, or peripheral tissue antigens incompletely tolerized against during development. When T cells recognize their cognate antigen in the presence of co-inhibitory ligands, they can undergo a tolerogenic fate induction program resulting in apoptosis, anergy/exhaustion, or a dominant regulatory fate. It has been previously shown in adoptive transfer experiments of ex vivo activated cells that memory and effector T cells can undergo peripheral tolerance induction and deletion.[65,68] Nevertheless, current therapies for autoimmunity, allergy, and drug hypersensitivity utilize global immune suppression, which require life-long treatment and leave patients vulnerable to infection, malignancy, and other comorbidities.

We previously devised a strategy for robust antigen-specific tolerance induction in circulating T cells by targeting protein antigen to tolerogenic APC networks. By conjugating a protein or peptide of interest to a glycopolymer consisting of repeating GalNAc units (pGal), we can target antigen for rapid uptake in hepatic APCs.[65] We theorize that presentation of antigen to circulating T cells in the hepatic environment coopts the endogenous immunosuppressive APC network to drive tolerance in cognate T cells.

Using a variety of mouse models, we explore the ability of intravenous pGal-antigen therapy to mediate suppression of previously established T cell immunity within the insulted host. Interventional treatment with pGal-ovalbumin (pGal-OVA) was able to dampen antigen-specific T cell recall responses across multiple OVA challenge models, in both transgenic and endogenous repertoires. Transcriptional analysis of T cells after antigen treatment revealed co-inhibitory pathways to be the top causal networks induced by pGal-antigen therapy. Congruently, we experimentally demonstrated a partial dependence on PD-1 for tolerance induction in this setting. Finally, we show therapeutic tolerance induction in a relapsing-remitting MS mouse model of experimental autoimmune encephalomyelitis (RR-EAE).

2.3 Results

2.3.1 Antigen-mediated suppression of CFA/IFA recall response in transgenic T cells

We first sought to demonstrate therapeutic AIT with pGal-OVA in a proof-of-principle model using transgenic T cells specific for OVA. The experimental time frame for this experiment is shown in **Figure 2.1 a**, below. After first adoptively transferring transgenic $CD8^+$ and $CD4^+$ T cells specific for OVA (OTI and OTII, respectively) into WT hosts, mice received a primary immunization with OVA emulsified in Complete Freund's Adjuvant (CFA). This immunization induces potent T cell activation along with T_H17 and T_H1 fate skewing, as well as IgG antibodies against the target antigen.[69] We then tracked OT cells using their congenic label CD45.1 and the specific TCR component, Vα2.

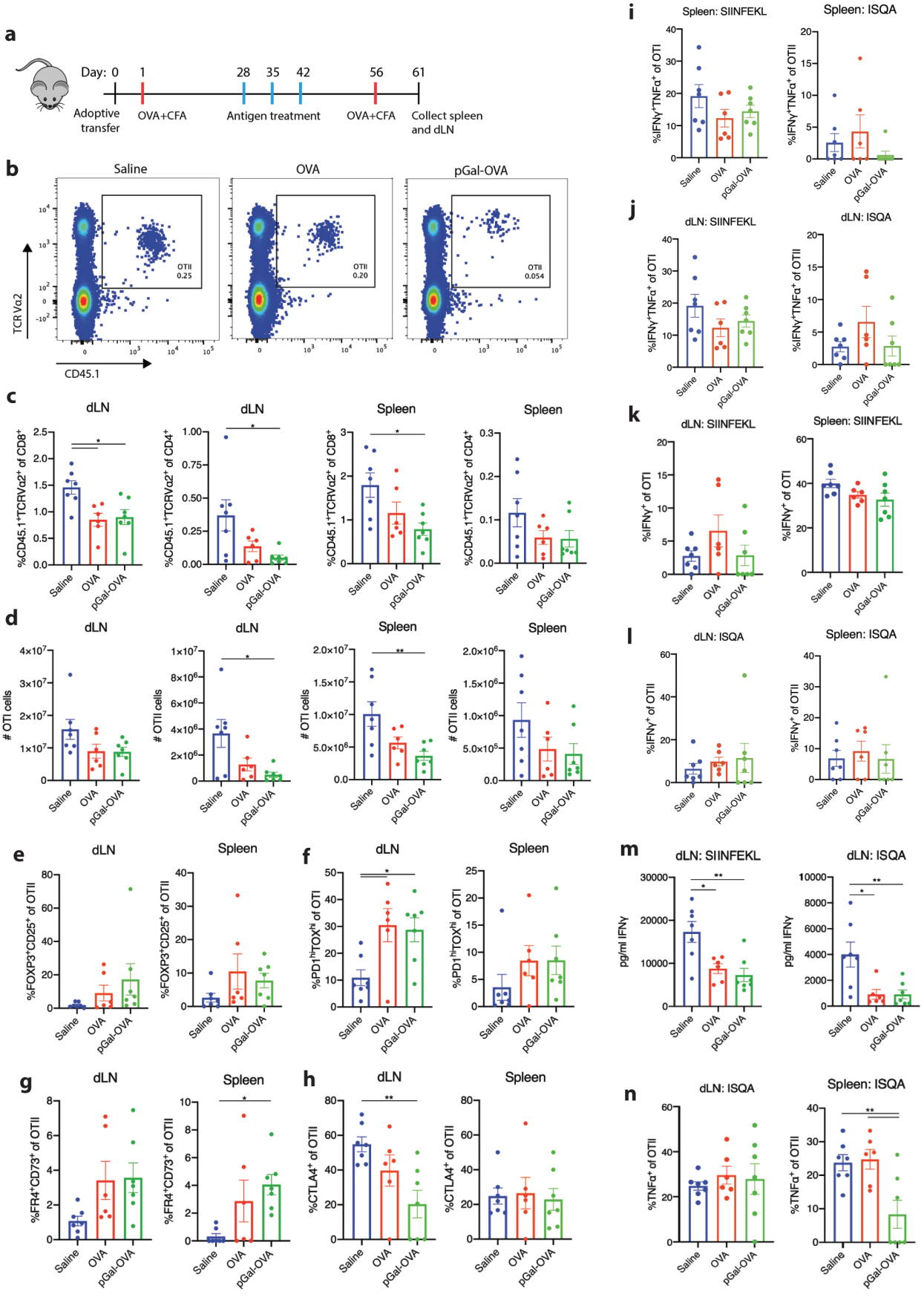
a
Day: 0
1
28
35
42
56
61
Adoptive transfer
OVA+CFA
Antigen treatment
OVA+CFA
Collect spleen and dLN
b
Saline
OVA
pGal-OVA
OTII 0.25
OTII 0.20
OTII 0.054
TCR Vα2
CD45.1
c
dLN
Spleen
%CD45.1+TCRVα2+ of CD8+
%CD45.1+TCRVα2+ of CD4+
d
OTI cells
OTII cells
e
%FOXP3+CD25+ of OTII
f
%PD1hiTOXhi of OTI
%PD1hiTOXhi of OTII
g
%FR4+CD73+ of OTII
h
%CTLA4+ of OTII
i
Spleen: SIINFEKL
Spleen: ISQA
%IFNγ+TNFα+ of OTI
j
dLN: SIINFEKL
dLN: ISQA
k
%IFNγ+ of OTI
l
%IFNγ+ of OTII
m
pg/ml IFNγ
n
%TNFα+ of OTII
Saline
OVA
pGal-OVA

Figure 2.1 | Antigen-mediated suppression of CFA/IFA recall response in transgenic T cells (previous page). a) Experimental design: WT B6 hosts received adoptive transfer of ~75k OTI and OTII, then s.c. immunized in the forelimbs with OVA in CFA. After waiting one month for memory responses to stabilize, mice were i.v. treated with either 5μg OVA or equimolar pGal-OVA (or saline as negative control). Mice received three treatment doses, each one week apart. Two weeks after the final dose, a secondary challenge of OVA emulsified in Incomplete Freund's Adjuvant (IFA) was injected s.c. in the forelimbs. Mice were sacrificed five days after rechallenge for collection of the secondary lymphoid organs (SLO), spleen and dLNs. **b)** Representative flow cytometry profiles of recovered OTII cells in the dLN across treatments. **c)** Percent recovery of OTI and OTII cells in dLN and spleens as a proportion of parent population. **d)** Total OTI&II cell numbers recovered, calculated by multiplying the percent recovery of live cells by the total number of lymphocytes recovered from each organ. **e-h)** Expression frequencies of the specified protein markers as indicated on the y-axes on recovered OTI&II cells from SLO. **i-l)** Six-hour ex vivo antigen restimulations were performed with recovered lymphocytes and peptides as indicated above each graph, and intracellular flow cytometry was used to detect production of the indicated cytokines in OTI&II cells. **m,n)** Three-day restimulations were also carried out for ELISA-based analyses of the indicated cytokines in culture supernatants. All statistical comparisons were performed by one-way ANOVA using Tukey correction.

The recovery of OTI&II cells by flow cytometry is shown in **Figure 2.1 b**. Recovery is quantified as a frequency of parent population (CD8 or CD4) in **Figure 2.1 c**, or total cell number in **Figure 2.1 d**. Essentially, we see a consistent and statistically significant reduction in the recovery of OTI&II cells in pGal-OVA treated mice compared to those treated with saline, and a consistent observable difference to plain OVA. We interpreted this key result as indication of successful AIT via pGal-antigen therapy, particularly the near absence of OTII cells in the dLN in this immunization setting.

While OVA treatment also led to some statistical degree of recovery impairment compared to saline, it was not consistently discernable. Overall, a stair-step pattern can be seen in the data: starting with saline as the highest level of secondary challenge recovery, then OVA with some minor impairment in recall response, and finally pGal-OVA with the lowest level of cell recovery. This pattern is representative of what has been observed in many prophylactic antigen immunotherapy experiments, such as with ERY1 or pGal. Unmodified antigen therapy can induce a minor level of tolerance, but

engineered variants that facilitate improved APC uptake lead to a more complete level of suppression.[65] It was noteworthy to see no adverse effects of i.v. antigen therapy given the strong circulating antibody titers induced by CFA at the time of treatment (**Supplemental Figure 2.1.1 a**). Ultimately the efficacy of OVA in our model fit with the moderate level of effectiveness of AIT realized in clinical practice, and it was reaffirming to see substantial improvement with pGal conjugation. We measured the affinity for polyclonal anti-OVA IgG against plain OVA and pGal-OVA using surface plasmon resonance (SPR) and discovered a five-fold decrease in affinity with pGal conjugation (**Supplemental Figure 2.1.1 b**). We postulate the carbohydrate polymer may act as a shield against antibody recognition. Taken together, we interpret these data to indicate that pGal-OVA conjugation may contribute to therapeutic tolerance induction via its ability to avoid antibody-mediate capture and opsonization of antigen upon i.v. injection, and deliver the antigen to its subversive destination.

Confirming recall impairment led us to consider possible mechanisms that contributed to T cell tolerance. One possible outcome of T cell – p:MHC interaction that could have led to reduced cell recovery is induction of apoptosis upon tolerogenic antigen encounter, prior to secondary challenge. Alternatively, cells could have been suppressed (anergized/exhausted) upon tolerogenic antigen encounter and thus could not expand upon secondary challenge. The localization of effects to specific SLO or cell type is an additional layer of complexity. The absence of OTII cells in the dLN upon rechallenge was the most noticeable impact of pGal on cell recovery. The largest differences for OTI cells

were seen in the spleen. It's difficult to speculate on what may be causing these tropic patterns, but it may be related to the types of tolerance imparted.

Flow cytometric analysis of cell protein expression at the experimental endpoint revealed phenotypic signatures of cell suppression. We saw a non-significant trend towards increased Treg frequencies with antigen treatment (**Figure 2.1 e**). When we looked for populations of exhausted $CD8^+$ T cells using the surface marker PD-1 and the transcription factor thymocyte selection associated high mobility group box (TOX), we found a notable increase of double positives in antigen-treated mice compared to saline (**Figure 2.1 f**).[70] Further investigation into markers of tolerance in CD4 T cells led us to discern an increase in the population of anergic cells defined by FR4 and CD73 (**Figure 2.1 g**), which showed a significant increase in pGal-OVA versus saline in the spleen.[71] Expression of the co-inhibitory ligand Cytotoxic T lymphocyte-associated protein 4 (CTLA4) on OTII cells in the dLN was somewhat counterintuitive in its opposite stair-step pattern, where pGal-OVA treatment led to the lowest level of expression (**Figure 2.1 h**). Overall, cells that experienced antigen treatment had a more suppressed surface phenotype than those that were treated only with saline.

Lymphocytes collected from spleen and dLNs at the experimental endpoint were subjected to ex vivo peptide restimulations. OVA-derived class I peptide SIINFEKL ($OVA_{257-264}$) was used to interrogate OTI cells as their cognate antigen, and class II peptide ISQAVHAAHAEINEAGR ($OVA_{323-339}$) for OTII cells. Cells were stimulated for either six hours for intracellular flow cytometry, or for three days for ELISA analysis of supernatant. The short-term stimulation consisted of three hours with peptide, and

another three hours with the addition of brefeldin A (BFA) and monensin to prevent secretion of cytokines. **Figure 2.1 i and j** show the frequency of OTI&II cells from the dLN that produced both IFNγ and TNFα upon restimulation with the indicated peptide. **Figure 2.1 k and l** show the frequency of IFNγ-producing OTs. The restim data mentioned thus far does not demonstrate any clear distinction between treatment groups. However, when we looked at the amount of IFNγ in the three-day supernatant, we saw a clear reduction with antigen treatment compared to saline (**Figure 2.1 m**). When we looked at TNFα production in the six-hour restim by flow, we saw a clear decrease only in pGal-OVA treated mice (**Figure 2.1 n**). Taken together, we see a reduction in recall magnitude, suppression of cell phenotype, and impairment in cytokine production of cognate T cells with pGal antigen modification.

This experiment confirmed results from our earlier pilot studies that pGal-OVA can inhibit recall responses across a variety of adjuvants (**Supplemental Figure 2.1.2**). Even before these pilot studies, our initial immunization approach involved no adjuvant at all, and we found that by simply injecting endotoxin-free OVA s.c. we could achieve weak but tractable anti-OVA IgG titers (10^3, data not shown). We reasoned this approach could offer the best chance of successfully culling an "established' immune response. However, we then learned about traditional AIT and realized we must use an adjuvant in order to drive a bona fide memory response that would provide a rigorous test for pGal. We had our first hint of success utilizing LPS as adjuvant, which is historically used in our lab for prophylactic challenges, but it did not yield a sufficient dynamic range to show statistically significant improvement in AIT-mediated recall

suppression with pGal conjugation (data not shown). Essentially, LPS did not produce a legitimate memory recall response; the secondary response was of a lower magnitude than the primary response. Eventually we decided to screen pGal against various adjuvants (CFA, R848, and CpG) in our pilot memory model experiments shown in Supplemental Figure 2.3.1.2.

We interpreted our results from Figure 2.1 as evidence for therapeutic antigen-specific tolerance induction, since pGal was designed as an inert antigen carrier that is not expected to be affecting APC state. We performed a simple test for innate suppression by pre-incubating pGal-OVA with R848-activated APCs and observed no impairment in the induction of activated $CD86^{+}MHC\text{-}II^{+}$ double positive cells (**Supplemental Figure 2.1.3**).

2.3.2 Antigen-mediated suppression of R848 recall response in transgenic T cells

We next tested the ability of pGal-OVA to suppress the OTI&II recall response in an effector stage intervention between R848 immunizations. The experimental setup was identical to Figure 2.1 (a), except the first treatment was given only five days after primary immunization, instead of one month later. We designed this in attempt to interrogate therapeutic suppression of an effector population, as compared to Figure 2.1 which focused on suppression of a memory population. We changed adjuvants to avoid the depot effect of Freund's adjuvant, which could complicate therapy if there was ongoing generation of potent pro-inflammatory signals at the time of treatment.

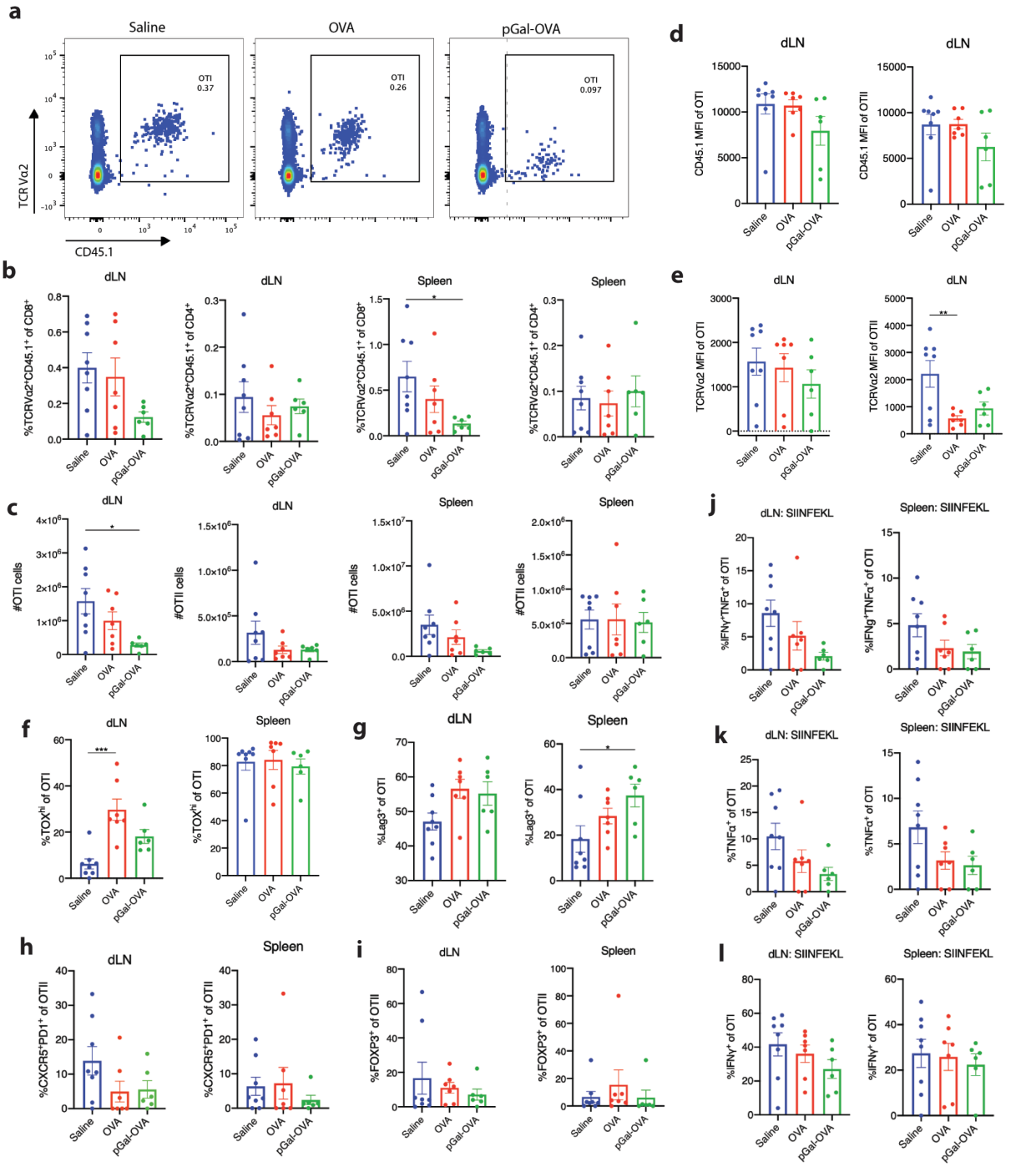

Figure 2.2 | Antigen-mediated suppression of R848 recall response in transgenic T cells. Experimental setup as in Figure 2.1 but here using R848 for both immunizations, and mice received first treatment dose 5 days after immunization. **a)** Representative flow cytometry profiles of recovered OTI cells in the dLN across treatments. **b)** Percent recovery of OTI and OTII cells in dLN and spleens as a proportion of parent population. **c)** Total OTI&II cell numbers recovered. **d-i)** Expression frequencies of the specified protein markers as indicated on the y-axes on recovered OTI&II cells from SLO. **j-k)** Six-hour ex vivo antigen restimulations were performed with recovered lymphocytes and peptides as indicated above each graph, and intracellular flow cytometry was used to detect production of the indicated cytokines in OTI&II cells. All statistical comparisons were performed by one-way ANOVA using Tukey correction.

OTI&II cell recovery by flow is shown in **Figure 2.2 a**, quantified as a frequency of parent cell type in **Figure 2.2 b**, or total cell number in **Figure 2.2 c**. Importantly, we saw a significant reduction in OTI cells compared to saline in only the pGal-OVA treated mice. There were no obvious differences in OTII cell recovery. The differential suppression of OTI observed here versus suppression of OTII in the previous experiment could be due to the change in timing of intervention and/or adjuvant used. The stair-step pattern was again observable here in the OTI cell recovery, with saline treatment generating the strongest recall response, then OVA, and finally pGal-OVA with the least.

The stair-step pattern was also seen in the OTI expression levels of CD45 (**Figure 2.2 d**) and TCR (**Figure 2.2 e**), although there were no statistically significant differences. In the OTII cell compartment, a stair-step pattern is observable in CD45 expression, but TCR expression was clearly decreased with OVA versus saline showing statistical significance. Puzzlingly, while a reduction in TCR expression level is associated with lower T cell avidity for APC, with fewer p:MHC interactions possible, a reduction in CD45 is associated with higher TCR sensitivity as CD45 has an intracellular phosphatase domain that inhibits TCR kinase signaling cascades.

When we looked at the expression of TOX in OTI cells, we saw a large increase with plain OVA treatment, while pGal-OVA showed a trend toward increase (**Figure 2.2 f**). Investigation into co-inhibitory markers on OTI cells revealed a stair-step increase in Lymphocyte-activation protein 3 (Lag3) across treatments, with pGal-OVA being significantly higher than saline in the spleen (**Figure 2.2 g**). We looked into the OTII frequencies of T_{FH} cells using the markers PD-1 and C-X-C chemokine motif receptor 5

(CXCR5; **Figure 2.2 h**), as well as Tregs (**Figure 2.2 i**), but saw no major differences. pGal-OVA trended towards having the lowest frequency of splenic T_{FH}.

Analysis of cytokine production upon six-hour restim revealed a consistent stair-step pattern whereby pGal-OVA exhibited a trend towards the least amount of single and double producers of IFNγ and TNFα (**Figure 2.2 j-l**). Overall, the data from this experiment demonstrate further evidence of therapeutic tolerance induction with pGal-OVA.

2.3.3 Antigen-mediated suppression of LmOVA/CFA recall response in endogenous CD8$^+$ T cell

After demonstrating consistent induction of therapeutic tolerance using pGal-OVA in our transgenic OT cell model, we moved to test our ability to tolerize the endogenous T cell compartment under rigorous conditions. Utilizing a similar experiment approach as above, we setup a system to induce robust endogenous CD8 memory against OVA by first inoculating WT B6 mice with a genetically modified strain of the bacterial pathogen *Listeria monocytogenes*, which expresses OVA as one of its own antigens (LmOVA). After mice naturally clear the infection over the course of a week, they acquire adaptive memory against OVA as a pathogen-associated antigen.

We then waited another month for the memory response to stabilize before beginning our treatment regimen involving three doses of either saline, OVA, or pGal-OVA. Two weeks after the last treatment, mice were challenged subcutaneously in the forelimbs with OVA emulsified in CFA. Five days after the CFA challenge mice were

euthanized to collect spleens and dLNs. OVA-specific CD8 T cells were then analyzed by flow cytometry using a pentamer of H2Kb:SIINFEKL fused to a fluorophore, which allows tracking antigen-specific T cells in an endogenous repertoire.

F**igure 2.3 a** displays the quantification of pentamer-reactive CD8 T cells in the dLN and spleen as a percentage of total CD8s, as well as total cell number. We observed a non-significant trend towards reduction of cognate T cell recovery in antigen-treated mice. The flow cytometry gate for detecting pentamer-reactive $CD8^+$ T cells is shown in **Figure 2.3 b**.

Phenotypic analysis of cognate CD8s revealed a stair-step pattern of increased frequencies of $TOX^+PD\text{-}1^+$ double positives (**Figure 2.3 c**), as well as PD-1 single positives (**Figure 2.3 d**). We detected a significant increase in TOX expression only in pGal-OVA treated mice compared to saline (**Figure 2.3 e**). Analysis of the transcription factor Eomesodermin (Eomes) revealed an opposite stair-step pattern, with pGal-OVA having the lowest levels of expression (**Figure 2.3 f**). Since Eomes expression is associated with maintenance of cellular function, or a precursor exhaustive state, and loss of its expression is associated with terminal exhaustion, these data collectively illustrated a fate outcome resembling exhaustion.

Intracellular staining after six-hour restimulation was also performed. A consistent stair-step pattern of tolerance was observed, with pGal-OVA driving the lowest levels of IFNγ and TNFα double producers and IFNγ single producers (**Figure 2.3 g,h**). An alternate restimulation was performed with the pan T cell activators phorbol myristate

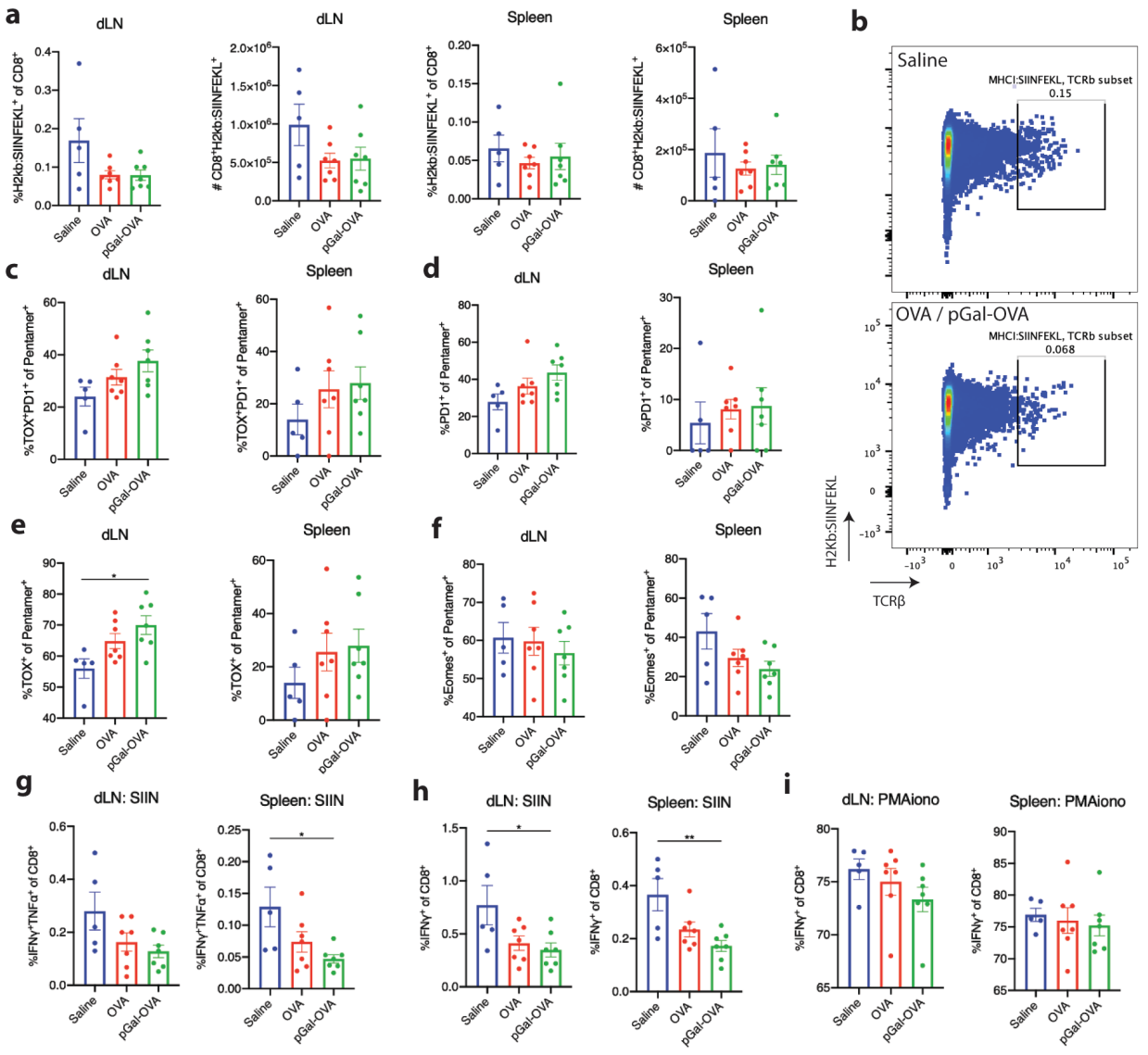

Figure 2.3 | Antigen-mediated suppression of LmOVA/CFA recall response in endogenous CD8$^+$ T cell. Mice were first inoculated with LmOVA and allowed to clear the infection, then one month later given antigen therapy as described previously, and finally challenged two weeks after the last antigen dose with OVA+CFA s.c. **a)** Quantification of endogenous OVA-specific CD8$^+$ T cells recovered in dLN and spleens as a proportion of total CD8$^+$ as well as total cell number. **b)** Representative flow cytometry profiles of recovered pentamer reactive CD8$^+$ T cells in the dLN comparing effects of saline and antigen treatments. **c-f)** Expression frequencies of the specified protein markers as indicated on the y-axes on recovered pentamer-specific CD8$^+$ T cells from SLO. **g-i)** Six-hour ex vivo antigen restimulations were performed with recovered lymphocytes and peptides as indicated above each graph, and intracellular flow cytometry was used to detect production of the indicated cytokines in pentamer-reactive CD8$^+$ T cells. All statistical comparisons were performed by one-way ANOVA using Tukey correction.

acetate (PMA) and ionomycin, which activates signaling downstream of the TCR via protein kinase C and calcium flux, respectively. Under these rigorous conditions the stair-step pattern was somewhat preserved, with pGal-OVA trending toward the lowest amount of IFNγ production (**Figure 2.3 i**).

2.3.4 Transcriptional profile of therapeutic T cell tolerance induction

Through our experiments described above, we were able to gain a picture for how previously activated cognate T cells that experienced pGal-OVA looked and acted after being submitted to a secondary challenge. In order to gain a deeper understanding for how pGal-antigen therapy mediates tolerogenic fate outcomes in circulating memory T cells, we subjected cells to RNAseq shortly after they experienced antigen treatment in vivo.

Mice first received ~600k OTI and OTII cells, each. Such a high number was used because pilot experiments resulted in a very low recovery of cells from saline treated mice (data not shown). After adoptive transfer, mice were immunized in the forelimbs with OVA emulsified in CFA. One month later, mice received a single therapeutic treatment dose of saline, OVA, or pGal-OVA. Mice were euthanized four days after treatment for collection of liver and forelimb dLN, along with spleen. All recovered lymphocytes were pooled together. We then used fluorescently activated cell sorting (FACS) to isolate the OTI and separately OTII cells from each mouse. Finally, RNA extraction and sequencing were performed on each cell population.

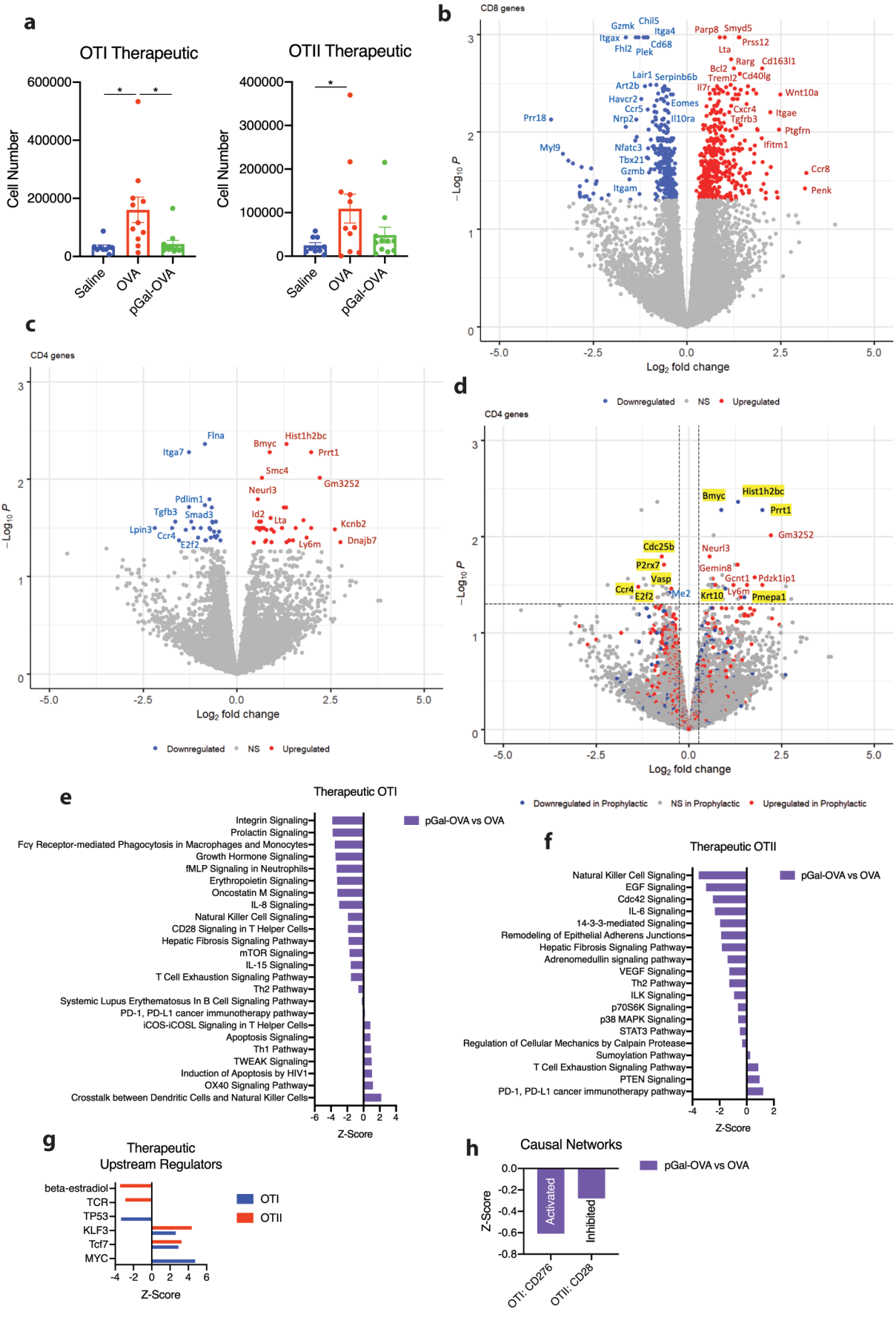
a
OTI Therapeutic
OTII Therapeutic
Cell Number
Saline
OVA
pGal-OVA
b
CD8 genes
Log2 fold change
c
CD4 genes
Downregulated
NS
Upregulated
d
e
Therapeutic OTI
pGal-OVA vs OVA
Integrin Signaling
Prolactin Signaling
Fcγ Receptor-mediated Phagocytosis in Macrophages and Monocytes
Growth Hormone Signaling
fMLP Signaling in Neutrophils
Erythropoietin Signaling
Oncostatin M Signaling
IL-8 Signaling
Natural Killer Cell Signaling
CD28 Signaling in T Helper Cells
Hepatic Fibrosis Signaling Pathway
mTOR Signaling
IL-15 Signaling
T Cell Exhaustion Signaling Pathway
Th2 Pathway
Systemic Lupus Erythematosus In B Cell Signaling Pathway
PD-1, PD-L1 cancer immunotherapy pathway
iCOS-iCOSL Signaling in T Helper Cells
Apoptosis Signaling
Th1 Pathway
TWEAK Signaling
Induction of Apoptosis by HIV1
OX40 Signaling Pathway
Crosstalk between Dendritic Cells and Natural Killer Cells
Z-Score
f
Therapeutic OTII
Natural Killer Cell Signaling
EGF Signaling
Cdc42 Signaling
IL-6 Signaling
14-3-3-mediated Signaling
Remodeling of Epithelial Adherens Junctions
Hepatic Fibrosis Signaling Pathway
Adrenomedullin signaling pathway
VEGF Signaling
Th2 Pathway
ILK Signaling
p70S6K Signaling
p38 MAPK Signaling
STAT3 Pathway
Regulation of Cellular Mechanics by Calpain Protease
Sumoylation Pathway
T Cell Exhaustion Signaling Pathway
PTEN Signaling
PD-1, PD-L1 cancer immunotherapy pathway
g
Therapeutic
Upstream Regulators
beta-estradiol
TCR
TP53
KLF3
Tcf7
MYC
OTI
OTII
h
Causal Networks
Activated
Inhibited
OTI: CD276
OTII: CD28

Figure 2.4 | Transcriptional profile of therapeutic T cell tolerance induction (previous page). Mice received adoptive transfer of ~600k OTI and OTII cells each, then given one i.v. antigen treatment the next day, and five days later were sacrificed to harvest SLOs. **a)** Number of recovered cells by FACS. **b)** Volcano plot displaying DEGs for OTI cells between pGal-OVA and OVA (blue = significantly downregulated in pGal-OVA, red = upregulated). **c)** Volcano plot displaying DEGs for OTII cells between pGal-OVA and OVA. **d)** As in (c), but color overlay indicates directionality in the prophylactic dataset (blue = significantly downregulated in prophylactic pGal-OVA and OVA, red = upregulated in prophylactic pGal-OVA and OVA). **e)** Canonical pathway analysis performed with IPA of OTI pGal-OVA vs OV. **f)** As in (e) for OTII cells. **g)** Upstream regulator analysis performed with IPA separately for OTI and OTII, comparing pGal-OVA vs OVA. **h)** Causal network analysis performed with IPA separately for OTI and OTII, comparing pGal-OVA vs OVA.

In conjunction with RNAseq following therapeutic treatment, we performed an analogous experiment in the prophylactic setting. Here, mice received adoptive transfer followed by antigen treatment (no challenge). SLO were harvested and pooled four days after treatment. OTI and OTII cells were separately isolated by FACS and subjected to RNA sequencing.

Figure 2.4 a shows the number of OTI and OTII cells recovered by FACS in the therapeutic setting. Here, treatment with OVA led to a significant increase in cell recovery of both OTI&II compared to saline, while pGal-OVA was not different than saline, indicating suppression of cell proliferation when antigen was delivered via pGal. Quantification of prophylactic recovery can be found in **Supplemental Figure 2.4.1 a**, where pGal-OVA shows a (transient) increase in OTII cells.

Differentially expressed genes (DEGs) between pGal-OVA and OVA in the therapeutic setting are displayed using a volcano plot for OTI cells in **Figure 2.4 b**. Genes upregulated in pGal-OVA treated cells compared to cells experiencing plain OVA are shown in red, while downregulated genes are shown in blue. **Figure 2.4 c** displays DEGs for OTII cells in pGal-OVA versus OVA. In both cell compartments, we see a somewhat mixed pattern of pro- and anti-inflammatory associated markers. For example, in OTI

cells we see upregulation of Tgfbr3, and downregulation of Tbx21, integrins, and granzymes; but also upregulation of Il7r and Ccr8, with downregulation of Havcr2 (TIM3) and Il10r. Many fewer DEGs between pGal-OVA and OVA were detected in OTII cells.

In an effort to understand the different transcriptional programs involved in the endogenous suppression of naïve or memory T cells, we overlayed prophylactic DEGs onto the therapeutic volcano plots. **Figure 2.4 d** is the same plot as in (c), but the colors represent directionality of those genes in the prophylactic data set. For example, Bmyc is upregulated with pGal-OVA treatment in the therapeutic setting, but it is significantly downregulated in the prophylactic OTII comparison of pGal-OVA versus OVA. Genes of opposite directionality are highlighted in yellow. Alternatively, Neurl3 is significantly upregulated in both settings and remains colored red. The other comparison overlays are included in **Supplemental Figure 2.4.1 b-f**. Unfortunately, there were no significant DEGs detected in OTI cells between pGal-OVA and OVA in the prophylactic setting. This was likely due to high noise in the prophylactic biological samples, as each of those replicates was a pool of three mice due to technical limitations. We subsequently improved our technique and achieved single-mouse samples for the therapeutic setting.

Using Ingenuity Pathway Analysis (IPA), we performed canonical pathway analyses separately for OTI and OTII cells in the therapeutic setting for pGal-OVA versus OVA (**Figure 2.4 e,f**). This revealed an understandable downregulation of integrin signaling, CD28 signaling, and IL-15 signaling, along with an upregulation of PD-1 signaling and apoptosis in OTI cells. However, we also detected some counterintuitive

results such as reduced T cell exhaustion signaling. For OTII cells, we detected a decrease in IL-6 signaling and an increase in T cell exhaustion and PD-1 signaling.

IPA was used to identify upstream regulators from the transcriptional data (**Figure 2.4 g**). In OTI cells, TP53-regulated pathways were inhibited, while pathways involving KLF3, TCF7, and MYC were induced. In OTII cells, beta-estradiol and TCR-regulated pathways were inferred to be inhibited, while those of KLF3 and TCF7 were induced as in OTI cells.

Further analysis was performed using IPA to identify causal networks (**Figure 2.4 f**). In OTI cells, activation of the co-inhibitory ligand CD276 (B7-H3) was inferred to be the most important causal network that could drive the observed transcriptional programs. Inhibition of the co-activating ligand CD28 was inferred to be the most important causal network for OTII cells. While each cell type has a unique identified causal factor, both involve inhibitory context at the synapse for tolerogenic T cell re-education.

2.3.5 Effects of PD-1 blockade or IL-10 depletion during antigen-mediated suppression of CFA/IFA recall response in transgenic T cells

Transcriptional analysis revealed an important role for co-inhibitory ligands in the T cell programming imparted by pGal-OVA treatment. We chose to focus on PD-1 as a canonical co-inhibitory ligand. The experimental design from Figure 2.1 was repeated, but with the addition of blocking antibodies against PD-1 given throughout the treatment regimen. We also included a group of mice that received IL-10 depletion antibodies, in

attempt to interrogate the contribution of soluble factors to pGal-mediated therapeutic tolerance. Saline and pGal-OVA plus IgG isotype control were included as separate control groups. An additional difference to the timeline shown in Figure 2.1 (a) is the time between primary immunization and first treatment: here we waited three months, as compared to one month in the previous experiment. This was not originally planned but was forced by lab closure due to COVID-19. Having the mice sit in their cages for this extended period of time did grant the advantage of a more stable immune environment upon manipulation with antibodies and antigen treatment.

The quantification of cell recovery at endpoint is shown in **Figure 2.5 a** as a percent of parent population, and in **Figure 2.5 b** as total cell number. Comparing saline and pGal-OVA+IgG isotype control groups confirmed our previous observations of a reduction in cell recovery with pGal-OVA treatment. Interestingly, while pGal-OVA+αIL-10 and pGal-OVA+IgG isotype control groups appeared similar in their overall level of cell recovery, pGal-OVA+αPD-1 exhibited an average level of cell recovery more like that of saline treatment. This defect in suppression of recall magnitude was more pronounced in the OTII compartment, although it was not completely penetrant in all mice. These results suggested that PD-1 signaling is partially required for pGal-mediated tolerance in a therapeutic setting, while IL-10 is dispensable.

Levels of TCR and CD45 expression are shown in **Figure 2.5 c** and **d**, respectively. While the effect of IL-10 depletion during pGal-OVA treatment was similar to isotype control, there were some unique features in the αIL-10 group, such as low CD45 expression in dLN OTIIs. The frequency of TOX expression in OTI cells is shown **Figure**

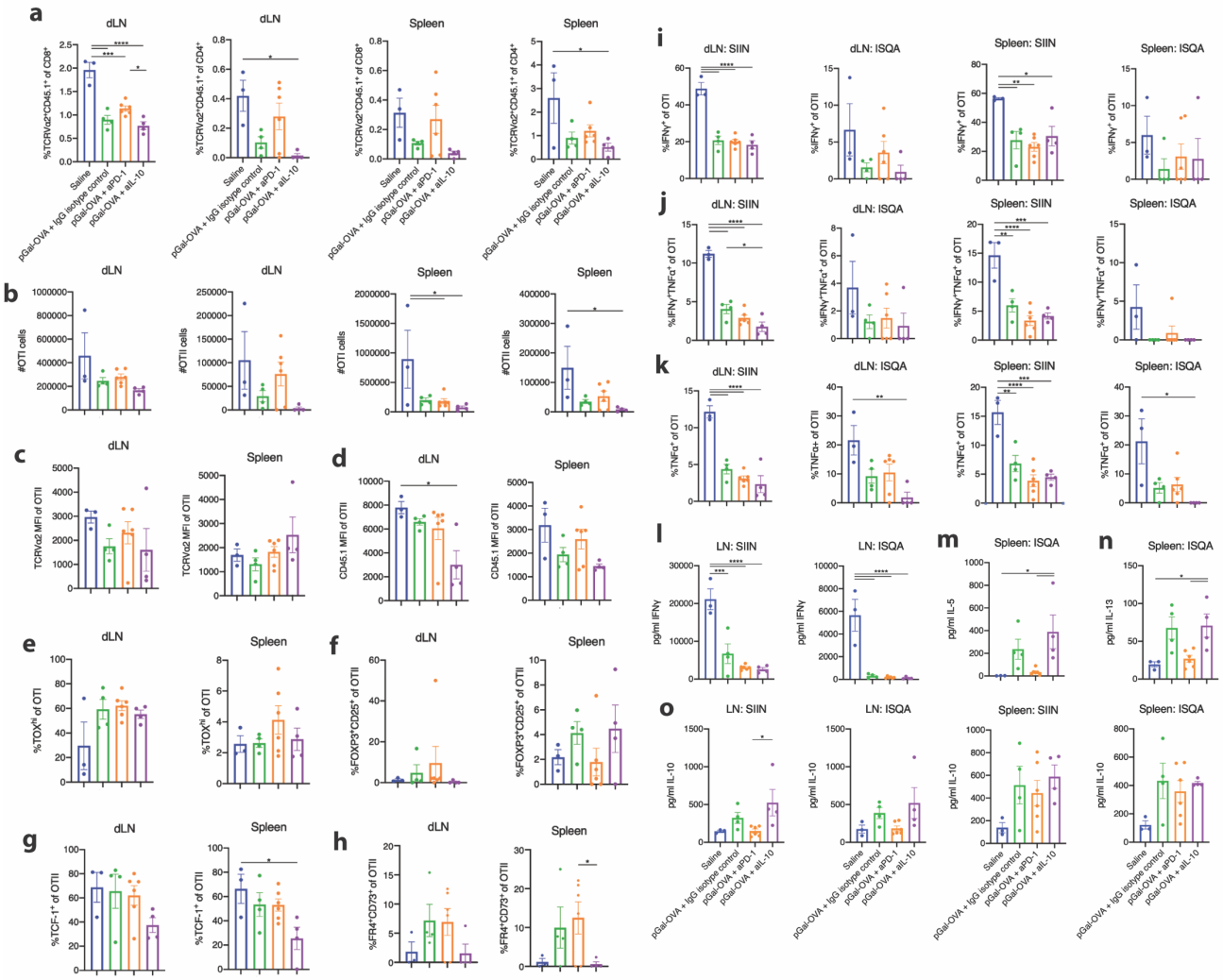

Figure 2.5 | Effects of PD-1 blockade or IL-10 depletion during antigen-mediated suppression of CFA/IFA recall response in transgenic T cells. Identical experimental setup as Figure 2.1, but pGal-OVA treatment was administered under conditions of antibody manipulation. Mice received either 100μg αPD-1, 1mg αIL-10, or 1mg IgG isotype control i.p. every four days across the antigen treatment (**Figure 2.5 continued**) window. **a)** Percent recovery of OTI and OTII cells in dLN and spleens as a proportion of parent population. **b)** Total OTI&II cell numbers recovered. **c,d)** Median fluorescence intensity of the indicated markers on the y-axes in recovered OTI&II cells. **e-h)** Expression frequencies of the specified protein markers as indicated on recovered OTI&II cells from SLO. **i-k)** Six-hour ex vivo antigen restimulations were performed with recovered lymphocytes and peptides as indicated above each graph, and intracellular flow cytometry was used to detect production of the indicated cytokines in OTI&II cells. **l-o)** Three-day restimulations were also carried out for ELISA-based analyses of the indicated cytokines in culture supernatants. All statistical comparisons were performed by one-way ANOVA using Tukey correction.

2.5 e, and Treg frequency is shown in **Figure 2.5 f.** No statistically significant differences were found across these parameters. The expression of transcription factor TCF-1 in OTII cells was lowest in the αIL-10 group (**Figure 2.5 g**). Induction of anergy markers was most similar between pGal-OVA + isotype IgG and αPD-1 groups, while saline and αIL-10 groups did not exhibit expression (**Figure 2.5 h**).

OVA peptide restimulation was performed with recovered lymphocytes. Given the increased recovery with PD-1 blockade, we were surprised to find that intracellular flow cytometry of six-hour restims revealed no obvious differences amongst the various pGal-OVA treatment groups with regards to IFNγ and TNFα, which were all lower than saline (**Figure 2.5 i-k**). Analysis of three-day restim supernatants by ELISA produced a similar pattern as seen by flow for IFNγ (**Figure 2.5 l**).

We decided to look for other ways in which our manipulations of IL-10 or PD-1 axes during treatment could have affected cellular programming. Analysis of the T_H2 cytokines IL-5 and IL-13 in the three-day restim supernatant elucidated a pattern of induction in the isotype and αIL-10 pGal-OVA conditions, while αPD-1 mirrored saline with a paucity of these cytokines (**Figure 2.5 m,n**). Production of IL-10 in the dLN mirrored the pattern of IL-5 and -13 to some extent, but in the spleen there was no differences across the pGal-OVA treatment groups (**Figure 2.5 o**).

Taken together, the results from this experiment indicate that PD-1 engagement is partially required for reduction of cell magnitude but does not affect the activity of cells instigated by recall challenge with IFA. Furthermore, IL-10 depletion may aid the type 2 skewing of CFA-induced memory T cells away from pathogenic T_H1 and T_H17 programs.

2.3.6 Therapeutic suppression of relapsing-remitting experimental autoimmune encephalomyelitis

Our attempt at a rigorous estimate of the potential for pGal-mediated AIT to suppress established immunity gave us confidence to go forward with a mouse model of human disease. Experimental autoimmune encephalomyelitis (EAE) is a murine model for multiple sclerosis. The basic approach involves s.c. immunization of mice in the back with a myelin peptide, such as MOG or PLP emulsified in CFA, which drives an autoimmune attack against the myelin sheath of the CNS ultimately resulting in paralysis. On the day of immunization and two days later, pertussis toxin (PTX) can be administered intraperitoneally (i.p.) to help destabilize the blood brain barrier and allow activated T cells easier access to their targets.

Onset of paralysis occurs about a week after immunization and is measured using a clinical score rubric. Symptoms begin with tail drooping (score of 1) and progress through minor motor defects (score of 2) into severe rear leg paralysis (score of 3), with possible front leg impairment as well (score of 4). Mice are euthanized if the severity of their paralysis prevents access to food or water.

Two different EAE models are commonly used, presenting either a chronic or a relapsing-remitting (R/R) disease course. The chronic model is generated using the MOG antigen in B6 mice, while the R/R model uses the PLP antigen in SJL mice. The causative mechanisms for the different disease courses are not well understood. Here, we employed the R/R model because it offers a therapeutic window after the primary wave of disease remits, and before the relapse phase begins.

Here, mice were immunized and the first wave of paralysis was allowed to occur. Upon remission, when mice begin to show improvement in their motor functionality, we began treatment regimens including plain PLP peptide, pGal-PLP, fingolimod (FTY720, used clinically), or saline as negative control. Mice receiving antigen therapy or saline were given three doses total, each three days apart, while FTY720 was given daily via oral delivery for three weeks.

The disease courses are plotted in F**igure 2.6 a**. Astoundingly, pGal-PLP treatment was able to prevent relapse and maintain motor function throughout the remainder of our 50-day study, whereas plain PLP treatment prolonged the remission phase by only one week. FTY720 was able suppress disease as long as it was applied, after which a dramatic relapse was observed as lymphocytes were able to reacquire their targets. Statistical comparisons were performed using area under the curve (AUC) analysis beginning either one week after the last antigen treatment, or one week after ceasing FTY720 treatment, separately. AUC after AIT revealed a significant difference between pGal-PLP treatment and treatment with either PLP or saline. Endpoint scores were also compared, illuminating significant differences between pGal-PLP and saline as well as FTY720.

Mouse weight was measured periodically during the experiment, as shown in **Figure 2.6 b**. AUC analysis one week after the last antigen dose found a significant difference between pGal-PLP treatment and treatment with FTY720 or saline. Endpoint analysis revealed the FTY720 group having the lowest weight compared to all other groups, while pGal-OVA was significantly higher than saline.

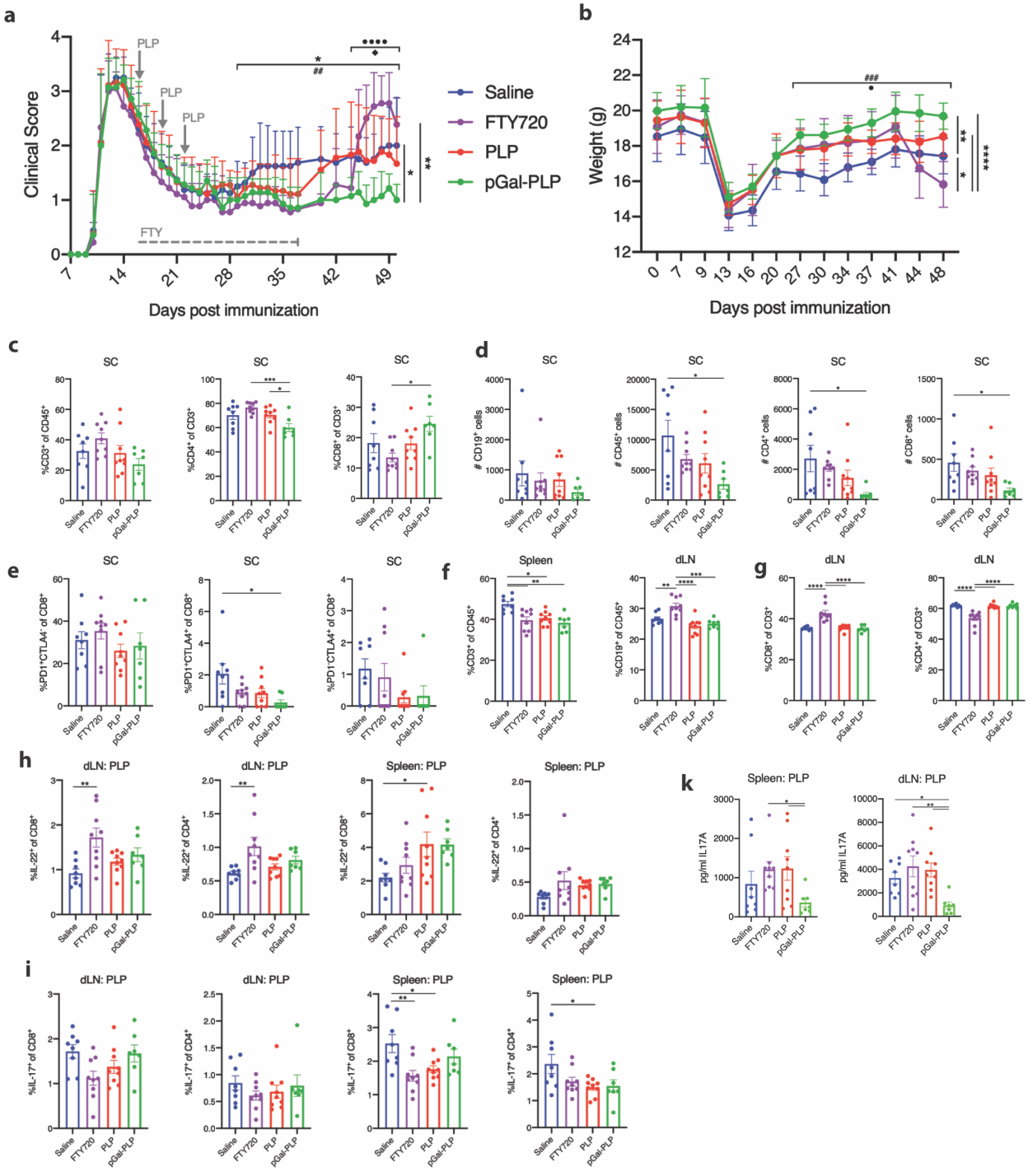

Figure 2.6 | Therapeutic suppression of relapsing-remitting experimental autoimmune encephalomyelitis. RR-EAE was induced on day 0 and followed with two 100µg PTX doses i.p. **a)** Disease course was measured by clinical scoring of paralysis severity; treatments are indicated using gray arrows for single antigen doses and gray dashed line for continuous daily therapy. Horizontal bars atop the graph indicate significant differences via AUC as follows: * = pGal-PLP vs PLP, # = pGal-PLP vs Saline. Vertical bars at the endpoint indicate significant differences via Tukey-corrected ANOVA as follows: • = pGal-PLP vs FTY720,◆ = PLP vs FTY720. **b)** Mouse weight measurements, statistical comparisons performed as in (a). **c)** Quantification of T cell infiltrates in the spinal column at the experimental endpoint as frequencies of parent population

(**Figure 2.6 continued**) indicated on the y-axes. **d)** Quantification of cells as in (c) but reporting total cell numbers recorded by flow cytometry. **e**) Frequency of $CD8^+$ T cells in the SC expressing PD-1 and CTLA4 as indicated. **f)** Quantification of cell recovery in the spleen and dLN as a percentage of parent population. **h,i)** Six-hour ex vivo antigen restimulations were performed as indicated and intracellular flow cytometry was used to detect production of the indicated cytokines in $CD8^+$ and $CD4^+$ T cells. **k)** Three-day restimulations were carried out for analysis of IL-17A production in culture supernatants. All statistical comparisons were performed by one-way ANOVA using Tukey correction unless otherwise indicated.

Mice were euthanized at the experimental endpoint where a lumbar spinal column (SC), spleens, and a subset of spinal dLNs were collected. Lymphocytes were analyzed by flow cytometry. **Figure 2.6 c** shows the quantification of T cells in the SC as a percentage of indicated parent population, and **Figure 2.6 d** shows total cell numbers. pGal-PLP led to the lowest level of SC lymphocyte infiltration at the time of collection, predominated by a loss in the CD4 compartment. Again, a stair-step pattern is observed whereby saline treatment leads to the highest level of cellular response, plain antigen (PLP) leads to a moderate level of reduction, and pGal-antigen therapy drives the lowest level of lymphocyte number.

Assessment of SC T cell co-inhibitory marker expression was performed with PD-1 and CTLA4, as shown in **Figure 2.6 e**. pGal-PLP was associated with the lowest frequencies of these marker subsets. Examination of bulk T and B cell populations in SLO revealed a dominance for T cells in the spleen of saline treated mice, and a dominance of B cells in the dLN of FTY720 mice at the time of collection (**Figure 2.6 f**). **Figure 2.6 g** shows the relative frequencies of CD8 and CD4 populations in the dLN.

Lymphocytes from the dLN and spleen were restimulated with PLP peptide for six hours or three days and analyzed by intracellular flow cytometry or ELISA, respectively. The frequency of T cells producing the pathological cytokines IL-22 or IL-17A as detected

by flow are shown in **Figure 2.6 h and i**. The FTY720 treatment group had an induction of IL-22 alongside a reduction in IL-17 compared to saline. Importantly, while pGal-PLP did not show evidence of cytokine suppression in the short term restimulation, analysis of the long term restim clearly demonstrated a reduction of IL-17A production in mice treated with pGal-PLP compared to all other groups (**Figure 2.6 k**).

The diminishment of CNS-infiltrating lymphocytes along with the impairment in IL-17A production elucidate how pGal was able to improve the disease course. By tolerizing the circulating T cells specific for PLP, we were able to prevent relapse while maintaining an otherwise fully competent repertoire able to maintain proper immune functionality. The lasting tolerance observed here after just a few doses of pGal-antigen is an enticing avenue for clinical application, as compared to the transient protection mediated by FTY720.

2.4 Discussion

AIT has been in practice for decades, but traditional approaches fail to reach a level of effectiveness required for application beyond a limited range of allergens, such as in the case of drug hypersensitivity or autoimmunity. Here we have advanced the development of pGal as a novel antigen engineering approach for immunotherapy. We demonstrated intervention of T cell immunity in multiple immunization models and suppression of previously established disease with pGal-antigen therapy. Furthermore, we explored the underlying biology of therapeutic tolerance mediated by pGal to discover a

myriad of tolerized phenotypes involving induction of apoptosis, hyporesponsiveness, and possible T_H2 skewing, predominantly mediated by co-inhibitory ligand signaling.

When I first set out to evaluate pGal in a therapeutic setting, we had little experience in our lab with attempting suppression of established immunity. The establishment of viable adjuvants for the interrogation of memory intervention was an important first step (Supplemental Figure 2.3.1.2). These early results showed clear suppression of recall responses in pGal-OVA treated mice, with distinct differences across adjuvants. While using a weaker adjuvant would test for sensitivity of T cell immunity after tolerance, a strong adjuvant would test for durability of tolerance – we wanted a balance of the two. For example, CpG seemed the least amenable to impact via pGal-antigen therapy, so we did not pursue it further. We then performed a separate pilot experiment (data not shown) using a CFA/IFA adjuvant regimen to test suppression with plain OVA treatment, which suggested there was sufficient dynamic range to demonstrate improvement with pGal-antigen conjugation in this setting.

Results from Figure 2.1 indicated an improvement in therapeutic tolerance induction with pGal-antigen therapy compared to plain antigen alone. Our primary readout was a reduction of cell recovery upon secondary challenge. We reasoned this readout would be reflective of the remaining inflammatory potential of antigen-specific cells, since induction of apoptosis, anergy, exhaustion, Treg, etc. would contribute to an overall weaker recall response. Phenotypic analysis revealed an induction of exhausted and anergized populations of OTI and OTII with pGal-OVA treatment compared to saline, although OVA induced similar levels of exhaustion. Impairment of cytokine

production was observed in cells isolated from pGal-treated mice, particularly TNFα in this setting. Specific suppression of TNFα, rather than IFNγ, has been reported to be indicative of exhaustive fate.[72]

Although the differences between OVA and pGal-OVA were not consistently different via statistical analyses, there was a repeated observable stair-step pattern whereby saline exhibited the strongest recall response as expected, then OVA showed minor impairment of immunity, and finally pGal-OVA had the lowest recall response. This pattern was also evident in the expression of CTLA4, albeit in reverse. The induction of co-inhibitory markers such as PD-1 or CTLA4 can be negative-feedback mechanisms implemented by over-activation.[73] Thus it can be difficult to interpret whether high expression of these markers is representative of a tolerized, hyporesponsive population or instead of a highly activated population. In the case of PD-1, we co-stained for the exhaustion-associated transcription factor TOX, known to increase surface levels of PD-1 expression of tumor-infiltrating $CD8^+$ T cells.[74] The induction of TOX and PD-1 therefore gave strong evidence for exhaustion, and we can interpret the low level of CTLA4 expression on OTII cells the experienced with pGal-OVA as indication that these cells did not experience the same level of activation as saline or plain OVA treatment.

Comparing our results of therapeutic intervention with Scott's prophylactic data reveals some differences between these two settings. Our primary readout of cell magnitude was importantly conserved, but only in some cases of therapeutic intervention could we achieve complete suppression of recall response and ablation of cognate T cells. Such a limitation in the therapeutic context was somewhat expected due to the

established T cell immunity. In a prophylactic setting pGal was found to induce Treg programming in OTII cells, and furthermore that pGal-induced tolerance could be ablated with αCD25. We did not find strong evidence for Treg programming with pGal-antigen therapy in a therapeutic context. Treg induction of naïve T cells is a well-established feature of the adaptive immune system, but conversion of a proinflammatory $CD4^+$ T cell into a Treg is more complicated due to the presence of canonical T_H transcription factors. Fate mapping experiments have shown conversion of T_H17 into Treg, so while conversion may be a theoretical possibility we did not generate sufficient evidence to demonstrate this convincingly with pGal-antigen therapy.[75] We were able to show induction of exhaustion and anergy associated markers, as well as reduced cytokine production upon ex vivo restimulation. While we could not ablate the cognate cellular compartment, we could reduce it and suppress activity in the remaining cells.

Using OTI and OTII cells provided a key advantage of tracking antigen specific $CD8^+$ and $CD4^+$ T cells, but demonstration of tolerance induction in an endogenous repertoire was important to validate the biology we observed in our transgenic T cell models. Using LmOVA and H2Kb:SIINFEKL pentamers, we were able to induce and track a bona fide population of memory $CD8^+$ T cells. Here again we were able to show evidence of improved tolerance induction with pGal-antigen therapy. The observed inhibition of endogenous immunity supported the general outcome from our transgenic experiments. Unfortunately, due to a limitation of effective class-II tetramer reagents for OVA, we did not track endogenous $CD4^+$ T cells.

Our transcriptional analysis of OTI&II cells four days after therapeutic dose provided insight into the underlying mechanisms that could be driving pGal-mediated tolerance. FACS isolation of OT cells recovered a greater number in plain antigen treated mice, suggesting that pGal-mediated p:MHC encounter did not facilitate lasting cellular expansion. Further evidence of a tolerogenic encounter was found in the gene and pathway analyses that revealed a decrease in integrin signaling and proinflammatory molecules, with an increase in co-inhibitory ligand signaling. Inferred upstream regulators and causal networks pointed towards programs of T cell quiescence and co-inhibitory ligands as master regulators in differences observed between pGal-OVA and plain OVA. Comparisons between therapeutic and prophylactic gene sets revealed similar and contrasting effects across the two settings.

Equipped with the knowledge of potential mechanisms, we attempted to interfere with pGal-mediated therapeutic tolerance induction. PD-1 blockade is a common tool used in cancer biology and was readily available in the lab. IL-10 is considered an important cytokine in the immunosuppressive hepatic environment, but we hypothesized that co-inhibitory ligands were the primary means by which tolerance was imposed on T cells. Including IL-10 depletion alongside PD-1 blockade provided an interesting comparison in the end, since their effects contrasted quite boldly. While PD-1 signaling proved to be important in tolerance induction, the absence of IL-10 seemed to possibly benefit AIT. Furthermore, the induction of T_H2 cytokines in the IgG isotype and αIL-10 groups corresponded to their patterns of cellular inhibition. IL-10 is widely considered an immunosuppressive cytokine, but it is pleotropic and there is evidence that it can

mediate proinflammation. For example, IL-10 neutralization has displayed therapeutic efficacy in lupus patients.[76] It's difficult to speculate on how the presence of IL-10 could impair tolerance induction, but perhaps it inhibits a signaling feedback loop that would normally help drive induction of apoptosis or exhaustion.

Scott also demonstrated reliance upon TGFβ during prophylactic treatment, where its depletion severely crippled tolerance induction. Relatedly, past work on ERY1 demonstrated reliance upon the PD-1 and CTLA4 pathways for tolerance induction, where blocking these receptors prevented tolerance induction as follows: CTLA4 blockade alone caused minor defects in tolerance induction, PD-1 blockade caused major defects, and co-blockade abrogated tolerance entirely. Taken together, these data support our results using PD-1 blockade during therapeutic treatment and suggest there may be additional mechanisms required for therapeutic tolerance induction than we tested here.

The RR-EAE model gave us the opportunity to test pGal-antigen immunotherapy in a clinically relevant disease model. Surprisingly, we were able to prevent relapse with pGal-antigen therapy, while plain antigen alone could only delay relapse. Improved weight retention, reduction in SC cellular infiltrates, as well as systemic inhibition of IL-17 production in PLP-reactive lymphocytes corroborated our clinical scores and described underlying features of pGal-antigen therapy that likely contributed to the observed protection from disease. The ability of pGal to mediate therapeutic intervention in RR-EAE is the first example of successful AIT in this model, as far as we are aware, without the aid of immunoregulatory molecules like rapamycin. Here, we co-opt endogenous peripheral tolerance networks for suppression of the antigen-specific population.

Because i.v. pGal-antigen delivery can theoretically only affect circulating lymphocytes that pass through the liver, a potential weakness in this approach is the inability to directly tolerize tissue-resident lymphocytes. We performed a separate tolerance experiment in a model of airway inflammation, whereafter establishment of immunity the pathogenic cells do not circulate (data not shown). Under these conditions, pGal-antigen therapy looked similar to saline, while OVA treatment exacerbated immunity. We interpret these results to indicate that pGal-antigen did not affect the cognate T cell repertoire resident in the lung at the time of treatment, while plain OVA was encountered by the target lymphocytes in a proinflammatory manner. Future work in the lab along these lines aims to utilize s.c. administration of tolerogenic constructs in the affected tissue area. Our success in RR-EAE suggests that we are able to impact tissue-specific immunity, but without clear induction of dominant regulatory cells the ability to suppress diseases mediated predominantly by tissue-resident immunity is somewhat questionable. Ongoing clinical trials in celiac disease will be a good test for the ability of pGal-antigen therapy to suppress tissue-resident immunity.

Targeting hepatic APCs for AIT drives effective tolerance induction in cognate T cells but pinpointing a specific mechanism responsible for pGal's efficacy is difficult. In a prophylactic setting, depletion of TGFβ during treatment or depletion of CD25+ cells after treatment prevented tolerance induction against antigen challenge. In a therapeutic setting, blocking PD1 during treatment prevented tolerance induction, while depletion of IL-10 during treatment did not. Our transcriptional analysis revealed an importance for co-inhibitory ligands; specifically in the therapeutic setting we identified CD276 as a

causal factor in driving OTII cell tolerance. Together, these data illustrate a complex, multifaceted biology whereby T cells are (re)educated via immune context at the immunological synapse between T cell and APC. Our studies are not comprehensive enough to ascertain the full network of signals involved in our model of tolerance induction. For example, further studies should repeat our experiment utilizing PD1 blockade during therapeutic tolerance induction with a myriad of blocking antibodies against other co-inhibitory ligands alone and in combination. Co-blockade of PD1 and CTLA4 could yield a more complete level of tolerance inhibition, compared to the partial effect we saw with PD1 alone. Blockade of other co-inhibitory molecules such as Lag3 would be required to illuminate the full landscape of contributing ligands. A similar approach would be useful for confirming the network of soluble factors at play, for example confirming if TGFβ is relevant in a therapeutic context as it is in prophylactic. Ultimately, in a therapeutic context, pGal seems to force T cells to receive inhibitory signals alongside antigen recognition from the synapse and surrounding milieu, which then suppresses activation and drives a hyporesponsive fate. Comparatively, antigen therapy without pGal modification drives proliferation of memory T cells and incomplete hyporesponsiveness. Upon secondary rechallenge, the lasting tolerance imparted by pGal-antigen therapy prevents activation of cognate T cells and ultimately cripples the antigen specific immune response of interest.

2.5 Methods

2.5.1 Mice

Mice were maintained in a specific pathogen-free facility at the University of Chicago. The experiments and procedures in this study were performed in accordance with the Institutional Animal Care and Use Committee. 9 to 10 week-old female C57BL/6 mice were purchased from The Jackson Laboratory and used as wild type mice in all studies unless otherwise indicated. OT-I (stock no: 003831) and OT-II (stock no: 004194) were crossed to CD45.1 mice (stock no: 002014) to yield congenically labeled OT-I and OT-II.

2.5.2 Transgenic T cell adoptive transfer

Spleens and lymph nodes (axillary, brachial, inguinal, and popliteal) were isolated from TCR transgenic mice. OTI and OTII T cells were isolated by negative magnetic bead selection using a CD8 and CD4 (Stemcell) negative selection kit, respectively. Cell purity was assessed by flow cytometry. Indicated numbers of OT-I and OT-II cells in DMEM were injected through the tail vein.

2.5.3 Subcutaneous immunization to OVA

All OVA challenges consisted of 20 μg EndoFit OVA (Sigma) mixed with the indicated adjuvant, distributed evenly across each forelimb injection into the hock while mice were anesthetized with isofluorane. CFA/IFA (Sigma) emulsifications were each prepared as 1:1 mixture with antigen from stock solutions (final 0.5 mg/ml), 10μltotal injection volume per hock, vortexed immediately upon addition of adjuvant for 1 hour. R848 (Sigma) and CpG-B ODN 1826 (InvivoGen) were prepared with 20ug per mouse, 25μlinjection volume.

2.5.4 pGal antigen constructs

A detailed explanation of the synthesis of the pGal polymer, linker, and intermediates is provided in the supplementary methods of our previous publication.[65]

2.5.5 Antibody affinity measurements

SPR measurements were made using a Biacore X100 SPR system (Cytiva). At the beginning of each cycle, 2 μg mL^{-1} anti-OVA antibody (Abcam) in running buffer (0.01 M HEPES pH 7.4, 0.15 M NaCl, 0.005% v/v Surfactant P20) was flowed over a Protein A coated sensor chip (Cytiva) at a flowrate of 5 μl min^{-1} for 780 seconds, resulting in ~700-1100 resonance units corresponding to ligand coating. pGal-OVA or native OVA protein was then flowed at decreasing concentrations (ranging from 250 nM to 7.8125 nM) in running buffer for contact time of 180 seconds at 30 μl min^{-1}, followed by running buffer for a dissociation time of 300 seconds. At the end of each cycle, the sensor chip surface was regenerated with two 30-second pulses of 10 mM glycine pH 1.5 at 30 μl min^{-1}. Specific binding of pGal-OVA and OVA to the anti-OVA antibody was calculated by comparison to a non-functionalized channel used as a reference and blank subtraction. The experimental results were fitted with Langmuir binding kinetics using the BIAevaluation software (Cytiva, version 2.0.2).

2.5.6 Tissue Processing

Draining lymph nodes (axillary, brachial, inguinal, and popliteal), spleen, or spinal column were isolated from mice and kept on ice in DMEM until processing. Lymph nodes

were mechanically disrupted and digested at 37°C for 45 min in collagenase D. Digested lymph nodes, spleens, or spinal columns were processed into single-cell suspensions via mechanical disruption and passage through a sterile 70 μm screen. Red blood cells in splenocyte suspensions were lysed by resuspending in ACK lysing buffer (Gibco) and incubating for 5 min at room temperature. Lysis reaction was quenched using 15 mL DMEM + 10% FBS. The single cell suspensions were then washed once with DMEM and resuspended in IMDM + 10% FBS + 1% pen/strep. These single cell suspensions were then used in restimulation experiments or directly stained for flow cytometry analysis.

2.5.7 Antibody titer ELISA

ELISA plates (Nunc Maxisorp, ThermoFisher) were coated overnight with 10 μg/mL OVA. Blood was collected in a heparinized capillary tube per IACUC protocol. Blood was spun down at 700g for 7 minutes to pellet erythrocytes, and plasma was collected. Plasma was diluted in PBS. After washing and blocking plates coated with OVA, diluted plasma was added for 2 hours at room temperature and washed. Antibodies were detected using an HRP-conjugated anti-mouse IgG antibody for one hour at room temperature diluted in 2% BSA (Southern Biotech). TMB solution was added, and 10% sulfuric acid to stop the reaction. Titers were calculated using a background level of two-fold the average optical density (OD) readings of two blank wells. The reciprocal of the last dilution with detectable signal is the titer plotted.

2.5.8 Ex vivo restimulation

Single-cell suspensions from spleen or lymph nodes were prepared as described above. 1-2 million cells from spleen or lymph node were restimulated in vitro with the addition of peptide epitopes as described: PLP-SH (HCLGKWLGHPDKFGGSGCRG) 10.0 µg/mL, OVA MHC class I (SIINFEKL) and MHC class II (ISQAVHAAHAEINEAGR) 2.0 µg/mL (Genscript). For ELISA analysis, following a 72hr restimulation cells are spun down and supernatant collected for the measurement of secreted cytokines. Cytokine ELISAs were performed using the Ready-Set-Go Kit (eBioscience), according to manufacturer's protocol. An unstimulated (no peptide added) control well to determine background levels of non-specific activation. For flow cytometric analysis, cells were restimulated with peptide for 6 hrs total. Cytokines were retained intracellularly via addition of GolgiPlug and GolgiFix (BD) for final 4hrs of restimulation. Following 6hr restimulation, cells were immediately washed and stained for flow cytometry analysis.

2.5.9 Cytokine ELISA

3-day restimulations were removed from incubation and put on ice for 20 min, followed by centrifugation at 2000g for 5 min. Supernatants were removed via pipetting and stored at -20 degrees Celsius until cytokine ELISAs were performed. Culture supernatants were assessed for IFNγ, TNFα, IL-17A using ELISA, Ready-Set-Go Kit (eBioscience), following the manufacturer's instructions. Culture supernatants were also measured using the LEGENDplex (BioLegend) T_H cytokine multi-analyte kit, following the manufacturer's instructions.

2.5.10 Flow cytometry

For phenotypic analysis, 2-4x106 cells were stained in PBS with 1:200 CD16/CD32 Fc Block (Biolegend) and 1:500 Live/Dead fixable dye (ThermoFisher) at 4°C for 15 minutes. Cells were washed in PBS + 2% FBS. Cells were stained with 1:200 surface antibodies at 4°C for 20 minutes. Cells were washed in PBS + 2% FBS and fixed in 2% paraformaldehyde. For intracellular staining, cells were fixed and permeabilized using Cytofix/Cytoperm (BD Biosciences) at 4°C for 20 minutes, and cells stained intracellularly in Perm Wash Buffer (Biolegend) with 1:200 antibodies at 4°C for 30 minutes. For transcription factor stain, FoxP3 Transcription Factor Kit (eBioscience) was used per manufactures protocol, and nuclear stains were applied for 1 hour at 4°C. Tetramer staining was conducted after Live/Dead staining. Tetramers were first spun down at 4000g for 5 minutes, and then incubated with cells for 1 hr at room temperature. H2-Kb-SIINFEKL pentamer was purchased from ProImmune and used at a final dilution of 1:10. After tetramer stain, cells were washed and surface stain performed as described above.

2.5.11 Listeria inoculation

An attenuated Listeria strain (ΔactA) encoding for OVA antigen (Lm-OVA) was used for investigating endogenous CD8 memory. The characterized generation time is about 40 min, where an OD of 0.1 corresponds to $1x10^8$ CFU/mL. The day before inoculation, Lm-OVA was put in culture in 5 mL of BHI broth (DIFCO cat 237500) with 10 µg/mL chloramphenicol antibiotic, at 37 °C with shaking. The morning of inoculation, the starter culture was diluted 20-fold in BHI broth and shaken at 37 °C for a further 3 h. The OD

was measured at 600 nm and, using the growth curve, the total amount required to inoculate mice at 10^8 CFU in a volume of 100 µL for each mouse was calculated and measured out. Mice received an i.v. injection of 10^8 CFU of Lm-OVA, via the tail vein. The exact inoculation dose was confirmed by preparing serial dilutions of the injected dose in BHI broth, plating on BHI-chloramphenicol plates and counting the number of Lm-OVA colonies 36 h later. At the experimental endpoint, well after clearing the infection, mice were sacrificed and the spleens and forelimb dLNs (axillary, brachial, inguinal, popliteal) were isolated in a BSL2 facility. Spleens and LNs were processed as previously described.

2.5.12 RNAseq data collection

For the prophylactic setting, mice were adoptively transferred with 750k OTI and OTII each at day 0. At day 1, mice received saline, 5 µg pGal-OVA, or molar equivalent of plain OVA (Endograde). Four days later, mice were sacrificed and spleens and liver and peripheral lymph nodes were pooled. OT-I and OT-II were sorted into Trizol using fluorescence activated cell sorting (FACS) and frozen at -80°C. RNA was extracted (Qiagen, RNeasy Micro), and three mice were pooled per replicate. For the therapeutic setting, mice were adoptively transferred with 600k OTI and OTII cells at day 0. At day 1, mice received s.c. immunization with OVA in CFA. Four weeks later, mice received i.v. saline, 5µg pGal-OVA, or equimolar OVA. Four days later, mice were sacrificed and spleens and liver and peripheral draining lymph nodes were pooled. OT-I and OT-II were sorted into DMEM+10%FBS using FACS and put on ice, then spun down, decanted, and snap frozen in liquid nitrogen and stored at -80°C. RNA was extracted as above, using

each individual mouse per biological replicate. RNA integrity was measured by the Agilent 2100 Bioanalyzer. RNA was converted to cDNA using SmartSeq-v4 (Takara, cat no. R400752). Library was prepared using Nextera XT DNA library preparation kit (Illumina, cat no. FC-131-1096). For each setting, all samples were pooled and sequenced using Illumina HiSeq 4000 (2x100 paired end).

2.5.13 RNAseq analysis

Unless otherwise specified, all data analyses were performed under the R programming and software environment for statistical computing and graphics version 3.6 (R Core Team, 2019). FastQ file for each sample was assessed for quality using the FastQC tool (version 0.11.5). For mRNAseq, raw reads were aligned to the GRCh38 primary genome assembly using Spliced Transcripts Alignment to a Reference (STAR) aligner (version 2.7.2a) 1-pass algorithm.[77] After sorting the bam files in lexicographical order with the sambamba program (v0.5.4), we assigned the reads to exon features annotated in Ensembl Mus musculus GRCm38 annotation (release 97) using the FeatureCounts tool from the subread package (version 1.5.2) and summarized the read counts by genes. [78,79] The post alignment quality control was carried out with Picard tools (version 2.18.7). Specifically, we examined the QC data regarding the alignment summary, gene body coverage, read distribution, and ribosomal RNA depletion rate. We used alignment-free transcriptome quantification method kallisto (v0.46.1) to estimate the transcript abundance of each sample.[80] We then summarize the transcript-level estimates for gene-level analysis using R package tximport and GRCm38 annotation. After removing the

genes with zero read counts across all samples, we calculated the normalization factors to scale the raw library sizes using the calcNormFactors function in the edgeR R package with trimmed mean of M-values (TMM) option enabled.[81] The normalized count per million (CPM) value was log2-transformed for each gene. We removed heteroscedascity from the count data using the voomWithQualityWeights function from the limma package. We then fit a linear model for each gene using the limma algorithm, adjusted for any batch effects, and ranked the genes for differential expression using the empirical Bayes method. The differentially expressed genes were identified using the Benjamini-Hochberg procedure for multiple testing correction. The adjusted P-value threshold was set at 0.05. The Ingenuity Pathway Analysis Fall 2020 release (Qiagen) was used to identify canonical pathways, upstream regulators, and causal networks that related to significant differentially expressed genes in the pGal-OVA to OVA comparisons.

2.5.14 Antibody depletion experiments

Rat IgG2a Isotype control (Clone C1.182) antibody 1mg per injection were purchased from BioXCell. Rat anti-mouse PD-1 (Clone 29F.1A12, Bio X Cell) 100 µg per injection was used for coinhibitory ligand blockade and IL-10 (Clone JES5-2A5, Bio X Cell) 1mg per injection was used for depletion. Antibodies were administered every four days throughout the entire treatment window, starting two days prior to first antigen treatment dose.

2.5.15 EAE model

SJL/JCrHsd mice (Envigo) were vaccinated with $PLP_{139-151}$ (Hooke Labs) emulsified in complete Freud's adjuvant at each shoulder blade. 100µg PTX was administered i.p. day of vaccination and again two days later. Fifty days after vaccination, spleens were harvested, and single cell suspensions created. To enhance the encephalitogenic T cells, cells were restimulated with PLP-SH peptide (10 µg/mL) for 6 hours or 3 days. Three antigen doses of PLP-SH peptide or pGal conjugated to PLP-SH were administered i.v., schedule as indicated in the figure. As a positive control for maintaining EAE remission, FTY720 was orally administered every day as indicated in the figure. Mice were scored daily starting from day 7 until the experimental endpoint. Scoring was performed consistently with two overlapping researchers, blind to treatment or previous scores.

2.5.16 Statistical Analysis

Statistically significant differences between experimental groups were determined using Prism software (v9, GraphPad). All statistical analyses are stated specifically in the figure legends for all experiments. For most experiments, unless otherwise specified in figure legend, one-way ANOVA was performed with a Tukey's post-hoc test to correct for multiple comparisons. Comparisons were significant if $p < 0.05$. For showing statistical significance ***P≤0.001; **P≤0.01; *P≤0.05, unless otherwise stated. For all transgenic T cell experiments, mice exhibiting outliers for percent OTI or OTII recovery in the dLN calculated as 1.5-fold outside the upper or lower quartiles were removed from all analyses.

For the RNA-seq experiment, a detailed description of the statistical analysis can be found in Methods.

2.6 Appendix A: Supplementary Figures

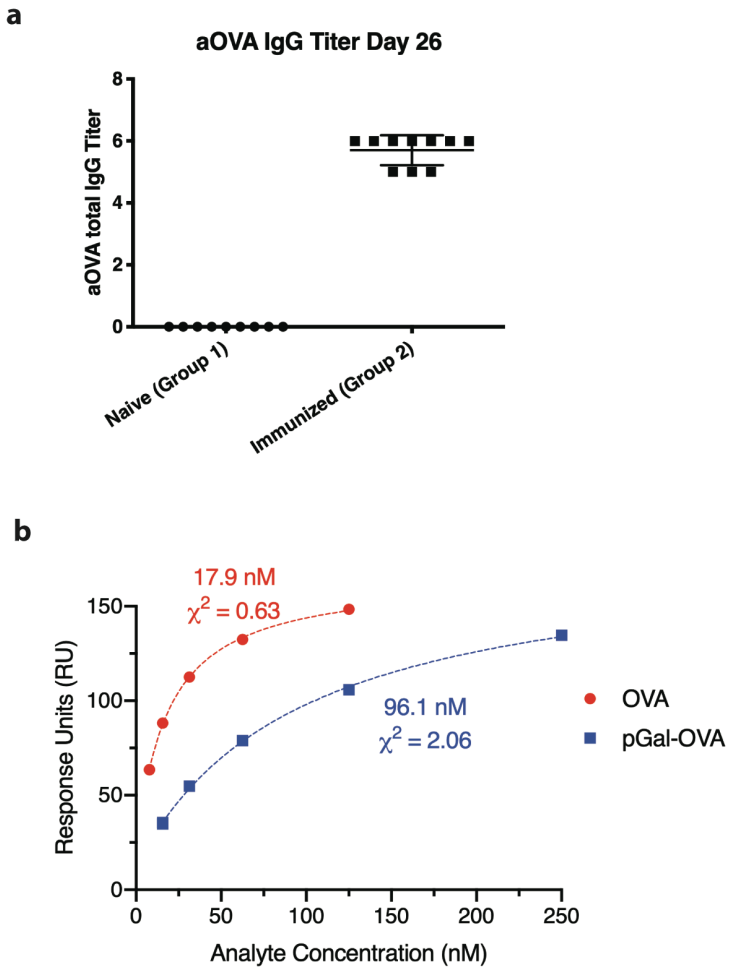

Supplemental Figure 2.1.1 | Anti-OVA IgG CFA-induced titers and SPR. a) Mice received adoptive transfer of 75k OTI&II cells each, followed by s.c. immunization with OVA+CFA in the forelimbs. 25 days later blood was collected and anti-OVA IgG was measured by ELISA. **b)** SPR was performed using purchased polyclonal anti-OVA IgG as substrate. Affinity to plain OVA or pGal-OVA was measured.

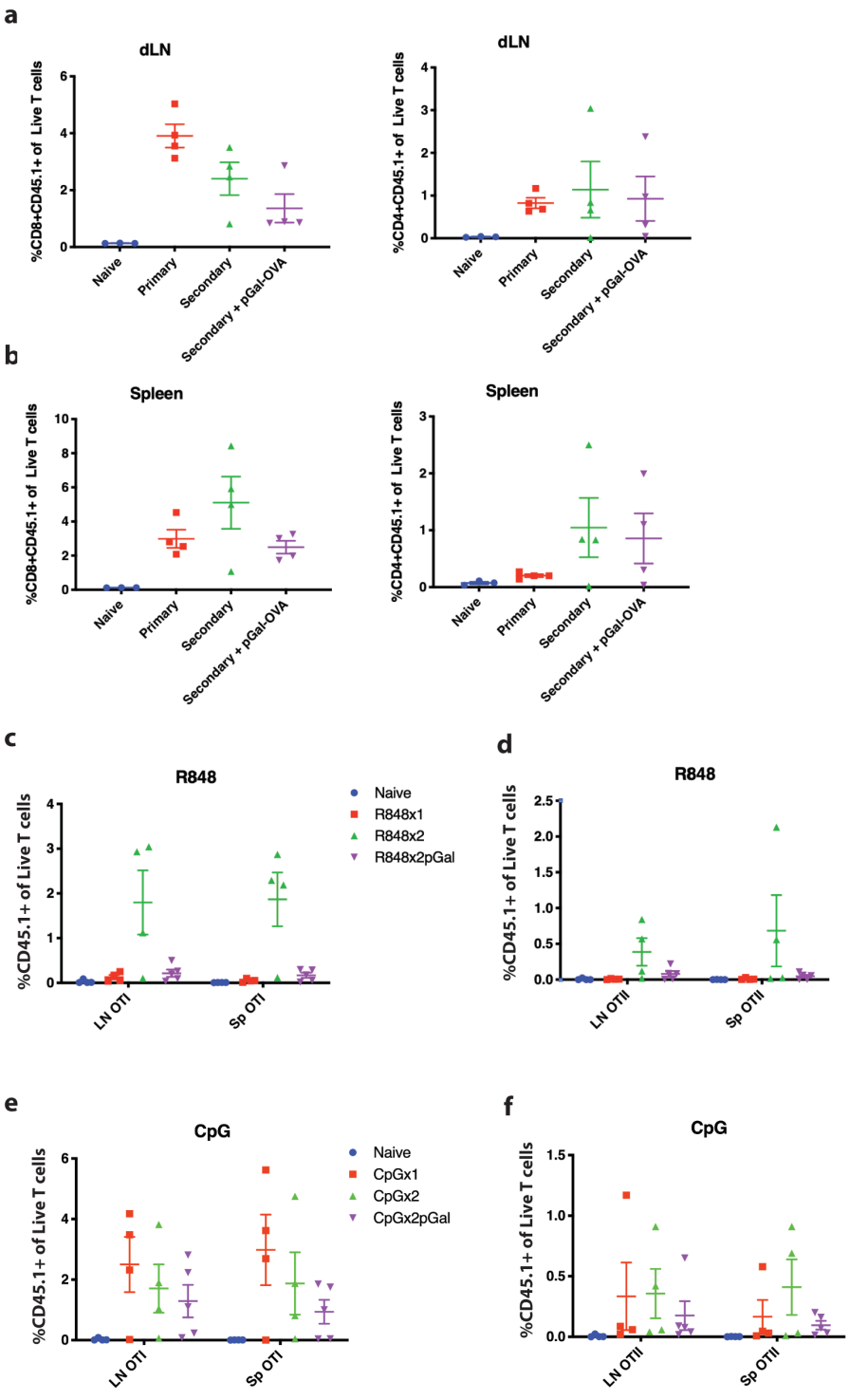

Supplemental Figure 2.1.2 | Memory model setup. Experimental setup as in Figure 2.1 with the addition of a primary immunization group that received its only challenge five days before sac. Quantification of OTI&II cell recovery as a frequency of parent population. **a,b)** CFA/IFA challenge was used for "Secondary" groups, CFA was used for the "Primary" group. **c,d)** R848 immunization was used for both primary "x1" and secondary "x2" groups. **e,f)** as in (c,d) but with CpG immunization.

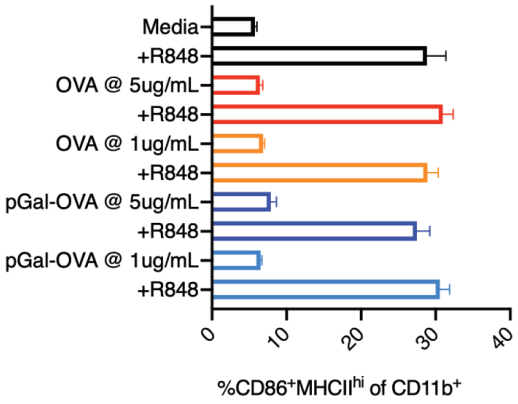

Supplemental Figure 2.1.3 | pGal innate suppression assay. BMDC were cultured with antigen or media overnight in the presence or absence of R848 (1μg/ml). Cell phenotype was assayed by flow cytometry.

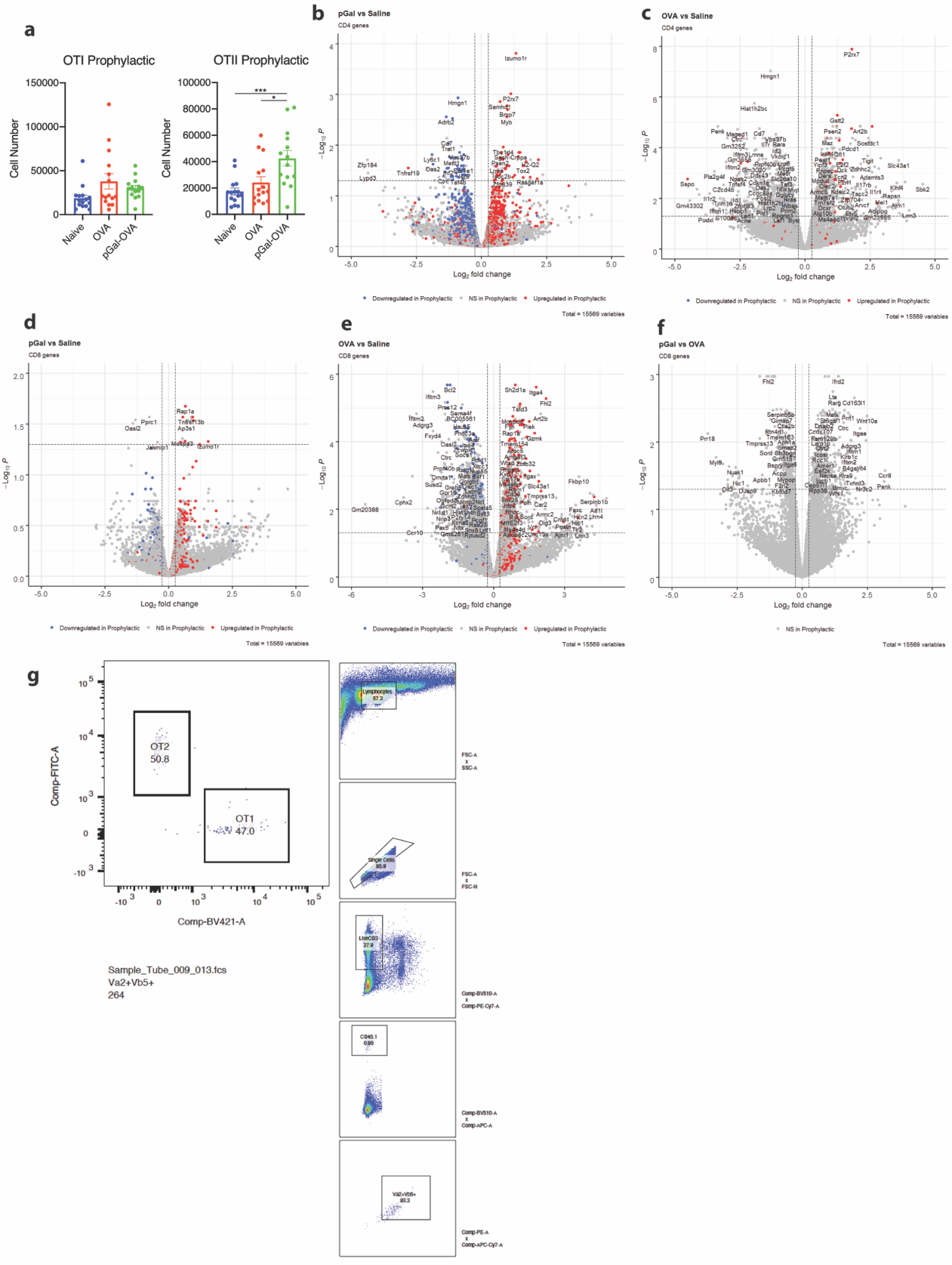
a
OTI Prophylactic
OTII Prophylactic
Cell Number
Naive
OVA
pGal-OVA
***
*
b
pGal vs Saline
CD4 genes
c
OVA vs Saline
CD4 genes
d
pGal vs Saline
CD8 genes
e
OVA vs Saline
CD8 genes
f
pGal vs OVA
CD8 genes
Log2 fold change
−Log10 P
Downregulated in Prophylactic
NS in Prophylactic
Upregulated in Prophylactic
Total = 15569 variables
g
OT2
50.8
OT1
47.0
Comp-FITC-A
Comp-BV421-A
Sample_Tube_009_013.fcs
Va2+Vb5+
264
Lymphocytes
57.3
Single Cells
99.9
Live/CD3
37.9
CD45.1
0.85
Va2+Vb5+
99.3
FSC-A
SSC-A
FSC-A
FSC-H
Comp-BV510-A
Comp-PE-Cy7-A
Comp-BV510-A
Comp-APC-A
Comp-PE-A
Comp-APC-Cy7-A

Supplemental Figure 2.4.1 | RNAseq extended data (previous page). a) FACS recovery of OTI and OTII cells from pooled SLO 4 days after prophylactic treatment. **b-f)** Therapeutic setting volcano plot with prophylactic overlay coloring for indicated cell type and group comparison. **g)** Representative FACS gating strategy for isolating OTI&II cells for RNAseq .

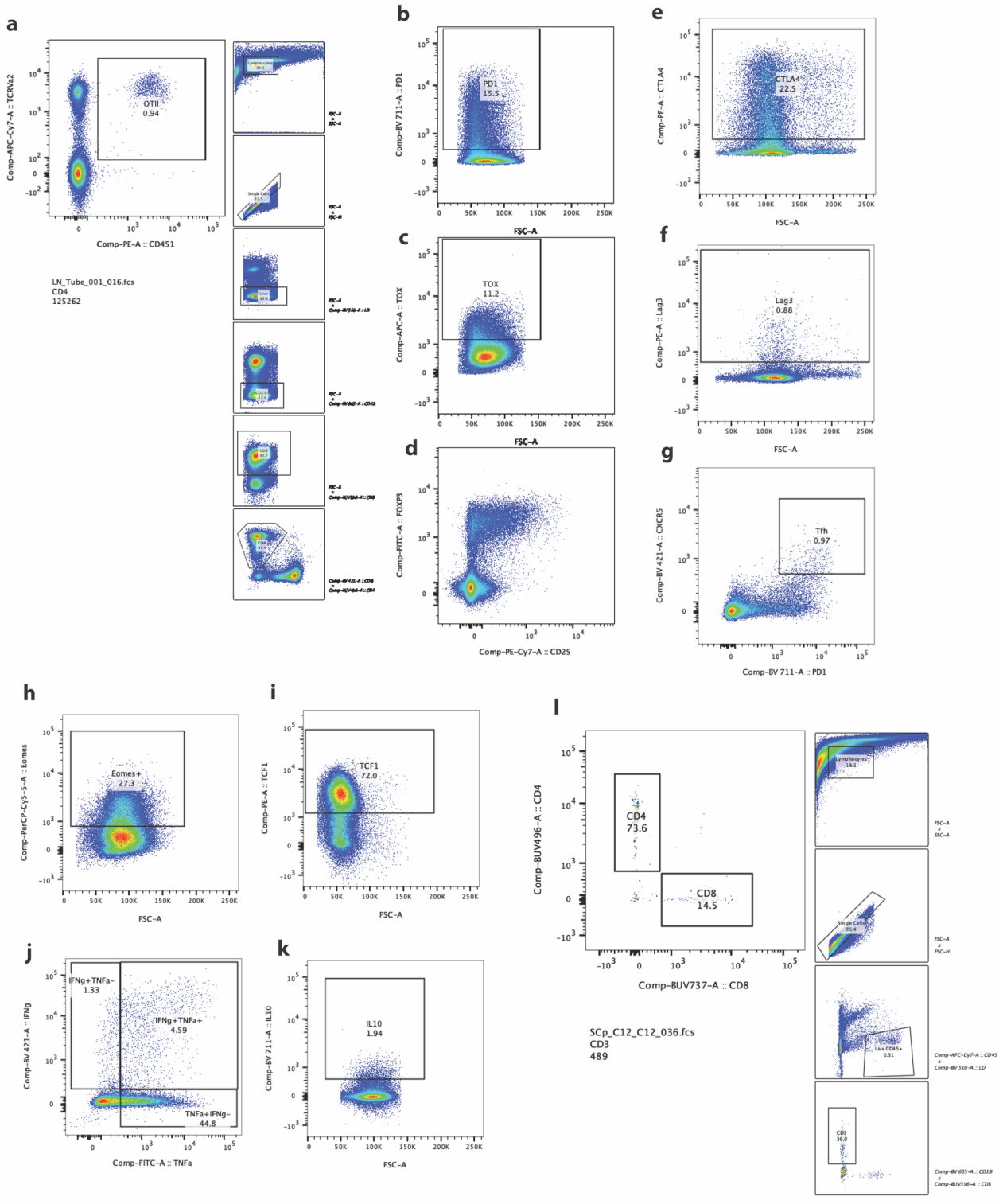

Supplemental Figure 2.5 | Flow cytometry gating. Representative gating schemes. **a)** Gating ancestry for OTII cells. **b)** PD1. **c)** TOX. **d)** Treg. **e)** CTLA4. **f)** Lag3. **g)** T_{FH}. **h)** Eomes. **i)** TCF1. **j)** IFNγ and TNFα. **k)** IL-10. **l)** Representative T cell gating and ancestry from SC isolations.

2.7 Appendix B: Supplementary Tables

2.7.1 Prophylactic DEGs CD4 (OTII) OVA vs Saline

	gene_name	ENTREZID	logFC	AveExpr	t	P.Value	adj.P.Val	B
1	Chst2	54371	2.145	3.708	10.238	3.67E-08	0.0004	9.184
2	Jdp2	81703	2.507	1.656	9.770	6.79E-08	0.0004	8.254
3	Eomes	13813	1.908	3.211	9.514	9.59E-08	0.0004	8.227
4	Cxcr5	12145	2.689	5.488	9.341	1.22E-07	0.0004	7.919
5	Zfp821	75871	1.592	3.482	9.236	1.41E-07	0.0004	7.865
6	Cd86	12524	1.647	4.624	8.569	3.66E-07	0.0008	6.844
7	Il2rb	16185	1.174	7.634	8.554	3.74E-07	0.0008	6.590
8	Cd200	17470	1.235	5.820	8.150	6.85E-07	0.0012	6.071
9	Ybx3	56449	1.191	5.169	8.077	7.66E-07	0.0012	6.020
10	P2rx7	18439	1.439	5.104	8.067	7.77E-07	0.0012	6.003
11	Wnt10a	22409	3.036	3.130	8.007	8.53E-07	0.0012	6.107
12	Acot7	70025	0.875	4.807	7.781	1.21E-06	0.0014	5.595
13	Gng2	14702	0.850	5.276	7.748	1.28E-06	0.0014	5.481
14	Gimap7	231932	0.744	6.870	7.705	1.36E-06	0.0014	5.291
15	Epsti1	108670	0.575	6.783	7.588	1.64E-06	0.0016	5.107
16	Prr13	66151	0.739	7.134	7.357	2.38E-06	0.0022	4.699
17	Tox2	269389	1.789	3.046	7.146	3.36E-06	0.0027	4.746
18	Gm5157	381937	3.815	-1.376	7.131	3.44E-06	0.0027	3.760
19	Ctla4	12477	1.341	5.676	7.112	3.56E-06	0.0027	4.380
20	Ccnb2	12442	2.902	2.289	7.108	3.58E-06	0.0027	4.713
21	Gm2237	100039441	2.157	1.606	6.999	4.29E-06	0.0030	4.530
22	Bcl2a1b	12045	0.919	5.157	6.965	4.54E-06	0.0031	4.198
23	Endod1	71946	1.318	5.018	6.898	5.08E-06	0.0032	4.129
24	Mki67	17345	2.959	3.345	6.882	5.22E-06	0.0032	4.331
25	Tns1	21961	1.588	4.525	6.799	6.00E-06	0.0035	4.002
26	E2f2	242705	1.502	4.165	6.791	6.09E-06	0.0035	4.032
27	Bcl2a1d	12047	1.099	3.595	6.692	7.21E-06	0.0038	3.937
28	Acvr1	11477	4.360	-3.111	6.682	7.33E-06	0.0038	2.049
29	Casp1	12362	0.842	4.756	6.682	7.34E-06	0.0038	3.757
30	Nmral1	67824	1.228	3.055	6.640	7.88E-06	0.0039	3.921
31	Ms4a4c	64380	1.572	5.622	6.527	9.57E-06	0.0044	3.398
32	Smim24	72273	1.766	0.972	6.525	9.61E-06	0.0044	3.708
33	Lrmp	16970	0.688	7.191	6.496	1.01E-05	0.0044	3.204
34	Adap1	231821	1.574	3.391	6.492	1.02E-05	0.0044	3.631
35	Ctnnbip1	67087	2.372	0.258	6.483	1.03E-05	0.0044	3.586
36	Plpp1	19012	3.047	0.130	6.448	1.10E-05	0.0045	3.343
37	Cxcr3	12766	1.378	5.224	6.366	1.27E-05	0.0051	3.176
38	Ttf2	74044	0.873	4.125	6.262	1.52E-05	0.0060	3.113
39	Itgb1	16412	0.660	7.955	6.236	1.59E-05	0.0060	2.699
40	Capn3	12335	1.901	3.537	6.230	1.61E-05	0.0060	3.118
41	Top2a	21973	1.502	4.186	6.217	1.65E-05	0.0060	3.027
42	Gm3411	100042149, 100861615	4.016	-2.660	6.111	1.99E-05	0.0070	1.927
43	Dusp6	67603	0.757	6.308	6.103	2.02E-05	0.0070	2.547
44	Arhgap20	244867	2.906	1.344	6.043	2.25E-05	0.0076	2.956
45	Gstt2	14872	0.806	4.688	6.028	2.31E-05	0.0076	2.582
46	Bcas1	76960	3.413	-0.789	6.013	2.38E-05	0.0077	2.452

47	Aspm	12316	5.318	-0.436	5.987	2.49E-05	0.0079	2.147
48	Fam124b	241128	3.298	-0.907	5.902	2.90E-05	0.0090	2.319
49	Epc1	13831	-0.523	6.138	-5.871	3.07E-05	0.0093	2.161
50	Ildr1	106347	1.586	1.637	5.858	3.15E-05	0.0094	2.640
51	Cd44	12505	0.605	6.820	5.814	3.41E-05	0.0098	1.970
52	Cyp1a1	13076	5.758	-4.632	5.805	3.47E-05	0.0098	0.067
53	Gpr55	227326	1.963	2.038	5.799	3.51E-05	0.0098	2.521
54	Klf2	16598	-0.443	9.214	-5.777	3.66E-05	0.0101	1.816
55	Izumo1r	64931	1.070	7.228	5.740	3.91E-05	0.0106	1.803
56	Ccdc50	67501	1.142	4.884	5.725	4.02E-05	0.0107	2.008
57	Atf4	11911	-0.474	7.132	-5.698	4.23E-05	0.0110	1.756
58	Rec8	56739	1.934	0.895	5.684	4.34E-05	0.0111	2.331
59	Mlf1	17349	4.147	-4.138	5.675	4.41E-05	0.0111	0.617
60	Tnfsf14	50930	1.566	2.258	5.649	4.63E-05	0.0115	2.242
61	Chrm4	12672	3.137	-2.135	5.561	5.45E-05	0.0133	1.529
62	Birc5	11799	2.423	2.434	5.547	5.59E-05	0.0134	2.065
63	Pnrc2	52830	0.429	7.060	5.540	5.67E-05	0.0134	1.444
64	Slc29a4	243328	4.349	-1.124	5.519	5.90E-05	0.0137	1.473
65	Tfdp1	21781	0.530	6.148	5.472	6.43E-05	0.0147	1.374
66	Casp3	12367	0.676	4.607	5.434	6.91E-05	0.0153	1.485
67	Ccnb1	268697	2.173	2.631	5.434	6.92E-05	0.0153	1.827
68	Kdelc2	68304	1.846	0.651	5.425	7.03E-05	0.0154	1.877
69	Rundc3a	51799	1.219	2.723	5.413	7.19E-05	0.0154	1.732
70	Tnfsf4	22164	3.665	0.796	5.408	7.27E-05	0.0154	1.837
71	Ebi3	50498	1.866	1.974	5.379	7.67E-05	0.0160	1.784
72	Mcoln3	171166	0.828	3.709	5.334	8.35E-05	0.0171	1.482
73	Synpo	104027	1.822	3.330	5.331	8.39E-05	0.0171	1.517
74	Lpxn	107321	0.571	6.689	5.247	9.85E-05	0.0198	0.897
75	Kif18b	70218	4.826	0.366	5.185	1.11E-04	0.0213	1.206
76	Sspo	243369	3.416	-2.026	5.185	1.11E-04	0.0213	1.021
77	Frat2	212398	-0.794	6.117	-5.182	1.12E-04	0.0213	0.853
78	Srsf5	20384	-0.448	8.959	-5.180	1.12E-04	0.0213	0.674
79	Nlrx1	270151	0.888	4.092	5.173	1.14E-04	0.0213	1.073
80	Gm10406	100038847	4.149	-3.248	5.162	1.16E-04	0.0215	0.609
81	Cpq	54381	1.136	2.914	5.130	1.23E-04	0.0226	1.165
82	Cmya5	76469	1.818	1.651	5.121	1.26E-04	0.0227	1.308
83	Mxd4	17122	0.705	6.388	5.084	1.35E-04	0.0241	0.590
84	Tpx2	72119	2.989	1.635	5.076	1.37E-04	0.0242	1.253
85	Akap12	83397	0.775	4.620	5.030	1.49E-04	0.0259	0.703
86	Fhl2	14200	1.771	1.169	5.028	1.50E-04	0.0259	1.174
87	Ncapg	54392	2.248	1.613	4.968	1.69E-04	0.0288	1.041
88	Tnp2	21959	3.540	-2.934	4.940	1.78E-04	0.0300	0.235
89	Depdc1a	76131	5.219	-1.814	4.931	1.81E-04	0.0302	0.427
90	Glrx	93692	0.737	6.011	4.915	1.87E-04	0.0307	0.286
91	Adamtsl2	77794	3.569	0.049	4.911	1.88E-04	0.0307	0.941
92	Bmp7	12162	1.155	4.020	4.900	1.92E-04	0.0311	0.526
93	Myo9a	270163	1.083	5.064	4.892	1.96E-04	0.0312	0.362
94	2610042L04Rik	554327	4.266	-2.792	4.885	1.98E-04	0.0313	0.287
95	Pear1	73182	0.673	5.361	4.873	2.03E-04	0.0317	0.281
96	Fbxw8	231672	0.850	4.579	4.856	2.10E-04	0.0325	0.379
97	Spryd7	66674	-0.779	3.492	-4.850	2.12E-04	0.0325	0.644
98	E2f5	13559	-0.690	3.784	-4.819	2.25E-04	0.0342	0.529
99	Uhrf1	18140	0.942	4.070	4.796	2.36E-04	0.0353	0.387
100	Cnrip1	380686	1.833	0.815	4.792	2.38E-04	0.0353	0.749
101	Elmo3	234683	0.742	2.775	4.760	2.53E-04	0.0371	0.535
102	Gstt3	103140	1.633	0.632	4.756	2.55E-04	0.0371	0.685

103	Nfatc1	18018	0.376	8.788	4.748	2.59E-04	0.0374	-0.191
104	Selp	20344	4.996	-2.754	4.733	2.67E-04	0.0381	0.004
105	Cpt2	12896	0.554	4.347	4.728	2.69E-04	0.0381	0.194
106	Adam19	11492	1.607	3.855	4.721	2.73E-04	0.0383	0.270
107	Ier2	15936	-0.738	8.617	-4.706	2.82E-04	0.0391	-0.251
108	Nek5	330721	4.407	-3.665	4.686	2.93E-04	0.0403	-0.628
109	Cdkn3	72391	2.410	0.107	4.668	3.03E-04	0.0413	0.506
110	Acta2	11475	2.821	-0.332	4.659	3.09E-04	0.0417	0.456
111	E2f1	13555	1.227	2.732	4.615	3.37E-04	0.0451	0.253
112	Ntn1	18208	3.290	0.015	4.604	3.44E-04	0.0455	0.403
113	Aunip	69885	3.755	-2.600	4.599	3.48E-04	0.0455	-0.102
114	Cenph	26886	1.225	0.669	4.597	3.49E-04	0.0455	0.394
115	Pdzk1ip1	67182	2.902	-0.065	4.589	3.55E-04	0.0459	0.351
116	Cdca5	67849	1.892	1.154	4.569	3.69E-04	0.0472	0.329
117	Tnk2	51789	0.720	4.406	4.565	3.72E-04	0.0472	-0.170
118	Trim59	66949	0.607	6.740	4.555	3.79E-04	0.0477	-0.493
119	Kif11	16551	1.691	1.747	4.549	3.84E-04	0.0477	0.236
120	Chn2	69993	0.898	3.377	4.548	3.85E-04	0.0477	-0.015

2.7.2 Prophylactic DEGs CD4 (OTII) pGal vs OVA

	gene_name	ENTREZID	logFC	AveExpr	t	P.Value	adj.P.Val	B
1	Endod1	71946	2.959	5.018	17.238	2.69E-11	4.00E-07	16.176
2	Nrn1	68404	2.826	2.334	13.897	5.68E-10	4.22E-06	12.558
3	Casp1	12362	1.557	4.756	12.980	1.47E-09	5.78E-06	12.338
4	Nrp1	18186	1.853	5.402	12.927	1.55E-09	5.78E-06	12.298
5	Dntt	21673	-4.109	4.307	-12.390	2.79E-09	8.25E-06	11.390
6	Cd200	17470	1.756	5.820	12.147	3.66E-09	8.25E-06	11.446
7	Ppic	19038	2.886	3.370	12.044	4.12E-09	8.25E-06	11.232
8	Slc9b2	97086	3.149	1.987	11.897	4.87E-09	8.25E-06	10.664
9	Atp1b1	11931	-2.042	5.738	-11.868	5.03E-09	8.25E-06	11.130
10	Wnt10a	22409	2.892	3.130	11.783	5.55E-09	8.25E-06	11.013
11	Tbc1d4	210789	1.724	6.460	11.627	6.66E-09	8.74E-06	10.836
12	Enpp4	224794	-2.632	4.336	-11.538	7.39E-09	8.74E-06	10.574
13	Pdlim4	30794	-3.049	3.686	-11.509	7.65E-09	8.74E-06	10.337
14	Evi2a	14017	1.278	5.588	11.433	8.36E-09	8.88E-06	10.632
15	Ccr9	12769	-3.070	4.171	-11.200	1.10E-08	1.09E-05	10.123
16	Fbxw8	231672	1.811	4.579	10.995	1.42E-08	1.18E-05	10.121
17	Cd44	12505	1.119	6.820	10.949	1.50E-08	1.18E-05	10.008
18	Izumo1r	64931	1.991	7.228	10.924	1.55E-08	1.18E-05	9.962
19	Ly6c1	17067	-3.735	6.844	-10.906	1.58E-08	1.18E-05	10.013
20	Ctla4	12477	1.945	5.676	10.900	1.59E-08	1.18E-05	9.970
21	Ephx1	13849	1.195	7.835	10.847	1.70E-08	1.20E-05	9.858
22	Spry1	24063	2.446	3.472	10.780	1.85E-08	1.25E-05	9.820
23	Rgs1	50778	1.414	5.389	10.641	2.19E-08	1.42E-05	9.673
24	Ccdc28b	66264	1.530	3.087	10.552	2.45E-08	1.50E-05	9.442
25	Synpo	104027	3.029	3.330	10.530	2.53E-08	1.50E-05	9.532
26	Scd2	20250	1.064	6.690	10.358	3.14E-08	1.80E-05	9.260
27	Tns1	21961	2.114	4.525	10.310	3.34E-08	1.84E-05	9.264
28	Chst2	54371	1.751	3.708	10.248	3.62E-08	1.92E-05	9.198
29	Lclat1	225010	1.874	4.088	10.187	3.92E-08	1.92E-05	9.115
30	Tnfsf11	21943	2.015	4.484	10.159	4.06E-08	1.92E-05	9.080
31	Prr13	66151	1.004	7.134	10.153	4.10E-08	1.92E-05	8.977

32	Casp3	12367	1.210	4.607	10.105	4.36E-08	1.92E-05	9.009
33	Gng2	14702	1.069	5.276	10.105	4.36E-08	1.92E-05	8.982
34	Bcl2a1b	12045	1.272	5.157	10.077	4.52E-08	1.92E-05	8.951
35	Il2rb	16185	1.355	7.634	10.075	4.53E-08	1.92E-05	8.857
36	Plscr1	22038	1.709	3.276	9.830	6.27E-08	2.53E-05	8.626
37	Smpdl3a	57319	1.031	6.864	9.827	6.29E-08	2.53E-05	8.551
38	Bmp7	12162	2.083	4.020	9.714	7.32E-08	2.86E-05	8.501
39	St3gal2	20444	1.154	5.375	9.528	9.41E-08	3.55E-05	8.214
40	Gpr55	227326	2.610	2.038	9.506	9.70E-08	3.55E-05	8.128
41	Slamf6	30925	1.117	8.244	9.499	9.79E-08	3.55E-05	8.056
42	Zfp821	75871	1.441	3.482	9.477	1.01E-07	3.57E-05	8.190
43	Aqp11	66333	-3.083	1.785	-9.400	1.12E-07	3.76E-05	7.093
44	Mpp2	50997	4.004	0.791	9.396	1.13E-07	3.76E-05	7.400
45	Rilpl2	80291	1.305	5.472	9.376	1.16E-07	3.76E-05	7.997
46	Ccr10	12777	3.198	1.394	9.373	1.16E-07	3.76E-05	7.658
47	Gm2237	100039441	2.309	1.606	9.294	1.30E-07	4.09E-05	7.785
48	Il7r	16197	-1.028	7.351	-9.281	1.32E-07	4.09E-05	7.801
49	Tgtp1	21822	-1.525	7.878	-9.145	1.60E-07	4.85E-05	7.590
50	Slc29a1	63959	1.184	6.380	9.081	1.75E-07	5.20E-05	7.528
51	Gramd3	107022	-0.892	7.551	-9.015	1.92E-07	5.60E-05	7.407
52	Casp4	12363	2.331	3.354	8.930	2.17E-07	6.20E-05	7.443
53	Pxylp1	235534	-1.405	4.953	-8.881	2.33E-07	6.52E-05	7.371
54	Akap12	83397	1.306	4.620	8.855	2.41E-07	6.64E-05	7.299
55	Nfatc1	18018	0.686	8.788	8.795	2.63E-07	7.05E-05	7.030
56	Laptm4b	114128	-1.745	3.676	-8.782	2.68E-07	7.05E-05	7.185
57	Lrmp	16970	0.915	7.191	8.777	2.70E-07	7.05E-05	7.046
58	Ggt5	23887	-1.814	4.899	-8.753	2.80E-07	7.17E-05	7.194
59	Myo6	17920	-2.862	3.672	-8.721	2.93E-07	7.38E-05	7.072
60	Ttc39b	69863	1.283	5.793	8.694	3.05E-07	7.55E-05	6.982
61	Rundc3a	51799	1.789	2.723	8.650	3.25E-07	7.88E-05	7.032
62	Ccdc50	67501	1.607	4.884	8.642	3.29E-07	7.88E-05	6.962
63	Eea1	216238	1.591	3.811	8.581	3.60E-07	8.26E-05	6.948
64	Gm3739	#N/A	3.200	0.664	8.577	3.62E-07	8.26E-05	6.657
65	Syt11	229521	1.469	5.318	8.575	3.63E-07	8.26E-05	6.842
66	Smtn	29856	3.326	2.467	8.567	3.67E-07	8.26E-05	6.907
67	Dusp6	67603	1.034	6.308	8.524	3.91E-07	8.67E-05	6.706
68	Rgs3	50780	1.049	6.788	8.511	3.99E-07	8.71E-05	6.664
69	Clcf1	56708	-1.357	4.047	-8.448	4.38E-07	9.18E-05	6.751
70	Plekhb2	226971	0.757	6.909	8.445	4.39E-07	9.18E-05	6.562
71	Samhd1	56045	0.763	8.669	8.440	4.43E-07	9.18E-05	6.499
72	Wdr26	226757	1.055	6.926	8.435	4.46E-07	9.18E-05	6.546
73	Xdh	22436	1.410	4.943	8.428	4.51E-07	9.18E-05	6.654
74	Gm3591	100041958	5.795	-3.686	8.360	4.99E-07	1.00E-04	2.227
75	Gm3248	#N/A	5.618	-4.080	8.287	5.57E-07	1.07E-04	2.181
76	Pqlc3	217430	0.886	5.263	8.286	5.58E-07	1.07E-04	6.417
77	Bcl2a1d	12047	1.265	3.595	8.283	5.60E-07	1.07E-04	6.513
78	Psen2	19165	1.281	6.120	8.282	5.61E-07	1.07E-04	6.346
79	Mmd	67468	1.130	4.533	8.204	6.31E-07	1.19E-04	6.348
80	Vim	22352	0.822	7.562	8.172	6.62E-07	1.23E-04	6.120
81	Ly6m	67038	2.271	1.018	8.109	7.29E-07	1.32E-04	5.986
82	Gbp7	229900	-0.741	7.034	-8.107	7.32E-07	1.32E-04	6.056
83	Ybx3	56449	1.133	5.169	8.099	7.41E-07	1.32E-04	6.122
84	Tstd3	77032	1.187	3.725	8.094	7.46E-07	1.32E-04	6.232
85	Adamts20	223838	6.251	-3.659	8.066	7.79E-07	1.35E-04	2.137
86	Itgb1	16412	0.840	7.955	8.060	7.86E-07	1.35E-04	5.924
87	Nsd2	107823	1.457	5.062	8.056	7.91E-07	1.35E-04	6.074

	D830030K20							
88	Rik	320333	2.749	1.348	8.022	8.33E-07	1.39E-04	5.983
89	Acss2	60525	-0.906	6.357	-8.021	8.34E-07	1.39E-04	5.977
90	Nxpe3	385658	0.924	6.081	7.976	8.94E-07	1.48E-04	5.879
91	Il17rb	50905	2.031	2.348	7.954	9.25E-07	1.51E-04	5.947
92	Decr1	67460	1.429	4.199	7.919	9.77E-07	1.58E-04	5.929
93	Cnn3	71994	-1.816	6.731	-7.845	1.10E-06	1.75E-04	5.708
94	Tgtp2	100039796	-0.814	7.393	-7.812	1.15E-06	1.82E-04	5.574
95	Man1c1	230815	1.181	3.521	7.806	1.16E-06	1.82E-04	5.807
96	Bhlhe40	20893	1.752	4.344	7.767	1.24E-06	1.92E-04	5.682
97	Pear1	73182	1.042	5.361	7.752	1.27E-06	1.94E-04	5.569
98	Gm3636	100041151	2.670	1.428	7.736	1.30E-06	1.97E-04	5.651
99	Epb41	269587	-0.767	7.862	-7.712	1.35E-06	2.03E-04	5.392
100	Rictor	78757	-0.837	7.231	-7.695	1.39E-06	2.06E-04	5.394
101	1700025G04 Rik	69399	-1.521	3.598	-7.681	1.42E-06	2.08E-04	5.606
102	Qpct	70536	1.910	3.082	7.677	1.42E-06	2.08E-04	5.610
103	Ptger4	19219	0.867	6.417	7.670	1.44E-06	2.08E-04	5.368
104	Eml3	225898	0.674	6.226	7.649	1.49E-06	2.13E-04	5.350
105	Phactr2	215789	1.900	3.064	7.633	1.53E-06	2.15E-04	5.539
106	Clstn1	65945	1.508	3.985	7.630	1.54E-06	2.15E-04	5.503
107	Tmem65	74868	1.114	5.283	7.625	1.55E-06	2.15E-04	5.378
108	Daxx	13163	1.033	6.958	7.597	1.62E-06	2.22E-04	5.231
109	Ddit4	74747	1.663	5.259	7.591	1.63E-06	2.22E-04	5.331
110	Abcc4	239273	1.135	5.693	7.587	1.64E-06	2.22E-04	5.283
111	Unc119b	106840	0.619	7.052	7.562	1.71E-06	2.28E-04	5.161
112	Slc16a5	217316	-2.059	5.974	-7.559	1.72E-06	2.28E-04	5.317
113	Tlr12	384059	-2.538	2.886	-7.535	1.79E-06	2.35E-04	5.265
114	Gprasp2	245607	-2.668	1.270	-7.522	1.82E-06	2.38E-04	4.801
115	Sgk1	20393	-0.862	6.498	-7.489	1.92E-06	2.48E-04	5.112
116	Pprc1	226169	-0.750	6.400	-7.479	1.96E-06	2.51E-04	5.095
117	Sntb2	20650	1.249	4.319	7.468	1.99E-06	2.53E-04	5.206
118	Prkca	18750	1.065	6.169	7.459	2.02E-06	2.53E-04	5.037
119	Inppl1	16332	3.580	1.995	7.457	2.03E-06	2.53E-04	5.192
120	Hid1	217310	-1.316	5.902	-7.446	2.06E-06	2.55E-04	5.103

2.7.3 Prophylactic DEGs CD4 (OTII) pGal vs Saline

	gene_name	ENTREZID	logFC	AveExpr	t	P.Value	adj.P.Val	B
1	Endod1	71946	4.277	5.018	22.585	5.40E-13	8.02E-09	19.884
2	Cd200	17470	2.991	5.820	21.095	1.46E-12	9.57E-09	19.170
3	Il2rb	16185	2.529	7.634	20.442	2.30E-12	9.57E-09	18.768
4	Casp1	12362	2.399	4.756	20.284	2.58E-12	9.57E-09	18.513
5	Prr13	66151	1.743	7.134	19.395	4.93E-12	1.47E-08	18.010
6	Gng2	14702	1.919	5.276	18.795	7.76E-12	1.91E-08	17.528
7	Ctla4	12477	3.285	5.676	18.472	9.96E-12	1.91E-08	17.300
8	Cd44	12505	1.723	6.820	18.432	1.03E-11	1.91E-08	17.277
9	Izumo1r	64931	3.061	7.228	18.170	1.26E-11	1.99E-08	17.068
10	Chst2	54371	3.896	3.708	18.096	1.34E-11	1.99E-08	16.577
11	Bcl2a1b	12045	2.191	5.157	17.736	1.79E-11	2.30E-08	16.707
12	Zfp821	75871	3.033	3.482	17.689	1.86E-11	2.30E-08	16.253
13	Nrn1	68404	3.424	2.334	17.048	3.15E-11	3.60E-08	15.476
14	Lrmp	16970	1.603	7.191	16.860	3.69E-11	3.92E-08	15.986

15	Ybx3	56449	2.324	5.169	16.677	4.32E-11	4.28E-08	15.844
16	Casp3	12367	1.886	4.607	16.233	6.35E-11	5.89E-08	15.449
17	Scd2	20250	1.510	6.690	16.010	7.72E-11	6.47E-08	15.249
18	Fbxw8	231672	2.661	4.579	15.993	7.84E-11	6.47E-08	15.230
19	Itgb1	16412	1.500	7.955	15.873	8.73E-11	6.49E-08	15.097
20	Tns1	21961	3.702	4.525	15.872	8.73E-11	6.49E-08	15.098
21	Dusp6	67603	1.791	6.308	15.811	9.22E-11	6.53E-08	15.082
22	Evi2a	14017	1.613	5.588	15.587	1.13E-10	7.63E-08	14.893
23	P2rx7	18439	2.627	5.104	15.401	1.34E-10	8.65E-08	14.730
24	Nfatc1	18018	1.062	8.788	15.104	1.76E-10	1.09E-07	14.362
25	Nrp1	18186	1.936	5.402	14.987	1.97E-10	1.10E-07	14.335
26	Slamf6	30925	1.588	8.244	14.950	2.04E-10	1.10E-07	14.222
27	Ppic	19038	3.852	3.370	14.934	2.07E-10	1.10E-07	14.126
28	Ephx1	13849	1.484	7.835	14.895	2.15E-10	1.10E-07	14.179
29	Bcl2a1d	12047	2.364	3.595	14.890	2.16E-10	1.10E-07	14.128
30	Slc9b2	97086	4.246	1.987	14.857	2.23E-10	1.10E-07	13.530
31	Tbc1d4	210789	1.996	6.460	14.811	2.33E-10	1.11E-07	14.130
32	Pdlim4	30794	-3.637	3.686	-14.389	3.49E-10	1.52E-07	13.444
33	Ccdc50	67501	2.749	4.884	14.387	3.50E-10	1.52E-07	13.777
34	Akap12	83397	2.081	4.620	14.383	3.51E-10	1.52E-07	13.773
35	Wnt10a	22409	5.928	3.130	14.354	3.61E-10	1.52E-07	13.119
36	Enpp4	224794	-3.141	4.336	-14.337	3.67E-10	1.52E-07	13.577
37	Plscr1	22038	2.502	3.276	14.215	4.14E-10	1.66E-07	13.473
38	Gstt2	14872	1.751	4.688	14.086	4.70E-10	1.80E-07	13.483
39	Bmp7	12162	3.238	4.020	14.041	4.92E-10	1.80E-07	13.418
40	Ttc39b	69863	1.935	5.793	14.023	5.01E-10	1.80E-07	13.381
41	Atp1b1	11931	-2.268	5.738	-14.009	5.08E-10	1.80E-07	13.407
42	Gm2237	100039441	4.467	1.606	14.006	5.09E-10	1.80E-07	12.401
43	Dntt	21673	-4.537	4.307	-13.944	5.42E-10	1.87E-07	13.156
44	Ly6c1	17067	-4.538	6.844	-13.837	6.04E-10	2.00E-07	13.236
45	Ccdc28b	66264	1.897	3.087	13.834	6.06E-10	2.00E-07	13.094
46	Rundc3a	51799	3.008	2.723	13.780	6.40E-10	2.07E-07	12.950
47	Pxylp1	235534	-1.994	4.953	-13.671	7.15E-10	2.26E-07	13.065
48	Tgtp1	21822	-2.046	7.878	-13.586	7.79E-10	2.41E-07	12.877
49	Synpo	104027	4.851	3.330	13.510	8.43E-10	2.54E-07	12.724
50	Pear1	73182	1.716	5.361	13.499	8.53E-10	2.54E-07	12.866
51	Cd86	12524	2.543	4.624	13.460	8.88E-10	2.59E-07	12.853
52	Spry1	24063	3.041	3.472	13.402	9.43E-10	2.69E-07	12.754
53	Il7r	16197	-1.329	7.351	-13.322	1.02E-09	2.87E-07	12.609
54	Unc119b	106840	0.977	7.052	13.150	1.23E-09	3.38E-07	12.414
55	Gpr55	227326	4.573	2.038	13.063	1.35E-09	3.63E-07	11.867
56	Rgs1	50778	1.619	5.389	13.003	1.43E-09	3.74E-07	12.342
57	Tnfsf11	21943	2.520	4.484	13.002	1.44E-09	3.74E-07	12.377
58	Ccr9	12769	-3.404	4.171	-12.917	1.57E-09	4.03E-07	12.160
59	Gimap7	231932	1.121	6.870	12.896	1.61E-09	4.05E-07	12.145
60	Psen2	19165	1.820	6.120	12.833	1.72E-09	4.26E-07	12.106
61	Rgs3	50780	1.441	6.788	12.813	1.76E-09	4.28E-07	12.053
62	Xdh	22436	2.018	4.943	12.655	2.09E-09	5.00E-07	11.987
63	Tox2	269389	3.151	3.046	12.599	2.22E-09	5.20E-07	11.843
64	Map7d1	245877	1.051	6.355	12.590	2.24E-09	5.20E-07	11.828
65	Ms4a4c	64380	2.882	5.622	12.514	2.43E-09	5.57E-07	11.815
66	Leprot	230514	0.954	5.660	12.472	2.55E-09	5.74E-07	11.738
67	Cpq	54381	2.650	2.914	12.439	2.65E-09	5.87E-07	11.693
68	Smpdl3a	57319	1.181	6.864	12.415	2.72E-09	5.93E-07	11.602
69	Nod1	107607	1.441	6.178	12.373	2.84E-09	6.12E-07	11.600
70	Casp4	12363	3.575	3.354	12.343	2.94E-09	6.25E-07	11.606

71	Glrx	93692	1.687	6.011	12.299	3.09E-09	6.46E-07	11.518
72	Plekhb2	226971	0.997	6.909	12.287	3.13E-09	6.46E-07	11.453
73	Mmd	67468	1.618	4.533	12.237	3.31E-09	6.74E-07	11.542
74	Tstd3	77032	1.726	3.725	12.201	3.45E-09	6.92E-07	11.510
75	Eml3	225898	0.976	6.226	12.139	3.70E-09	7.32E-07	11.321
76	Samhd1	56045	0.980	8.669	12.041	4.13E-09	8.07E-07	11.112
77	Ggt5	23887	-2.285	4.899	-11.997	4.34E-09	8.38E-07	11.285
78	Cars	27267	-1.041	5.873	-11.852	5.13E-09	9.76E-07	11.046
79	Ifi27l2a	76933	1.571	8.423	11.816	5.34E-09	1.00E-06	10.849
80	Pqlc3	217430	1.159	5.263	11.771	5.63E-09	1.05E-06	10.950
81	Tgtp2	100039796	-1.107	7.393	-11.732	5.89E-09	1.08E-06	10.803
82	Decr1	67460	2.062	4.199	11.721	5.97E-09	1.08E-06	10.965
83	E2f2	242705	2.498	4.165	11.553	7.26E-09	1.30E-06	10.778
84	Gramd3	107022	-1.027	7.551	-11.516	7.58E-09	1.33E-06	10.535
85	Sh3bgrl	56726	1.315	6.017	11.514	7.59E-09	1.33E-06	10.600
86	Epsti1	108670	0.784	6.783	11.493	7.79E-09	1.35E-06	10.527
87	Bhlhe40	20893	2.701	4.344	11.474	7.97E-09	1.36E-06	10.683
88	Cxcr5	12145	3.309	5.488	11.459	8.11E-09	1.37E-06	10.642
89	Pdcd1	18566	1.967	4.967	11.397	8.73E-09	1.46E-06	10.540
90	Nsd2	107823	1.964	5.062	11.377	8.93E-09	1.47E-06	10.506
91	Rilpl2	80291	1.463	5.472	11.370	9.01E-09	1.47E-06	10.462
92	Trim59	66949	1.358	6.740	11.364	9.07E-09	1.47E-06	10.361
93	Chn2	69993	2.124	3.377	11.335	9.40E-09	1.49E-06	10.514
94	Jdp2	81703	2.934	1.656	11.330	9.45E-09	1.49E-06	10.005
95	Syt11	229521	1.775	5.318	11.281	1.00E-08	1.57E-06	10.350
96	Ly6m	67038	3.367	1.018	11.261	1.03E-08	1.59E-06	9.845
97	Ccr10	12777	3.739	1.394	11.203	1.10E-08	1.68E-06	10.059
98	Acss2	60525	-1.140	6.357	-11.113	1.23E-08	1.86E-06	10.117
99	Coro7	78885	0.927	8.343	11.101	1.25E-08	1.87E-06	9.976
100	Sntb2	20650	1.777	4.319	11.084	1.27E-08	1.89E-06	10.199
101	Ifnar2	15976	0.712	7.046	11.035	1.35E-08	1.98E-06	9.943
102	Tmem254b	100039257	1.207	5.639	11.001	1.41E-08	2.04E-06	9.986
103	Nsmaf	18201	1.013	7.014	10.997	1.41E-08	2.04E-06	9.896
104	Tspan31	67125	1.427	5.278	10.989	1.43E-08	2.04E-06	10.006
105	Gbp7	229900	-0.909	7.034	-10.974	1.45E-08	2.04E-06	9.885
106	Igflr1	101883	1.689	6.303	10.973	1.45E-08	2.04E-06	9.893
107	Ubash3b	72828	1.347	5.343	10.950	1.50E-08	2.06E-06	9.945
108	Unc119	22248	1.887	4.603	10.949	1.50E-08	2.06E-06	10.030
109	Sgk1	20393	-1.143	6.498	-10.921	1.55E-08	2.11E-06	9.865
110	Ptpn7	320139	1.225	8.131	10.883	1.62E-08	2.19E-06	9.706
111	Tram2	170829	1.965	2.904	10.870	1.65E-08	2.21E-06	9.935
112	Itgal	16408	0.982	9.624	10.846	1.70E-08	2.26E-06	9.619
113	Myo6	17920	-3.442	3.672	-10.826	1.74E-08	2.29E-06	9.855
114	Ttf2	74044	1.437	4.125	10.751	1.91E-08	2.49E-06	9.812
115	Phactr2	215789	2.711	3.064	10.720	1.99E-08	2.57E-06	9.781
116	Zc3h12d	237256	1.312	5.912	10.698	2.04E-08	2.62E-06	9.576
117	Gprasp1	67298	-1.256	5.669	-10.684	2.08E-08	2.64E-06	9.652
118	Gm3636	100041151	4.362	1.428	10.562	2.43E-08	3.06E-06	9.285
119	Pik3r5	320207	-0.931	7.467	-10.544	2.48E-08	3.10E-06	9.311
120	Ctnnbip1	67087	3.911	0.258	10.537	2.50E-08	3.10E-06	8.672

2.7.4 Prophylactic DEGs CD8 (OTI) OVA vs Saline

	gene_name	ENTREZID	logFC	AveExpr	t	P.Value	adj.P.Val	B
1	Itgb1	16412	2.614	8.719	11.751	1.79E-09	1.38E-05	12.060
2	Cxcr3	12766	1.908	7.274	11.471	2.57E-09	1.38E-05	11.716
3	Lag3	16768	3.414	1.325	11.407	2.79E-09	1.38E-05	9.026
4	Zbtb32	58206	4.662	3.576	11.070	4.35E-09	1.62E-05	10.200
5	Chst2	54371	3.167	3.521	10.389	1.10E-08	3.15E-05	9.864
6	Anxa2	12306	2.166	7.045	10.287	1.27E-08	3.15E-05	10.117
7	Slamf7	75345	2.364	5.618	9.884	2.26E-08	4.80E-05	9.589
8	Tbx21	57765	1.836	6.745	9.724	2.86E-08	5.31E-05	9.310
9	Itga4	16401	1.258	7.860	9.401	4.61E-08	6.55E-05	8.788
10	S100a6	20200	2.437	5.584	9.393	4.67E-08	6.55E-05	8.867
11	Stk39	53416	1.463	5.182	9.293	5.44E-08	6.55E-05	8.725
12	Ctla2a	13024	2.812	6.671	9.234	5.95E-08	6.55E-05	8.589
13	Lxn	17035	1.333	3.795	9.196	6.30E-08	6.55E-05	8.522
14	Capn3	12335	2.291	2.591	9.151	6.75E-08	6.55E-05	8.064
15	Klrk1	27007	2.752	6.409	9.111	7.17E-08	6.55E-05	8.416
16	Bcl2a1d	12047	1.687	3.374	9.087	7.45E-08	6.55E-05	8.269
17	Ikzf3	22780	1.156	7.185	9.083	7.49E-08	6.55E-05	8.314
18	Casp3	12367	1.504	4.788	8.995	8.58E-08	7.08E-05	8.286
19	Ptms	69202	2.642	1.403	8.944	9.29E-08	7.26E-05	7.224
20	Cxcr5	12145	1.599	5.821	8.855	1.07E-07	7.93E-05	8.038
21	Myb	17863	1.720	5.542	8.798	1.17E-07	8.25E-05	7.957
22	Arl4d	80981	1.755	3.581	8.619	1.55E-07	1.05E-04	7.630
23	Pdcd1	18566	2.510	3.662	8.346	2.40E-07	1.51E-04	7.213
24	Psen2	19165	1.163	5.875	8.338	2.44E-07	1.51E-04	7.189
25	Ccnb1	268697	2.128	3.440	8.277	2.69E-07	1.60E-04	7.074
26	Gm49391	#N/A	4.884	1.383	8.110	3.55E-07	2.03E-04	6.198
27	Unc119	22248	1.126	4.496	7.976	4.43E-07	2.44E-04	6.681
28	Ifi27l2a	76933	1.351	7.782	7.884	5.18E-07	2.62E-04	6.324
29	Lgals1	16852	1.493	7.296	7.861	5.38E-07	2.62E-04	6.299
30	Zdhhc2	70546	1.996	2.582	7.849	5.49E-07	2.62E-04	6.250
31	Jdp2	81703	2.706	1.860	7.843	5.54E-07	2.62E-04	5.922
32	Dop1b	70028	1.089	6.759	7.820	5.77E-07	2.62E-04	6.271
33	Ctla2b	13025	2.633	4.159	7.815	5.81E-07	2.62E-04	6.414
34	S100a4	20198	2.811	3.170	7.780	6.17E-07	2.69E-04	6.248
35	Pglyrp1	21946	1.218	5.556	7.688	7.21E-07	3.06E-04	6.119
36	Asap1	13196	0.794	6.785	7.624	8.06E-07	3.23E-04	5.917
37	Nrp1	18186	2.956	3.804	7.618	8.14E-07	3.23E-04	6.069
38	Bcl2a1b	12045	1.320	5.004	7.609	8.27E-07	3.23E-04	6.036
39	Ptpn7	320139	0.712	7.574	7.566	8.90E-07	3.39E-04	5.783
40	Bspry	192120	2.589	2.381	7.538	9.34E-07	3.45E-04	5.695
41	Plscr1	22038	1.900	3.071	7.527	9.53E-07	3.45E-04	5.868
42	Mki67	17345	2.196	4.563	7.463	1.06E-06	3.77E-04	5.835
43	Gm5157	381937	2.380	1.652	7.390	1.21E-06	4.09E-04	5.254
44	Hmgb2	97165	1.374	7.537	7.389	1.21E-06	4.09E-04	5.469
45	Ssh2	237860	-0.465	9.083	-7.354	1.29E-06	4.26E-04	5.365
46	Fhl2	14200	1.438	3.942	7.302	1.41E-06	4.56E-04	5.562
47	Crmp1	12933	1.553	1.782	7.275	1.48E-06	4.68E-04	5.165
48	Ctla4	12477	2.549	4.833	7.229	1.61E-06	4.97E-04	5.417
49	Atxn1	20238	1.211	4.285	7.210	1.66E-06	5.04E-04	5.391
50	Gpr55	227326	2.456	2.904	7.184	1.74E-06	5.13E-04	5.196
51	Klc3	232943	1.360	2.869	7.178	1.76E-06	5.13E-04	5.298
52	Ccdc50	67501	1.151	5.218	7.110	1.99E-06	5.68E-04	5.146
53	Cd44	12505	1.282	6.390	7.039	2.25E-06	6.32E-04	4.904

54	Cdkn3	72391	2.506	1.139	7.026	2.31E-06	6.36E-04	4.545
55	6330403K07Rik	103712	2.703	0.074	7.013	2.36E-06	6.39E-04	3.915
56	Ttc39b	69863	0.879	5.996	6.996	2.44E-06	6.47E-04	4.862
57	Sh2d1a	20400	1.262	6.108	6.962	2.59E-06	6.76E-04	4.774
58	Unc119b	106840	0.668	7.057	6.931	2.74E-06	7.03E-04	4.657
59	Tdrp	72148	-0.649	7.069	-6.883	2.99E-06	7.48E-04	4.573
60	Hip1	215114	2.266	2.954	6.866	3.09E-06	7.48E-04	4.755
61	Glrx	93692	0.851	5.749	6.862	3.11E-06	7.48E-04	4.629
62	Dclre1a	55947	1.408	1.826	6.858	3.13E-06	7.48E-04	4.573
63	Eea1	216238	1.029	3.474	6.851	3.17E-06	7.48E-04	4.784
64	Slamf6	30925	0.864	8.189	6.827	3.32E-06	7.69E-04	4.421
65	Pla2g16	225845	0.658	6.272	6.819	3.36E-06	7.69E-04	4.497
66	Top2a	21973	1.251	5.034	6.788	3.56E-06	8.01E-04	4.584
67	Ipo4	75751	-0.650	6.519	-6.758	3.76E-06	8.35E-04	4.382
68	Adap1	231821	2.068	3.903	6.748	3.83E-06	8.37E-04	4.602
69	Plek	56193	2.044	5.438	6.694	4.23E-06	9.05E-04	4.387
70	Ckap2l	70466	1.865	2.778	6.690	4.26E-06	9.05E-04	4.447
71	Birc5	11799	2.370	4.108	6.661	4.50E-06	9.42E-04	4.435
72	Gabarapl1	57436	1.283	3.146	6.652	4.57E-06	9.43E-04	4.429
73	Dtx3	80904	0.739	4.941	6.622	4.84E-06	9.62E-04	4.255
74	Gng2	14702	0.839	5.934	6.621	4.85E-06	9.62E-04	4.164
75	Nmral1	67824	0.950	3.192	6.620	4.86E-06	9.62E-04	4.373
76	Prr13	66151	0.887	7.587	6.596	5.07E-06	9.91E-04	4.004
77	Rnf122	68867	-0.754	5.105	-6.589	5.14E-06	9.92E-04	4.207
78	Hspa9	15526	-0.455	8.330	-6.565	5.38E-06	1.02E-03	3.924
79	Id3	15903	0.519	8.020	6.561	5.41E-06	1.02E-03	3.925
80	Cenpa	12615	1.183	5.733	6.551	5.52E-06	1.03E-03	4.035
81	Rhoc	11853	2.077	1.115	6.537	5.66E-06	1.04E-03	3.845
82	Aspm	12316	2.411	2.141	6.507	5.99E-06	1.07E-03	3.992
83	Tmem154	320782	1.157	5.427	6.503	6.04E-06	1.07E-03	3.996
84	Hnrnpll	72692	0.703	5.525	6.500	6.07E-06	1.07E-03	3.971
85	Cd86	12524	0.957	4.708	6.472	6.40E-06	1.12E-03	4.032
86	Gimap7	231932	0.840	8.045	6.432	6.90E-06	1.19E-03	3.676
87	S100a13	20196	0.733	5.960	6.427	6.96E-06	1.19E-03	3.779
88	Gstp3	225884	0.833	3.874	6.415	7.12E-06	1.20E-03	3.989
89	Gzmb	14939	2.911	4.420	6.408	7.22E-06	1.20E-03	3.958
90	Smap1	98366	0.662	5.597	6.405	7.26E-06	1.20E-03	3.775
91	Stmn1	16765	1.331	6.609	6.387	7.51E-06	1.23E-03	3.652
92	Pqlc3	217430	0.904	5.115	6.378	7.64E-06	1.23E-03	3.787
93	Tmem121	69195	5.408	-2.263	6.333	8.32E-06	1.33E-03	0.507
94	Hist1h2ab	319172	2.581	0.906	6.277	9.25E-06	1.45E-03	3.346
95	Cd28	12487	0.785	7.712	6.275	9.29E-06	1.45E-03	3.382
96	Pak6	214230	2.385	0.878	6.267	9.42E-06	1.46E-03	3.339
97	Nsd2	107823	1.188	4.920	6.242	9.89E-06	1.52E-03	3.578
98	Smyd1	12180	2.698	0.332	6.236	1.00E-05	1.52E-03	3.027
99	Mxd4	17122	0.635	5.876	6.225	1.02E-05	1.53E-03	3.408
100	Klhdc1	271005	-0.554	5.460	-6.203	1.06E-05	1.58E-03	3.425
101	Car5b	56078	1.818	1.666	6.173	1.13E-05	1.66E-03	3.425
102	Ptger2	19217	1.168	3.362	6.165	1.15E-05	1.67E-03	3.553
103	Ms4a4c	64380	0.517	7.670	6.132	1.22E-05	1.75E-03	3.113
104	Sh2d2a	27371	0.587	8.618	6.130	1.23E-05	1.75E-03	3.074
105	Gnpda1	26384	0.798	6.362	6.104	1.29E-05	1.81E-03	3.124
106	Ucp2	22228	0.569	10.111	6.103	1.29E-05	1.81E-03	2.991
107	Tmprss13	214531	4.192	-1.020	6.097	1.30E-05	1.81E-03	1.742
108	Ap2s1	232910	0.521	6.479	6.075	1.36E-05	1.87E-03	3.058
109	Ptpn13	19249	1.410	2.475	6.070	1.37E-05	1.87E-03	3.345

110	Itga2	16398	2.109	2.675	6.037	1.47E-05	1.98E-03	3.296
111	1110008P14Rik	73737	0.625	4.518	6.011	1.54E-05	2.05E-03	3.159
112	Il2rb	16185	0.911	9.725	6.008	1.55E-05	2.05E-03	2.811
113	P2rx7	18439	1.378	4.030	6.001	1.57E-05	2.05E-03	3.213
114	Pdgfb	18591	1.937	1.565	5.998	1.58E-05	2.05E-03	3.068
115	Taf4b	72504	-0.676	5.574	-5.995	1.59E-05	2.05E-03	3.018
116	Ttc39c	72747	2.872	1.323	5.985	1.62E-05	2.08E-03	2.913
117	Samd3	268288	1.664	5.108	5.971	1.67E-05	2.11E-03	3.029
118	Ccna2	12428	2.351	3.806	5.963	1.69E-05	2.13E-03	3.176
119	S100a10	20194	0.820	8.459	5.943	1.76E-05	2.20E-03	2.709
120	Gnl3	30877	-0.485	6.007	-5.934	1.79E-05	2.22E-03	2.835

2.7.5 Prophylactic DEGs CD8 (OTI) pGal-OVA vs OVA

	gene_name	ENTREZID	logFC	AveExpr	t	P.Value	adj.P.Val	B
1	Gm20503	#N/A	-2.288	-0.662	-5.332	5.93E-05	0.429	-0.528
2	Gm49391	#N/A	-2.028	1.383	-5.222	7.41E-05	0.429	1.467
3	Ly9	17085	0.327	7.924	5.146	8.66E-05	0.429	1.594
4	Lrrc17	74511	-2.276	-1.363	-5.002	1.16E-04	0.432	-1.156
5	Cx3cr1	13051	-1.129	3.195	-4.531	3.11E-04	0.651	0.259
6	Vdac1	22333	0.791	5.731	4.492	3.38E-04	0.651	0.366
7	Set	56086	0.287	8.661	4.288	5.21E-04	0.651	-0.162
8	Gm20425	#N/A	-3.750	-2.122	-4.251	5.63E-04	0.651	-1.848
9	S100a4	20198	-1.302	3.170	-4.177	6.60E-04	0.651	-0.272
10	Klf13	50794	-0.438	7.824	-4.147	7.04E-04	0.651	-0.439
11	Samd1	666704	-0.700	2.493	-4.128	7.34E-04	0.651	-0.498
12	Adamts17	233332	1.870	-0.442	4.101	7.77E-04	0.651	-1.955
13	Ccr10	12777	3.452	-1.355	4.089	7.97E-04	0.651	-2.183
14	Zfp101	22643	-0.548	4.167	-4.074	8.23E-04	0.651	-0.414
15	S100a6	20200	-0.965	5.584	-4.070	8.29E-04	0.651	-0.517
16	Ampd3	11717	0.443	4.299	4.047	8.71E-04	0.651	-0.464
17	Ipo4	75751	0.398	6.519	4.046	8.74E-04	0.651	-0.580
18	Nrp1	18186	-1.315	3.804	-3.991	9.82E-04	0.651	-0.573
19	Snapc1	75627	-0.404	4.971	-3.975	1.02E-03	0.651	-0.633
20	Ddx3x	13205	0.363	7.710	3.950	1.07E-03	0.651	-0.835
21	Pi4ka	224020	0.418	6.731	3.944	1.09E-03	0.651	-0.799
22	Cnot1	234594	0.491	7.863	3.926	1.13E-03	0.651	-0.885
23	Anapc1	17222	0.422	7.466	3.913	1.16E-03	0.651	-0.898
24	Josd2	66124	-0.460	4.944	-3.906	1.18E-03	0.651	-0.778
25	Zzef1	195018	0.409	6.124	3.895	1.21E-03	0.651	-0.863
26	Psap	19156	0.432	8.540	3.891	1.22E-03	0.651	-0.980
27	Gzmb	14939	-1.496	4.420	-3.845	1.35E-03	0.651	-0.881
28	Nasp	50927	0.328	5.930	3.840	1.36E-03	0.651	-0.975
29	Atp5k	11958	-0.550	5.112	-3.815	1.43E-03	0.651	-0.985
30	Uqcr11	66594	-0.402	6.010	-3.815	1.43E-03	0.651	-1.046
31	Taf4	228980	-0.728	4.450	-3.814	1.44E-03	0.651	-0.927
32	Asap3	230837	-4.062	-5.443	-3.730	1.72E-03	0.651	-3.660
33	Heatr1	217995	0.324	7.002	3.725	1.74E-03	0.651	-1.264
34	Retreg3	67998	0.517	6.410	3.703	1.82E-03	0.651	-1.273
35	Nufip1	27275	0.290	5.477	3.657	2.01E-03	0.651	-1.302
36	Hadha	97212	0.389	6.665	3.638	2.10E-03	0.651	-1.432
37	Neurl3	214854	0.238	7.263	3.627	2.15E-03	0.651	-1.488
38	Lmbrd2	320506	-1.077	1.445	-3.619	2.19E-03	0.651	-1.593

39	Frs3	107971	-2.447	-1.919	-3.610	2.23E-03	0.651	-2.718
40	U2af1	108121	0.424	5.967	3.609	2.23E-03	0.651	-1.445
41	Usp9x	22284	0.394	6.686	3.605	2.25E-03	0.651	-1.485
42	Adam19	11492	0.457	5.847	3.600	2.28E-03	0.651	-1.453
43	Cela2a	13706	-2.701	-3.289	-3.593	2.31E-03	0.651	-3.358
44	Prrt2	69017	-2.481	-2.577	-3.585	2.35E-03	0.651	-2.927
45	Gm45062	#N/A	4.135	-4.514	3.585	2.35E-03	0.651	-3.777
46	Gm2000	#N/A	-0.329	6.394	-3.583	2.36E-03	0.651	-1.540
47	Ap4m1	11781	0.588	3.327	3.568	2.44E-03	0.651	-1.384
48	Ier3ip1	66191	-0.335	5.803	-3.566	2.45E-03	0.651	-1.537
49	Pigo	56703	-0.295	5.897	-3.557	2.50E-03	0.651	-1.547
50	Htt	15194	0.577	5.446	3.549	2.54E-03	0.651	-1.496
51	Ccr8	12776	3.205	-1.717	3.549	2.54E-03	0.651	-2.921
52	Gna13	14674	0.237	7.071	3.542	2.58E-03	0.651	-1.656
53	Paip2b	232164	0.623	4.518	3.527	2.66E-03	0.651	-1.477
54	Slc30a3	22784	2.534	-5.693	3.525	2.68E-03	0.651	-3.836
55	Tuba1c	22146	0.357	6.943	3.512	2.75E-03	0.651	-1.706
56	Mindy1	75007	-0.317	4.916	-3.506	2.79E-03	0.651	-1.568
57	Polr1a	20019	0.341	6.260	3.480	2.95E-03	0.651	-1.719
58	Dolk	227697	-0.356	4.123	-3.467	3.03E-03	0.651	-1.578
59	Dok4	114255	-1.695	-0.757	-3.464	3.05E-03	0.651	-2.692
60	Nsd3	234135	0.232	7.231	3.457	3.10E-03	0.651	-1.836
61	Hdhd2	#N/A	4.041	-4.180	3.451	3.13E-03	0.651	-3.723
62	Tbc1d9	71310	-2.764	-2.177	-3.442	3.20E-03	0.651	-3.209
63	D430042O09Rik	233865	0.716	3.153	3.432	3.26E-03	0.651	-1.634
64	Cntnap1	53321	2.928	-4.239	3.426	3.31E-03	0.651	-3.410
65	Gm49380	#N/A	-1.932	-1.356	-3.426	3.31E-03	0.651	-2.917
66	Helz2	229003	0.527	6.005	3.425	3.32E-03	0.651	-1.814
67	Hnrnpll	72692	-0.372	5.525	-3.425	3.32E-03	0.651	-1.793
68	Trip12	14897	0.305	7.788	3.421	3.34E-03	0.651	-1.928
69	Prdm11	100042784	0.498	3.800	3.414	3.40E-03	0.651	-1.659
70	Prrg2	65116	-0.821	1.065	-3.414	3.40E-03	0.651	-1.948
71	Gm42420	#N/A	-2.828	-3.416	-3.412	3.41E-03	0.651	-3.522
72	1700029I15Rik	75641	-1.202	0.273	-3.397	3.52E-03	0.651	-2.251
73	Anapc13	69010	-0.497	4.329	-3.397	3.52E-03	0.651	-1.742
74	Kmt2b	75410	0.715	4.662	3.388	3.59E-03	0.651	-1.763
75	Cdk13	69562	-0.273	6.982	-3.384	3.62E-03	0.651	-1.980
76	Rbm38	56190	-0.340	5.974	-3.378	3.67E-03	0.651	-1.931
77	Naa38	78304	-0.341	5.118	-3.373	3.71E-03	0.651	-1.863
78	Naa30	70646	0.279	5.908	3.373	3.71E-03	0.651	-1.916
79	Tmprss3	140765	-3.066	-5.552	-3.367	3.75E-03	0.651	-3.945
80	Hdgfl3	29877	0.264	5.627	3.357	3.84E-03	0.651	-1.927
81	Srebf2	20788	-0.219	7.917	-3.353	3.87E-03	0.651	-2.077
82	Max	17187	1.062	5.119	3.344	3.95E-03	0.651	-1.875
83	Samd4	74480	3.679	-4.785	3.343	3.95E-03	0.651	-3.820
84	Tmprss11a	194597	-0.893	0.209	-3.339	3.98E-03	0.651	-2.235
85	Mettl21c	433294	4.290	-3.064	3.324	4.12E-03	0.651	-3.649
86	Ing1	26356	-0.260	6.150	-3.323	4.13E-03	0.651	-2.053
87	Mgat1	17308	-0.290	7.051	-3.321	4.14E-03	0.651	-2.112
88	Lsm7	66094	-0.286	5.766	-3.321	4.15E-03	0.651	-2.026
89	Ranbp2	19386	0.343	7.004	3.316	4.19E-03	0.651	-2.095
90	Csrnp1	215418	0.448	5.786	3.312	4.22E-03	0.651	-2.020
91	Plcb2	18796	0.293	6.614	3.291	4.42E-03	0.651	-2.137
92	Arih1	23806	0.312	6.590	3.288	4.44E-03	0.651	-2.130
93	Ptpa	110854	0.285	6.952	3.286	4.47E-03	0.651	-2.171
94	Bspry	192120	-1.004	2.381	-3.275	4.57E-03	0.651	-1.941

95	Peak1	244895	0.406	6.239	3.269	4.63E-03	0.651	-2.146
96	Plin2	11520	-0.548	4.059	-3.268	4.64E-03	0.651	-1.943
97	Dyrk1b	13549	-0.436	3.442	-3.266	4.66E-03	0.651	-1.931
98	Dock2	94176	0.255	9.988	3.265	4.67E-03	0.651	-2.300
99	Actr2	66713	0.301	8.154	3.264	4.68E-03	0.651	-2.265
100	Limk1	16885	0.460	4.894	3.263	4.69E-03	0.651	-2.024
101	Nup98	269966	0.328	6.411	3.262	4.70E-03	0.651	-2.167
102	Stx4a	20909	0.613	5.405	3.259	4.73E-03	0.651	-2.087
103	Mtmr14	97287	-0.244	5.905	-3.256	4.76E-03	0.651	-2.164
104	Csrnp2	207785	0.553	4.051	3.251	4.81E-03	0.651	-1.975
105	Ssh2	237860	0.209	9.083	3.247	4.85E-03	0.651	-2.318
106	S100a11	20195	-0.334	7.140	-3.235	4.98E-03	0.651	-2.295
107	Tsc22d4	78829	-0.249	7.714	-3.231	5.02E-03	0.651	-2.323
108	Ghrl	58991	3.191	-4.489	3.224	5.09E-03	0.651	-3.823
109	Hdlbp	110611	0.245	7.168	3.223	5.10E-03	0.651	-2.303
110	Itga4	16401	-0.436	7.860	-3.221	5.13E-03	0.651	-2.344
111	Anxa2	12306	-0.661	7.045	-3.214	5.21E-03	0.651	-2.340
112	Rnd2	11858	2.877	-3.936	3.196	5.41E-03	0.651	-3.753
113	Trim46	360213	-1.055	0.020	-3.196	5.42E-03	0.651	-2.563
114	Uggt1	320011	0.347	7.632	3.192	5.46E-03	0.651	-2.389
115	Amd1	11702	0.367	5.640	3.190	5.48E-03	0.651	-2.252
116	Foxj3	230700	0.357	5.767	3.180	5.60E-03	0.651	-2.281
117	Foxk2	68837	0.354	5.116	3.180	5.60E-03	0.651	-2.214
118	Dpm3	68563	-0.373	4.357	-3.177	5.64E-03	0.651	-2.165
119	E130116L18Rik	#N/A	-1.544	-2.830	-3.170	5.72E-03	0.651	-3.245
120	Gm19345	100502736	-1.468	-1.952	-3.164	5.79E-03	0.651	-3.194

2.7.6 Prophylactic DEGs CD8 (OTI) pGal-OVA vs Saline

	gene_name	ENTREZID	logFC	AveExpr	t	P.Value	adj.P.Val	B
1	Lag3	16768	3.067	1.325	9.975	1.98E-08	2.24E-04	6.524
2	Cxcr3	12766	1.561	7.274	9.232	5.96E-08	2.24E-04	8.631
3	Zbtb32	58206	3.954	3.576	9.078	7.54E-08	2.24E-04	7.247
4	Casp3	12367	1.499	4.788	8.993	8.61E-08	2.24E-04	8.234
5	Cd86	12524	1.291	4.708	8.989	8.66E-08	2.24E-04	8.232
6	Chst2	54371	2.805	3.521	8.960	9.05E-08	2.24E-04	7.608
7	Myb	17863	1.662	5.542	8.463	1.99E-07	3.63E-04	7.465
8	Itgb1	16412	1.918	8.719	8.445	2.05E-07	3.63E-04	7.384
9	Cxcr5	12145	1.526	5.821	8.344	2.41E-07	3.63E-04	7.277
10	Ms4a4c	64380	0.699	7.670	8.293	2.62E-07	3.63E-04	7.140
11	Capn3	12335	2.081	2.591	8.278	2.69E-07	3.63E-04	6.461
12	Slamf7	75345	1.994	5.618	8.136	3.40E-07	4.20E-04	6.945
13	Bcl2a1d	12047	1.491	3.374	8.058	3.87E-07	4.42E-04	6.556
14	Psen2	19165	1.105	5.875	8.002	4.24E-07	4.50E-04	6.711
15	Ctla2a	13024	2.464	6.671	7.932	4.77E-07	4.72E-04	6.591
16	Gpr55	227326	2.769	2.904	7.866	5.33E-07	4.95E-04	5.783
17	Ctla4	12477	2.762	4.833	7.774	6.23E-07	5.39E-04	6.336
18	Bcl2a1b	12045	1.320	5.004	7.729	6.73E-07	5.39E-04	6.280
19	Ttc39b	69863	0.962	5.996	7.715	6.90E-07	5.39E-04	6.229
20	Unc119	22248	1.050	4.496	7.563	8.95E-07	6.65E-04	5.999
21	Stk39	53416	1.181	5.182	7.510	9.81E-07	6.94E-04	5.910
22	Cd44	12505	1.345	6.390	7.402	1.18E-06	7.92E-04	5.672
23	Gng2	14702	0.916	5.934	7.376	1.24E-06	7.92E-04	5.642

24	Ptms	69202	2.153	1.403	7.358	1.28E-06	7.92E-04	4.662
25	Asap1	13196	0.759	6.785	7.321	1.37E-06	8.12E-04	5.508
26	Ccnb1	268697	1.922	3.440	7.286	1.45E-06	8.30E-04	5.335
27	Arl4d	80981	1.507	3.581	7.253	1.54E-06	8.48E-04	5.351
28	Dop1b	70028	1.009	6.759	7.177	1.76E-06	9.05E-04	5.268
29	Nr1d1	217166	-1.192	1.972	-7.175	1.77E-06	9.05E-04	4.989
30	Anxa2	12306	1.505	7.045	6.993	2.45E-06	1.15E-03	4.934
31	Lxn	17035	1.013	3.795	6.992	2.45E-06	1.15E-03	4.993
32	Klhdc1	271005	-0.568	5.460	-6.986	2.48E-06	1.15E-03	4.955
33	Adam19	11492	0.862	5.847	6.945	2.67E-06	1.18E-03	4.888
34	Jdp2	81703	2.457	1.860	6.939	2.70E-06	1.18E-03	4.128
35	Top2a	21973	1.276	5.034	6.912	2.84E-06	1.20E-03	4.883
36	Slamf6	30925	0.876	8.189	6.885	2.98E-06	1.23E-03	4.685
37	Ctla2b	13025	2.396	4.159	6.862	3.11E-06	1.25E-03	4.752
38	Ptpn13	19249	1.591	2.475	6.742	3.87E-06	1.48E-03	4.236
39	Nsd2	107823	1.278	4.920	6.737	3.91E-06	1.48E-03	4.574
40	Klrk1	27007	2.094	6.409	6.711	4.10E-06	1.48E-03	4.474
41	Ptpn7	320139	0.634	7.574	6.708	4.12E-06	1.48E-03	4.373
42	Tbl1xr1	81004	0.529	6.445	6.701	4.17E-06	1.48E-03	4.403
43	1110008P14Rik	73737	0.643	4.518	6.688	4.28E-06	1.48E-03	4.480
44	Tbx21	57765	1.284	6.745	6.657	4.53E-06	1.53E-03	4.328
45	Ikzf2	22779	0.932	3.942	6.566	5.37E-06	1.77E-03	4.279
46	Glrx	93692	0.789	5.749	6.460	6.55E-06	2.11E-03	3.997
47	Ccdc50	67501	1.042	5.218	6.450	6.67E-06	2.11E-03	4.033
48	Tlk1	228012	0.502	6.741	6.425	6.99E-06	2.13E-03	3.864
49	Pla2g16	225845	0.609	6.272	6.421	7.03E-06	2.13E-03	3.881
50	Ikzf3	22780	0.821	7.185	6.384	7.56E-06	2.23E-03	3.782
51	Crmp1	12933	1.357	1.782	6.365	7.83E-06	2.23E-03	3.434
52	Ifi27l2a	76933	1.092	7.782	6.364	7.84E-06	2.23E-03	3.714
53	Pglyrp1	21946	0.998	5.556	6.354	8.00E-06	2.23E-03	3.816
54	Ezh2	14056	0.968	4.917	6.343	8.16E-06	2.23E-03	3.839
55	Gstp3	225884	0.774	3.874	6.337	8.25E-06	2.23E-03	3.869
56	Smyd1	12180	2.724	0.332	6.327	8.41E-06	2.23E-03	2.579
57	Bcat1	12035	1.064	2.164	6.312	8.66E-06	2.23E-03	3.597
58	Scd2	20250	0.704	6.025	6.308	8.71E-06	2.23E-03	3.694
59	Plscr1	22038	1.619	3.071	6.274	9.30E-06	2.34E-03	3.639
60	Slc49a4	224132	-0.660	6.006	-6.242	9.88E-06	2.45E-03	3.541
61	Cblb	208650	0.496	7.474	6.198	1.08E-05	2.62E-03	3.407
62	Gm5157	381937	2.032	1.652	6.145	1.19E-05	2.82E-03	2.964
63	Zfpm1	22761	0.628	6.167	6.143	1.20E-05	2.82E-03	3.362
64	Ampd1	229665	-0.900	4.821	-6.094	1.31E-05	3.05E-03	3.346
65	Klc3	232943	1.124	2.869	6.072	1.37E-05	3.08E-03	3.317
66	Nlrx1	270151	1.008	3.818	6.066	1.39E-05	3.08E-03	3.375
67	Unc119b	106840	0.583	7.057	6.052	1.42E-05	3.08E-03	3.141
68	P2rx7	18439	1.370	4.030	6.052	1.43E-05	3.08E-03	3.348
69	Itga4	16401	0.823	7.860	6.049	1.43E-05	3.08E-03	3.119
70	Rgs1	50778	0.935	5.162	6.038	1.46E-05	3.11E-03	3.245
71	Mki67	17345	1.839	4.563	5.996	1.59E-05	3.26E-03	3.246
72	Irf4	16364	1.289	4.641	5.996	1.59E-05	3.26E-03	3.222
73	Ptger2	19217	1.097	3.362	5.992	1.60E-05	3.26E-03	3.228
74	Lmnb1	16906	0.889	4.906	5.944	1.76E-05	3.53E-03	3.095
75	Atp1b1	11931	-0.606	6.479	-5.918	1.85E-05	3.64E-03	2.888
76	Nr1d2	353187	-0.571	4.746	-5.915	1.86E-05	3.64E-03	3.032
77	Eea1	216238	0.867	3.474	5.903	1.90E-05	3.67E-03	3.069
78	Coro7	78885	0.536	7.882	5.860	2.07E-05	3.88E-03	2.737
79	Id3	15903	0.464	8.020	5.855	2.09E-05	3.88E-03	2.720

80	Adora2a	11540	1.048	4.321	5.854	2.10E-05	3.88E-03	2.966
81	Abhd15	67477	-0.779	4.638	-5.849	2.11E-05	3.88E-03	2.887
82	Gabarapl1	57436	1.094	3.146	5.837	2.16E-05	3.92E-03	2.933
83	Pdcd1	18566	1.817	3.662	5.827	2.21E-05	3.95E-03	2.912
84	Itgal	16408	0.527	9.790	5.796	2.34E-05	4.15E-03	2.574
85	Sh2d1a	20400	1.043	6.108	5.784	2.40E-05	4.18E-03	2.668
86	Gnl3	30877	-0.440	6.007	-5.770	2.47E-05	4.18E-03	2.618
87	Tle1	21885	-1.044	4.597	-5.765	2.49E-05	4.18E-03	2.747
88	Dnah8	13417	0.633	5.743	5.762	2.51E-05	4.18E-03	2.656
89	Stx2	13852	-0.704	6.074	-5.758	2.53E-05	4.18E-03	2.600
90	Icos	54167	0.601	6.290	5.757	2.53E-05	4.18E-03	2.593
91	Rras2	66922	-0.513	7.170	-5.743	2.61E-05	4.26E-03	2.516
92	Cpne3	70568	0.680	5.754	5.721	2.72E-05	4.39E-03	2.579
93	Hmgb2	97165	1.070	7.537	5.702	2.83E-05	4.52E-03	2.437
94	Pif1	208084	3.609	0.265	5.694	2.87E-05	4.53E-03	1.557
95	Pltp	18830	-0.733	3.842	-5.689	2.90E-05	4.53E-03	2.653
96	Lrmp	16970	0.549	7.619	5.681	2.95E-05	4.56E-03	2.389
97	Gpr174	213439	0.698	5.974	5.671	3.00E-05	4.60E-03	2.455
98	Atxn1	20238	0.939	4.285	5.664	3.04E-05	4.62E-03	2.605
99	Mdfic	16543	1.641	2.284	5.653	3.12E-05	4.68E-03	2.459
100	Gpr146	80290	-0.664	5.934	-5.637	3.22E-05	4.78E-03	2.366
101	Uspl1	231915	-0.423	6.543	-5.617	3.35E-05	4.92E-03	2.299
102	Apaf1	11783	0.713	5.605	5.577	3.62E-05	5.27E-03	2.316
103	Samd3	268288	1.560	5.108	5.543	3.88E-05	5.59E-03	2.316
104	S100a6	20200	1.472	5.584	5.528	4.00E-05	5.64E-03	2.249
105	Pqlc3	217430	0.763	5.115	5.526	4.01E-05	5.64E-03	2.246
106	Rhoc	11853	1.761	1.115	5.523	4.04E-05	5.64E-03	1.907
107	Ucp2	22228	0.518	10.111	5.516	4.09E-05	5.64E-03	2.002
108	Cdkn3	72391	1.983	1.139	5.515	4.10E-05	5.64E-03	1.863
109	Hspa9	15526	-0.381	8.330	-5.511	4.14E-05	5.64E-03	2.022
110	Sh3tc1	231147	-1.153	2.579	-5.480	4.40E-05	5.75E-03	2.235
111	Sgk3	170755	-0.453	5.479	-5.474	4.46E-05	5.75E-03	2.085
112	Adgrb2	230775	-0.723	3.509	-5.472	4.47E-05	5.75E-03	2.246
113	Rgs16	19734	2.081	1.874	5.472	4.47E-05	5.75E-03	2.041
114	Ccna2	12428	2.215	3.806	5.471	4.48E-05	5.75E-03	2.263
115	Ggt1	14598	-0.847	6.104	-5.468	4.50E-05	5.75E-03	2.019
116	Arhgap5	11855	-0.672	4.294	-5.466	4.53E-05	5.75E-03	2.182
117	Tspan3	56434	-0.487	5.029	-5.465	4.53E-05	5.75E-03	2.103
118	Prr13	66151	0.734	7.587	5.452	4.66E-05	5.82E-03	1.925
119	Ifrd2	15983	-0.623	5.216	-5.451	4.66E-05	5.82E-03	2.054
120	Pou2f2	18987	0.687	4.287	5.445	4.72E-05	5.84E-03	2.155

2.7.7 Therapeutic DEGs CD4 OVA (OTII) vs Saline

	gene_name	logFC	AveExpr	t	P.Value	adj.P.Val	B
1	P2rx7	1.799	6.798	11.930	8.32E-13	1.30E-08	19.082
2	Hmgn1	-1.330	6.575	-10.674	1.21E-11	9.45E-08	16.558
3	Hist1h2bc	-1.944	3.150	-9.222	3.45E-10	1.79E-06	12.690
4	Gstt2	1.241	5.492	8.653	1.38E-09	5.37E-06	11.955
5	Art2b	2.129	6.031	8.173	4.59E-09	1.43E-05	10.822
6	Tox2	2.575	7.240	8.034	6.54E-09	1.45E-05	10.487
7	Smtn	2.109	5.982	7.962	7.87E-09	1.45E-05	10.299
8	Psen2	1.067	7.142	7.943	8.25E-09	1.45E-05	10.260

9	Izumo1r	1.216	9.405	7.909	9.02E-09	1.45E-05	10.170
10	Penk	-3.346	4.603	-7.897	9.29E-09	1.45E-05	10.071
11	Cdc25b	1.212	6.750	7.828	1.11E-08	1.57E-05	9.972
12	Cd7	-1.752	4.199	-7.746	1.37E-08	1.76E-05	9.719
13	Cxcr5	1.781	7.629	7.720	1.47E-08	1.76E-05	9.698
14	Maged1	-2.591	2.913	-7.666	1.69E-08	1.88E-05	9.332
15	Vps37b	-1.124	6.643	-7.436	3.08E-08	2.95E-05	8.976
16	Ctrc	-2.603	2.986	-7.426	3.17E-08	2.95E-05	8.630
17	Rgmb	-1.755	4.024	-7.419	3.22E-08	2.95E-05	8.906
18	Pmepa1	-2.485	2.325	-7.333	4.03E-08	3.49E-05	8.241
19	Pdzk1ip1	-2.380	2.503	-7.248	5.06E-08	4.14E-05	8.197
20	Maz	0.858	6.987	7.186	5.96E-08	4.20E-05	8.331
21	Bmyc	-1.116	5.195	-7.186	5.96E-08	4.20E-05	8.348
22	Krt10	-1.605	2.372	-7.182	6.03E-08	4.20E-05	7.843
23	Lrmp	0.826	8.248	7.171	6.21E-08	4.20E-05	8.286
24	D830030K20Rik	-1.929	4.984	-7.128	6.95E-08	4.26E-05	8.197
25	Gm3488	-2.975	2.156	-7.123	7.06E-08	4.26E-05	7.655
26	Arl4c	-1.335	5.397	-7.077	7.98E-08	4.26E-05	8.064
27	Wdr26	0.982	7.691	7.072	8.08E-08	4.26E-05	8.031
28	Sostdc1	2.431	7.045	7.059	8.37E-08	4.26E-05	8.006
29	Crppa	1.821	4.895	7.055	8.45E-08	4.26E-05	7.990
30	Slc26a11	1.306	7.318	7.049	8.59E-08	4.26E-05	7.975
31	Btg3	-1.043	4.548	-7.045	8.67E-08	4.26E-05	7.985
32	Slc11a2	1.188	5.875	7.040	8.80E-08	4.26E-05	7.965
33	Tbc1d4	1.012	8.583	7.030	9.04E-08	4.26E-05	7.918
34	Camk2d	0.792	7.283	7.019	9.30E-08	4.26E-05	7.895
35	Sgsh	0.953	6.208	7.006	9.63E-08	4.28E-05	7.874
36	Cish	-2.363	4.632	-6.994	9.96E-08	4.31E-05	7.850
37	Creb5	-2.237	3.095	-6.971	1.06E-07	4.45E-05	7.592
38	Socs1	-0.968	6.333	-6.955	1.10E-07	4.52E-05	7.732
39	Rara	-1.001	5.183	-6.937	1.16E-07	4.62E-05	7.706
40	Trpv2	0.786	7.569	6.913	1.24E-07	4.81E-05	7.614
41	Il7r	-1.504	7.617	-6.899	1.28E-07	4.87E-05	7.578
42	Itga7	1.925	3.622	6.883	1.34E-07	4.97E-05	7.417
43	Akap12	1.307	5.665	6.865	1.41E-07	5.09E-05	7.515
44	Arhgap5	-1.022	4.870	-6.849	1.47E-07	5.19E-05	7.481
45	Pgd	0.742	5.999	6.810	1.63E-07	5.55E-05	7.362
46	Gm3252	-2.750	2.476	-6.805	1.65E-07	5.55E-05	6.924
47	Mettl1	-1.455	3.179	-6.800	1.68E-07	5.55E-05	7.227
48	H2-Q2	2.475	5.336	6.775	1.80E-07	5.82E-05	7.285
49	Prrt1	-2.330	1.457	-6.695	2.23E-07	6.97E-05	6.223
50	Pdcd1	1.754	7.128	6.693	2.24E-07	6.97E-05	7.040
51	Id2	-1.088	7.649	-6.611	2.80E-07	8.55E-05	6.814
52	Sdhaf1	-1.170	5.512	-6.573	3.10E-07	9.28E-05	6.749
53	Sh2d1a	1.119	7.035	6.538	3.41E-07	1.00E-04	6.628
54	Bcam	-2.352	2.197	-6.519	3.59E-07	1.04E-04	6.267
55	Tmem254c	1.026	5.338	6.511	3.67E-07	1.04E-04	6.593
56	Irak4	0.847	5.609	6.484	3.95E-07	1.10E-04	6.513
57	Gm3591	-2.237	2.467	-6.473	4.07E-07	1.11E-04	6.265
58	Ubash3b	1.069	5.490	6.460	4.22E-07	1.13E-04	6.455
59	Samhd1	0.643	8.825	6.444	4.40E-07	1.16E-04	6.369
60	Lmna	-1.876	4.057	-6.426	4.63E-07	1.18E-04	6.375
61	Ifitm3	-2.472	3.157	-6.423	4.67E-07	1.18E-04	6.289
62	Icam1	-1.089	5.389	-6.419	4.71E-07	1.18E-04	6.334
63	Gfi1	1.336	5.632	6.415	4.77E-07	1.18E-04	6.341
64	Crem	-1.084	3.786	-6.379	5.27E-07	1.28E-04	6.252

65	Jaml	-1.930	3.027	-6.363	5.49E-07	1.32E-04	6.135
66	Vkorc1	-0.942	3.579	-6.336	5.92E-07	1.40E-04	6.127
67	Zfp839	1.159	4.399	6.291	6.70E-07	1.56E-04	6.024
68	Ttll12	1.219	5.809	6.281	6.88E-07	1.58E-04	5.967
69	Bmp7	0.929	6.148	6.265	7.19E-07	1.62E-04	5.919
70	Rab37	0.826	7.262	6.260	7.29E-07	1.62E-04	5.882
71	Tuba1b	-0.952	8.439	-6.211	8.35E-07	1.83E-04	5.743
72	Gm3558	-2.512	2.088	-6.205	8.49E-07	1.84E-04	5.526
73	Tubb5	-0.745	6.955	-6.185	8.97E-07	1.91E-04	5.679
74	Pear1	0.685	7.201	6.179	9.11E-07	1.92E-04	5.666
75	St3gal1	0.722	6.701	6.145	1.00E-06	2.08E-04	5.578
76	Tigit	2.401	4.725	6.138	1.02E-06	2.09E-04	5.627
77	Cers4	0.995	6.310	6.112	1.10E-06	2.22E-04	5.506
78	Ddit4	1.061	6.378	6.078	1.20E-06	2.40E-04	5.407
79	Tgfb3	2.904	2.271	6.051	1.30E-06	2.56E-04	5.039
80	Ube2h	0.928	8.151	6.027	1.39E-06	2.70E-04	5.247
81	Camk4	0.801	6.610	6.023	1.40E-06	2.70E-04	5.250
82	Lrp6	-0.800	4.567	-6.011	1.45E-06	2.73E-04	5.274
83	Epas1	-1.636	1.636	-6.010	1.46E-06	2.73E-04	5.001
84	Cpq	1.159	4.532	6.001	1.49E-06	2.77E-04	5.266
85	Sdcbp2	1.168	4.908	5.981	1.58E-06	2.86E-04	5.205
86	Prpf40b	-1.510	3.357	-5.978	1.59E-06	2.86E-04	5.175
87	Uap1l1	0.903	5.767	5.972	1.62E-06	2.86E-04	5.144
88	Hist1h2bg	-1.762	1.621	-5.971	1.62E-06	2.86E-04	4.802
89	E2f2	1.444	4.855	5.954	1.70E-06	2.97E-04	5.140
90	Yipf3	0.590	6.979	5.945	1.74E-06	3.01E-04	5.035
91	Coro7	0.624	8.415	5.923	1.85E-06	3.17E-04	4.965
92	Slc43a1	3.594	2.637	5.914	1.90E-06	3.21E-04	4.699
93	Chchd10	-1.091	3.804	-5.888	2.04E-06	3.41E-04	4.970
94	Tbcel	0.867	5.484	5.874	2.12E-06	3.51E-04	4.886
95	Igfbp4	-1.807	2.978	-5.864	2.18E-06	3.51E-04	4.881
96	Ikzf4	-2.428	1.960	-5.864	2.18E-06	3.51E-04	4.714
97	Tnfrsf26	0.802	6.111	5.863	2.19E-06	3.51E-04	4.834
98	Gm3636	-1.140	4.280	-5.857	2.22E-06	3.53E-04	4.889
99	Gm3411	-2.197	1.714	-5.852	2.25E-06	3.54E-04	4.514
100	Gm5796	-3.025	0.823	-5.841	2.32E-06	3.62E-04	4.349
101	Nfkb2	-0.673	7.106	-5.822	2.45E-06	3.72E-04	4.694
102	Stim1	0.674	6.972	5.821	2.46E-06	3.72E-04	4.696
103	Ifitm2	-2.765	3.036	-5.820	2.46E-06	3.72E-04	4.750
104	Nolc1	-0.613	6.686	-5.807	2.56E-06	3.83E-04	4.659
105	Pfkp	0.827	8.366	5.795	2.64E-06	3.92E-04	4.617
106	Hist1h1c	-1.515	4.961	-5.786	2.71E-06	3.96E-04	4.674
107	Csnk1e	-0.714	4.443	-5.784	2.72E-06	3.96E-04	4.683
108	Gng2	0.953	6.240	5.769	2.84E-06	4.06E-04	4.577
109	Ezh1	0.791	7.143	5.768	2.85E-06	4.06E-04	4.551
110	Gpr55	1.346	3.506	5.759	2.92E-06	4.07E-04	4.599
111	Wnt10a	-2.471	5.047	-5.756	2.94E-06	4.07E-04	4.598
112	Slamf6	0.794	9.436	5.754	2.96E-06	4.07E-04	4.506
113	Lta	-1.092	5.293	-5.754	2.96E-06	4.07E-04	4.567
114	Rgs3	0.753	7.613	5.749	3.00E-06	4.07E-04	4.495
115	Hist2h4	-1.552	2.897	-5.748	3.01E-06	4.07E-04	4.542
116	Hspe1	-0.947	6.837	-5.737	3.10E-06	4.16E-04	4.468
117	Pcgf5	-0.696	5.786	-5.723	3.23E-06	4.28E-04	4.456
118	Rpa1	0.840	8.184	5.721	3.24E-06	4.28E-04	4.417
119	Zdhhc2	2.140	4.114	5.709	3.35E-06	4.39E-04	4.495
120	Gm2237	-1.016	4.249	-5.674	3.70E-06	4.80E-04	4.405

2.7.8 Therapeutic DEGs CD4 (OTII) pGal vs OVA

	gene_name	logFC	AveExpr	t	P.Value	adj.P.Val	B
1	Hist1h2bc	1.326	3.150	6.385	5.18E-07	0.004	5.921
2	Flna	-0.855	9.916	-6.358	5.58E-07	0.004	6.181
3	Bmyc	0.869	5.195	6.091	1.16E-06	0.005	5.503
4	Itga7	-1.279	3.622	-5.985	1.56E-06	0.005	5.188
5	Prrt1	1.974	1.457	5.956	1.69E-06	0.005	4.122
6	Gm3252	2.211	2.476	5.626	4.23E-06	0.010	3.828
7	Smc4	0.665	9.225	5.617	4.34E-06	0.010	4.193
8	Cdc25b	-0.731	6.750	-5.364	8.80E-06	0.016	3.517
9	Neurl3	0.561	6.463	5.344	9.30E-06	0.016	3.473
10	Pdlim1	-0.856	6.750	-5.257	1.19E-05	0.018	3.230
11	S100a6	-1.281	6.152	-5.209	1.36E-05	0.019	3.119
12	F830016B08Rik	1.251	3.465	5.143	1.63E-05	0.019	2.984
13	P2rx7	-0.665	6.798	-5.131	1.69E-05	0.019	2.885
14	D830030K20Rik	1.316	4.984	5.120	1.74E-05	0.019	2.951
15	Rhbdl3	0.901	3.602	5.003	2.41E-05	0.025	2.651
16	Gm3411	1.775	1.714	4.964	2.70E-05	0.026	2.172
17	Gemin8	0.648	4.116	4.888	3.33E-05	0.027	2.349
18	Tgfb3	-1.639	2.271	-4.881	3.40E-05	0.027	2.296
19	Pibf1	0.588	4.881	4.869	3.52E-05	0.027	2.272
20	Galnt6	-0.566	8.353	-4.858	3.62E-05	0.027	2.141
21	F2rl1	-1.222	2.715	-4.844	3.77E-05	0.027	2.217
22	Chst10	-0.661	5.694	-4.837	3.84E-05	0.027	2.126
23	Grk6	-0.649	9.074	-4.813	4.11E-05	0.028	2.019
24	Pdzk1ip1	1.561	2.503	4.715	5.41E-05	0.032	1.813
25	Gcnt1	1.198	4.634	4.701	5.62E-05	0.032	1.851
26	Adap1	-1.159	4.448	-4.683	5.91E-05	0.032	1.792
27	Id2	0.690	7.649	4.680	5.97E-05	0.032	1.666
28	Arhgap5	0.650	4.870	4.673	6.07E-05	0.032	1.754
29	Vars	0.525	8.309	4.665	6.21E-05	0.032	1.622
30	Gm3488	1.975	2.156	4.642	6.63E-05	0.032	1.502
31	Lpin3	-2.187	-0.505	-4.633	6.79E-05	0.032	0.881
32	Ryr1	-1.727	2.038	-4.623	7.00E-05	0.032	1.571
33	Ssbp2	0.591	5.374	4.618	7.08E-05	0.032	1.575
34	Hsd11b1	-0.729	7.269	-4.616	7.12E-05	0.032	1.495
35	Wdfy2	-0.968	4.185	-4.607	7.32E-05	0.032	1.617
36	Arhgap31	0.713	6.537	4.599	7.46E-05	0.032	1.472
37	Mib2	0.568	6.694	4.598	7.50E-05	0.032	1.461
38	Sh3gl3	0.927	3.343	4.572	8.06E-05	0.033	1.543
39	Rab6b	0.610	4.468	4.564	8.23E-05	0.033	1.478
40	Kcnb2	2.618	-3.507	4.547	8.63E-05	0.033	-0.628
41	Lrrc8c	-0.710	6.958	-4.547	8.65E-05	0.033	1.313
42	Hdgfl3	0.602	5.251	4.525	9.19E-05	0.033	1.330
43	Ccr4	-1.359	3.449	-4.524	9.22E-05	0.033	1.418
44	Lta	0.789	5.293	4.518	9.36E-05	0.033	1.317
45	Krt10	0.981	2.372	4.492	1.01E-04	0.035	1.218
46	Scarb2	-0.606	5.576	-4.486	1.02E-04	0.035	1.189
47	Vasp	-0.476	8.035	-4.479	1.04E-04	0.035	1.123
48	Me2	-0.523	6.741	-4.439	1.17E-04	0.038	1.029
49	Extl3	-0.595	5.689	-4.427	1.21E-04	0.038	1.033
50	Smad3	-0.695	5.728	-4.406	1.28E-04	0.040	0.974
51	Tbcel	-0.562	5.484	-4.396	1.31E-04	0.040	0.956
52	Penk	1.854	4.603	4.394	1.32E-04	0.040	1.084
53	Gk	-1.036	3.230	-4.387	1.35E-04	0.040	1.075

54	Igf1r	0.777	4.944	4.351	1.49E-04	0.042	0.885
55	Fhl2	-1.546	1.300	-4.350	1.50E-04	0.042	0.834
56	Vsir	-0.831	7.966	-4.329	1.58E-04	0.042	0.724
57	E2f2	-0.839	4.855	-4.325	1.60E-04	0.042	0.807
58	Pmepa1	1.497	2.325	4.325	1.60E-04	0.042	0.816
59	Ly6m	1.398	1.316	4.321	1.62E-04	0.042	0.757
60	Stim1	-0.444	6.972	-4.317	1.64E-04	0.042	0.698
61	Cep57l1	0.748	3.209	4.300	1.71E-04	0.044	0.856
62	Sytl1	0.924	3.791	4.278	1.82E-04	0.044	0.798
63	Ddx43	1.324	1.702	4.278	1.82E-04	0.044	0.642
64	Dnajb7	2.754	-2.605	4.277	1.83E-04	0.044	-0.610
65	Smc6	0.445	7.466	4.268	1.88E-04	0.045	0.565
66	Fam171b	-3.480	-2.032	-4.212	2.19E-04	0.052	-0.425
67	Taf2	-0.669	5.270	-4.200	2.26E-04	0.052	0.463
68	Cxcr5	-0.857	7.629	-4.199	2.27E-04	0.052	0.380
69	Acot11	-0.758	4.848	-4.191	2.32E-04	0.052	0.462
70	Lysmd3	-0.944	4.037	-4.187	2.34E-04	0.052	0.525
71	2010300C02Rik	1.411	2.148	4.169	2.46E-04	0.054	0.466
72	Gucd1	-0.682	5.431	-4.164	2.49E-04	0.054	0.352
73	Psat1	-0.892	4.909	-4.159	2.53E-04	0.054	0.361
74	Zbtb20	0.613	6.891	4.143	2.64E-04	0.055	0.249
75	Zmat1	0.572	4.363	4.143	2.65E-04	0.055	0.408
76	Pfkp	-0.527	8.366	-4.140	2.67E-04	0.055	0.223
77	Gm3739	0.885	3.945	4.130	2.74E-04	0.055	0.425
78	Tmie	0.632	3.737	4.129	2.74E-04	0.055	0.397
79	Pkn1	-0.333	8.429	-4.115	2.86E-04	0.055	0.156
80	Cxxc5	1.160	3.133	4.109	2.90E-04	0.055	0.384
81	Kcnab2	-0.507	7.154	-4.107	2.92E-04	0.055	0.143
82	Gm3591	1.420	2.467	4.103	2.96E-04	0.055	0.323
83	Slc25a42	0.643	4.117	4.097	3.00E-04	0.055	0.292
84	Slc39a6	-1.157	5.158	-4.097	3.00E-04	0.055	0.175
85	Txnrd1	-0.815	6.189	-4.095	3.02E-04	0.055	0.131
86	Dhcr7	-0.673	4.841	-4.094	3.03E-04	0.055	0.204
87	Ap1b1	-0.670	7.755	-4.085	3.10E-04	0.055	0.079
88	Thg1l	-1.164	1.137	-4.083	3.12E-04	0.055	0.119
89	Gm3558	1.650	2.088	4.067	3.26E-04	0.055	0.201
90	Nbeal2	-0.525	7.527	-4.064	3.29E-04	0.055	0.029
91	Ikzf1	-0.328	7.919	-4.058	3.34E-04	0.055	0.010
92	Rhobtb2	-0.495	5.542	-4.056	3.36E-04	0.055	0.066
93	Atp2a3	-0.810	8.936	-4.056	3.36E-04	0.055	0.001
94	Cd86	1.003	3.626	4.053	3.39E-04	0.055	0.235
95	Tigit	-1.132	4.725	-4.049	3.42E-04	0.055	0.068
96	Tacc2	-1.487	3.498	-4.047	3.44E-04	0.055	0.184
97	Gm8108	1.360	2.670	4.046	3.45E-04	0.055	0.202
98	Vgll3	2.260	-3.643	4.037	3.54E-04	0.056	-1.240
99	Ttc13	-0.520	6.210	-4.023	3.68E-04	0.058	-0.057
100	Rpa1	-0.526	8.184	-4.013	3.77E-04	0.058	-0.109
101	Gm2956	1.761	2.185	4.011	3.80E-04	0.058	0.078
102	Myh7b	-4.528	-2.886	-4.009	3.82E-04	0.058	-1.510
103	Pck2	0.515	5.352	4.004	3.87E-04	0.058	-0.055
104	Ovca2	-0.581	4.647	-3.992	4.00E-04	0.059	-0.039
105	S1pr1	-0.683	8.625	-3.991	4.01E-04	0.059	-0.167
106	Acss1	-0.650	5.851	-3.989	4.03E-04	0.059	-0.129
107	Kdm2a	-0.525	7.200	-3.979	4.14E-04	0.060	-0.191
108	Gbp8	0.430	7.243	3.978	4.15E-04	0.060	-0.190
109	Eea1	0.473	6.685	3.956	4.41E-04	0.063	-0.241

110	Slc16a5	-1.352	3.092	-3.946	4.53E-04	0.064	-0.015
111	Gm3500	1.703	2.319	3.942	4.59E-04	0.064	-0.082
112	Rnf125	-0.611	6.437	-3.936	4.65E-04	0.064	-0.292
113	Nfix	0.692	3.645	3.933	4.69E-04	0.064	-0.059
114	S1pr4	-0.483	6.443	-3.932	4.70E-04	0.064	-0.299
115	Slc43a1	-1.402	2.637	-3.931	4.72E-04	0.064	-0.077
116	Edem1	-0.486	7.978	-3.926	4.78E-04	0.064	-0.334
117	Man2b1	-0.404	7.893	-3.919	4.88E-04	0.064	-0.353
118	Snn	-0.931	3.336	-3.917	4.90E-04	0.064	-0.113
119	Zdhhc18	-0.606	7.865	-3.916	4.92E-04	0.064	-0.361
120	Gm3194	1.505	1.684	3.912	4.97E-04	0.064	-0.170

2.7.9 Therapeutic DEGs CD4 (OTII) pGal-OVA vs Saline

	gene_name	logFC	AveExpr	t	P.Value	adj.P.Val	B
1	Izumo1r	1.322	9.405	7.875	9.84E-09	1.53E-04	10.072
2	P2rx7	1.134	6.798	6.910	1.25E-07	9.71E-04	7.636
3	Hmgn1	-0.903	6.575	-6.692	2.24E-07	1.16E-03	7.074
4	Samhd1	0.710	8.825	6.520	3.58E-07	1.39E-03	6.624
5	Gstt2	0.984	5.492	6.369	5.42E-07	1.69E-03	6.225
6	Bmp7	1.001	6.148	6.244	7.63E-07	1.98E-03	5.904
7	Adrb2	-1.347	5.453	-6.037	1.35E-06	2.78E-03	5.362
8	Myb	0.970	5.925	6.016	1.43E-06	2.78E-03	5.305
9	Icam1	-1.107	5.389	-5.947	1.73E-06	3.00E-03	5.122
10	Cd7	-1.329	4.199	-5.587	4.71E-06	7.33E-03	4.179
11	Trat1	-1.267	5.650	-5.466	6.60E-06	9.34E-03	3.843
12	Lrp6	-0.784	4.567	-5.392	8.13E-06	1.06E-02	3.665
13	Tbc1d4	0.840	8.583	5.349	9.17E-06	1.10E-02	3.501
14	Crppa	1.437	4.895	5.219	1.32E-05	1.39E-02	3.217
15	Smtn	1.484	5.982	5.196	1.41E-05	1.39E-02	3.136
16	Sgsh	0.765	6.208	5.176	1.49E-05	1.39E-02	3.059
17	Ces2c	0.955	4.833	5.167	1.53E-05	1.39E-02	3.076
18	Vps37b	-0.845	6.643	-5.149	1.61E-05	1.39E-02	2.970
19	Tubb4b	-0.684	7.030	-5.069	2.01E-05	1.54E-02	2.751
20	Ly6c1	-1.902	1.063	-5.062	2.05E-05	1.54E-02	2.317
21	Slc26a11	1.020	7.318	5.057	2.08E-05	1.54E-02	2.723
22	Art2b	1.411	6.031	5.009	2.37E-05	1.68E-02	2.632
23	Rgmb	-1.226	4.024	-4.986	2.54E-05	1.72E-02	2.605
24	Mettl1	-1.136	3.179	-4.955	2.76E-05	1.79E-02	2.492
25	Psen2	0.724	7.142	4.942	2.87E-05	1.79E-02	2.415
26	Arl4c	-0.990	5.397	-4.908	3.15E-05	1.79E-02	2.355
27	Slamf6	0.737	9.436	4.892	3.29E-05	1.79E-02	2.271
28	Gfi1	1.098	5.632	4.892	3.30E-05	1.79E-02	2.330
29	Lmnb2	-0.757	4.734	-4.889	3.33E-05	1.79E-02	2.332
30	Decr1	0.830	5.519	4.852	3.68E-05	1.91E-02	2.222
31	H2-Q2	1.879	5.336	4.829	3.94E-05	1.94E-02	2.191
32	Slc9b2	2.185	3.880	4.824	3.99E-05	1.94E-02	2.156
33	Socs1	-0.727	6.333	-4.811	4.14E-05	1.95E-02	2.066
34	Zfp184	-4.377	-3.683	-4.801	4.25E-05	1.95E-02	-0.512
35	Vsig10l	1.718	2.799	4.762	4.75E-05	2.11E-02	1.872
36	Oas2	-1.866	2.292	-4.710	5.49E-05	2.37E-02	1.809
37	Eef1e1	-0.677	4.805	-4.655	6.39E-05	2.54E-02	1.715
38	Lrmp	0.585	8.248	4.652	6.44E-05	2.54E-02	1.629

39	Rrad	-0.922	6.091	-4.646	6.55E-05	2.54E-02	1.634
40	Bysl	-0.733	4.838	-4.618	7.08E-05	2.54E-02	1.613
41	Camk2d	0.568	7.283	4.617	7.10E-05	2.54E-02	1.542
42	Matk	1.052	7.112	4.615	7.14E-05	2.54E-02	1.540
43	Ephx1	0.968	8.241	4.604	7.37E-05	2.54E-02	1.499
44	Tubb5	-0.604	6.955	-4.600	7.45E-05	2.54E-02	1.495
45	Tuba1b	-0.769	8.439	-4.597	7.52E-05	2.54E-02	1.480
46	Pex6	0.494	7.026	4.596	7.53E-05	2.54E-02	1.487
47	Tox2	1.599	7.240	4.589	7.68E-05	2.54E-02	1.478
48	Pear1	0.552	7.201	4.568	8.16E-05	2.65E-02	1.411
49	Inf2	-1.264	3.203	-4.539	8.83E-05	2.80E-02	1.449
50	Tnfrsf19	-2.814	-0.205	-4.525	9.19E-05	2.84E-02	0.787
51	Nt5e	0.938	6.540	4.520	9.30E-05	2.84E-02	1.297
52	Acvrl1	-2.078	1.525	-4.507	9.67E-05	2.86E-02	1.228
53	Cers4	0.796	6.310	4.505	9.72E-05	2.86E-02	1.268
54	Akap12	0.927	5.665	4.493	1.00E-04	2.87E-02	1.262
55	Epas1	-1.330	1.636	-4.490	1.01E-04	2.87E-02	1.177
56	Tmie	0.894	3.737	4.481	1.04E-04	2.89E-02	1.313
57	Tuba4a	-0.828	7.596	-4.459	1.10E-04	2.94E-02	1.113
58	Ipcef1	0.642	7.271	4.458	1.11E-04	2.94E-02	1.117
59	Traf4	-0.677	4.960	-4.449	1.13E-04	2.94E-02	1.156
60	Bpnt1	-0.917	3.683	-4.445	1.15E-04	2.94E-02	1.220
61	Gimap7	0.926	6.938	4.442	1.16E-04	2.94E-02	1.080
62	Klf2	-0.879	9.411	-4.438	1.17E-04	2.94E-02	1.057
63	Isoc2b	0.783	4.784	4.388	1.34E-04	3.27E-02	1.042
64	Ier5	-0.674	8.063	-4.388	1.35E-04	3.27E-02	0.924
65	Hspe1	-0.787	6.837	-4.377	1.38E-04	3.32E-02	0.904
66	Dnajb1	-1.405	8.946	-4.363	1.44E-04	3.37E-02	0.857
67	Rab37	0.627	7.262	4.361	1.45E-04	3.37E-02	0.860
68	Lypd3	-4.352	-3.861	-4.338	1.54E-04	3.53E-02	-1.069
69	Sgk1	-0.960	6.072	-4.330	1.58E-04	3.56E-02	0.797
70	Abtb1	0.453	6.536	4.319	1.63E-04	3.62E-02	0.762
71	Ccs	0.562	5.645	4.314	1.65E-04	3.62E-02	0.784
72	Srm	-0.731	5.274	-4.287	1.78E-04	3.85E-02	0.716
73	Eva1b	0.701	5.281	4.276	1.83E-04	3.85E-02	0.716
74	Coprs	2.352	-0.203	4.276	1.83E-04	3.85E-02	-0.216
75	Hspa8	-0.669	11.732	-4.267	1.88E-04	3.85E-02	0.613
76	Uap1l1	0.699	5.767	4.263	1.90E-04	3.85E-02	0.651
77	Tox	0.591	7.344	4.263	1.90E-04	3.85E-02	0.599
78	Rell1	-0.626	4.470	-4.254	1.95E-04	3.89E-02	0.687
79	Nolc1	-0.488	6.686	-4.246	1.99E-04	3.92E-02	0.559
80	Mmd	1.280	4.542	4.241	2.02E-04	3.93E-02	0.687
81	Cenpa	0.605	5.864	4.225	2.11E-04	4.06E-02	0.538
82	Tgtp1	-0.967	6.132	-4.217	2.16E-04	4.09E-02	0.493
83	Ctrc	-1.445	2.986	-4.212	2.19E-04	4.11E-02	0.637
84	Nfkb2	-0.529	7.106	-4.199	2.27E-04	4.16E-02	0.430
85	Oasl2	-1.175	3.805	-4.198	2.27E-04	4.16E-02	0.573
86	Socs3	-1.096	7.027	-4.193	2.30E-04	4.17E-02	0.416
87	Rasgef1a	1.871	2.610	4.175	2.42E-04	4.29E-02	0.490
88	Taf4b	-0.890	4.199	-4.174	2.43E-04	4.29E-02	0.493
89	Gstt3	1.199	2.331	4.162	2.51E-04	4.31E-02	0.427
90	Cgas	-1.636	1.610	-4.162	2.51E-04	4.31E-02	0.392
91	Cish	-1.385	4.632	-4.160	2.52E-04	4.31E-02	0.411
92	Nrn1	1.604	2.991	4.151	2.59E-04	4.38E-02	0.476
93	Ddx51	-0.646	5.428	-4.129	2.75E-04	4.60E-02	0.301
94	Adamts3	2.134	1.527	4.124	2.78E-04	4.61E-02	0.183

95	Odf2l	-1.272	2.567	-4.109	2.90E-04	4.73E-02	0.337
96	Zfp839	0.817	4.399	4.107	2.92E-04	4.73E-02	0.354
97	Prpf40b	-1.091	3.357	-4.094	3.02E-04	4.83E-02	0.346
98	Rasa1	0.530	7.715	4.090	3.06E-04	4.83E-02	0.143
99	Sit1	-0.709	6.896	-4.080	3.14E-04	4.83E-02	0.124
100	Tmem220	1.866	0.005	4.079	3.15E-04	4.83E-02	-0.231
101	Lmna	-1.210	4.057	-4.078	3.16E-04	4.83E-02	0.254
102	Maged1	-1.326	2.913	-4.078	3.16E-04	4.83E-02	0.291
103	Creb5	-1.307	3.095	-4.072	3.21E-04	4.86E-02	0.292
104	Cxcl10	-1.804	2.720	-4.059	3.33E-04	4.98E-02	0.261
105	Ctdsp2	0.480	6.785	4.056	3.36E-04	4.98E-02	0.065
106	Maf	0.791	6.286	4.050	3.41E-04	5.01E-02	0.073
107	Gatd1	0.526	5.678	4.006	3.85E-04	5.60E-02	-0.021
108	Penk	-1.492	4.603	-4.002	3.89E-04	5.61E-02	-0.020
109	Proser3	0.720	2.990	3.996	3.96E-04	5.65E-02	0.101
110	Clec2i	0.783	5.799	3.983	4.10E-04	5.80E-02	-0.081
111	Sbk2	3.999	0.733	3.975	4.18E-04	5.87E-02	-0.553
112	Hcn2	3.358	-2.152	3.943	4.57E-04	6.36E-02	-1.549
113	Ccdc96	-3.698	-3.623	-3.921	4.85E-04	6.68E-02	-1.573
114	Tmem101	0.843	3.206	3.910	5.00E-04	6.73E-02	-0.101
115	Wdr26	0.591	7.691	3.902	5.12E-04	6.73E-02	-0.344
116	Yipf3	0.422	6.979	3.896	5.19E-04	6.73E-02	-0.349
117	Dnajb2	-0.652	5.462	-3.896	5.20E-04	6.73E-02	-0.310
118	Kcnq3	1.555	0.813	3.895	5.21E-04	6.73E-02	-0.461
119	Hk2	-1.454	1.453	-3.895	5.21E-04	6.73E-02	-0.237
120	Rnf128	1.488	3.507	3.893	5.23E-04	6.73E-02	-0.143

2.7.10 Therapeutic DEGs CD8 (OTI) OVA vs Saline

	gene_name	logFC	AveExpr	t	P.Value	adj.P.Val	B
1	Bcl2	-1.843	7.017	-8.944	3.91E-10	2.05E-06	13.197
2	Sh2d1a	0.909	6.881	8.940	3.95E-10	2.05E-06	13.187
3	Il7r	-1.956	8.420	-8.939	3.96E-10	2.05E-06	13.188
4	Itga4	1.797	8.102	8.763	6.20E-10	2.41E-06	12.751
5	Ifitm3	-2.560	3.258	-8.560	1.05E-09	3.27E-06	11.792
6	Fhl2	2.210	4.209	8.312	2.00E-09	5.19E-06	11.384
7	Prss12	-1.941	4.479	-8.110	3.42E-09	6.73E-06	11.019
8	Cd40lg	-2.055	3.364	-8.105	3.46E-09	6.73E-06	10.822
9	Tstd3	1.115	4.812	8.016	4.38E-09	7.58E-06	10.799
10	Gpatch4	-1.323	4.736	-7.961	5.07E-09	7.90E-06	10.679
11	Ap3s1	1.085	6.166	7.852	6.81E-09	9.00E-06	10.420
12	Mcu	1.038	4.881	7.845	6.93E-09	9.00E-06	10.380
13	Mettl1	-1.957	3.330	-7.766	8.57E-09	1.01E-05	9.928
14	Sema4f	-1.372	5.129	-7.746	9.05E-09	1.01E-05	10.143
15	Ifitm2	-3.262	3.147	-7.567	1.47E-08	1.48E-05	9.417
16	Art2b	1.981	5.304	7.551	1.53E-08	1.48E-05	9.627
17	BC005561	-1.362	4.250	-7.532	1.62E-08	1.48E-05	9.537
18	Spef2	-2.053	2.555	-7.506	1.73E-08	1.50E-05	9.146
19	Ifitm1	-3.540	4.945	-7.407	2.27E-08	1.77E-05	9.250
20	Mospd3	0.815	5.960	7.407	2.27E-08	1.77E-05	9.249
21	Ube2h	0.912	8.386	7.329	2.82E-08	2.09E-05	9.020
22	Treml2	-2.010	1.876	-7.275	3.26E-08	2.26E-05	8.123
23	Adgrg3	-2.978	1.676	-7.262	3.38E-08	2.26E-05	8.038

24	Gimap7	1.251	8.683	7.252	3.48E-08	2.26E-05	8.812
25	Eomes	0.866	7.250	7.216	3.84E-08	2.39E-05	8.724
26	Haus5	-1.346	5.647	-7.163	4.44E-08	2.49E-05	8.601
27	Fyn	0.683	10.189	7.147	4.64E-08	2.49E-05	8.525
28	Plek	1.509	7.417	7.142	4.71E-08	2.49E-05	8.522
29	Ifrd2	-1.640	4.340	-7.135	4.80E-08	2.49E-05	8.503
30	Vsig10l	1.150	4.300	7.126	4.92E-08	2.49E-05	8.472
31	Pycard	0.972	7.444	7.123	4.97E-08	2.49E-05	8.470
32	Sh3bgrl	1.264	6.113	7.037	6.31E-08	3.07E-05	8.256
33	Nsmaf	0.751	7.976	7.001	6.97E-08	3.18E-05	8.134
34	Ikzf3	1.115	8.113	7.000	6.98E-08	3.18E-05	8.131
35	Samd3	0.671	7.571	6.986	7.27E-08	3.18E-05	8.097
36	Serpinb6b	1.214	6.193	6.981	7.36E-08	3.18E-05	8.104
37	Bbc3	-1.239	5.138	-6.960	7.80E-08	3.28E-05	8.063
38	Fndc3a	-1.227	4.942	-6.887	9.58E-08	3.92E-05	7.868
39	Rap1a	0.742	7.431	6.859	1.03E-07	3.99E-05	7.753
40	Jaml	-1.094	7.270	-6.854	1.05E-07	3.99E-05	7.736
41	Tgtp1	-1.621	5.475	-6.854	1.05E-07	3.99E-05	7.769
42	Fxyd4	-2.564	0.279	-6.783	1.28E-07	4.75E-05	6.159
43	Stx1a	-1.525	3.553	-6.753	1.39E-07	4.93E-05	7.445
44	Ap1s2	1.014	5.443	6.748	1.41E-07	4.93E-05	7.487
45	Abhd11	-1.163	5.410	-6.745	1.42E-07	4.93E-05	7.475
46	Rasa4	-1.289	4.264	-6.715	1.55E-07	5.20E-05	7.404
47	Mmd	1.117	4.145	6.710	1.57E-07	5.20E-05	7.364
48	Gzmk	1.726	7.241	6.678	1.72E-07	5.57E-05	7.258
49	Aatf	-0.826	5.873	-6.638	1.92E-07	6.11E-05	7.170
50	Mecr	-1.250	4.196	-6.572	2.32E-07	7.21E-05	7.015
51	Smyd5	-1.191	4.843	-6.558	2.41E-07	7.21E-05	6.981
52	Gm5157	1.408	2.775	6.554	2.44E-07	7.21E-05	6.655
53	Ftsj3	-0.744	6.705	-6.551	2.45E-07	7.21E-05	6.911
54	Tspyl2	-1.044	4.934	-6.524	2.66E-07	7.54E-05	6.887
55	Cd68	1.336	4.030	6.523	2.66E-07	7.54E-05	6.874
56	Tmem154	0.881	6.249	6.493	2.89E-07	8.05E-05	6.765
57	Trp53inp1	1.204	6.802	6.480	3.01E-07	8.14E-05	6.719
58	Qtrt2	-1.194	3.613	-6.473	3.06E-07	8.14E-05	6.724
59	Arpc4	0.763	8.651	6.467	3.12E-07	8.14E-05	6.663
60	Znrf3	-0.986	4.758	-6.465	3.14E-07	8.14E-05	6.724
61	Oasl2	-1.893	3.151	-6.448	3.29E-07	8.39E-05	6.634
62	Srm	-1.108	5.508	-6.437	3.39E-07	8.39E-05	6.628
63	Il10ra	0.694	8.275	6.437	3.39E-07	8.39E-05	6.582
64	Prss16	-1.474	2.997	-6.429	3.47E-07	8.45E-05	6.556
65	Ipo4	-1.065	5.094	-6.412	3.64E-07	8.72E-05	6.574
66	Epsti1	0.844	9.064	6.392	3.86E-07	9.10E-05	6.452
67	Psen2	0.668	6.675	6.378	4.01E-07	9.26E-05	6.438
68	Ppan	-0.990	6.409	-6.371	4.09E-07	9.26E-05	6.422
69	Ctla2b	0.921	6.136	6.370	4.11E-07	9.26E-05	6.430
70	Vars	-0.735	8.248	-6.362	4.19E-07	9.33E-05	6.373
71	Prrt1	-2.206	0.525	-6.333	4.56E-07	1.00E-04	5.170
72	Fut7	-1.627	4.468	-6.325	4.66E-07	1.01E-04	6.351
73	Tespa1	-1.057	7.160	-6.313	4.82E-07	1.03E-04	6.248
74	2410002F23Rik	-0.949	6.456	-6.298	5.03E-07	1.06E-04	6.218
75	Mrpl38	-0.832	5.787	-6.265	5.52E-07	1.15E-04	6.145
76	Cnpy3	-0.670	5.793	-6.248	5.80E-07	1.19E-04	6.098
77	Zcwpw1	-1.225	3.205	-6.234	6.04E-07	1.22E-04	6.061
78	Arpc5	0.929	9.555	6.208	6.50E-07	1.30E-04	5.939
79	Jakmip1	-0.559	7.330	-6.196	6.73E-07	1.33E-04	5.916

80	Ccdc191	-1.554	3.545	-6.184	6.97E-07	1.35E-04	5.929
81	Nsun5	-1.054	5.608	-6.182	7.01E-07	1.35E-04	5.922
82	Top1mt	-1.361	3.014	-6.169	7.27E-07	1.35E-04	5.845
83	Gyg	1.044	5.387	6.167	7.31E-07	1.35E-04	5.897
84	Tnfrsf13b	1.017	5.052	6.166	7.34E-07	1.35E-04	5.914
85	Hist2h4	-1.502	2.426	-6.161	7.43E-07	1.35E-04	5.679
86	Macrod1	-1.389	2.438	-6.161	7.44E-07	1.35E-04	5.726
87	Dnajb2	-1.139	4.661	-6.151	7.65E-07	1.37E-04	5.875
88	Xdh	1.142	6.668	6.129	8.14E-07	1.42E-04	5.750
89	Ubash3b	1.046	6.138	6.127	8.18E-07	1.42E-04	5.757
90	Arl5a	1.130	6.103	6.127	8.19E-07	1.42E-04	5.756
91	Selenop	0.934	6.256	6.114	8.51E-07	1.45E-04	5.714
92	Tmem126a	0.671	5.481	6.111	8.56E-07	1.45E-04	5.739
93	Ifi209	0.910	8.657	6.094	9.01E-07	1.51E-04	5.624
94	Man2c1	-1.002	5.634	-6.070	9.63E-07	1.58E-04	5.609
95	Rrp9	-0.910	6.050	-6.068	9.69E-07	1.58E-04	5.588
96	Arhgap5	-1.525	4.003	-6.066	9.75E-07	1.58E-04	5.645
97	Tm6sf1	0.752	7.814	6.061	9.88E-07	1.59E-04	5.539
98	Cab39	0.795	8.328	6.046	1.03E-06	1.64E-04	5.492
99	Socs1	-1.252	5.990	-6.028	1.09E-06	1.71E-04	5.479
100	Eva1b	0.794	5.553	6.015	1.13E-06	1.75E-04	5.477
101	Arhgef3	0.909	8.491	5.970	1.28E-06	1.98E-04	5.279
102	Filip1l	-0.923	5.689	-5.953	1.35E-06	2.06E-04	5.288
103	Ctrc	-1.984	2.792	-5.949	1.36E-06	2.06E-04	5.159
104	Nacc2	-2.346	2.038	-5.936	1.41E-06	2.07E-04	5.082
105	Arl5c	0.744	6.416	5.936	1.42E-06	2.07E-04	5.211
106	Snx4	0.649	7.513	5.935	1.42E-06	2.07E-04	5.187
107	Gnl3	-1.165	5.652	-5.934	1.42E-06	2.07E-04	5.233
108	Smyd2	-1.119	3.150	-5.915	1.50E-06	2.16E-04	5.209
109	Chfr	0.721	6.802	5.913	1.51E-06	2.16E-04	5.136
110	Nolc1	-0.789	6.754	-5.908	1.53E-06	2.17E-04	5.122
111	Cbx7	-0.727	6.617	-5.888	1.62E-06	2.26E-04	5.069
112	Parp8	-0.939	5.204	-5.887	1.63E-06	2.26E-04	5.126
113	Cxcr4	-1.229	4.644	-5.882	1.65E-06	2.27E-04	5.134
114	Cep164	-1.133	4.525	-5.878	1.67E-06	2.28E-04	5.134
115	Atad3a	-1.099	5.685	-5.869	1.72E-06	2.32E-04	5.042
116	Pold1	-0.605	6.576	-5.846	1.83E-06	2.44E-04	4.949
117	Casp3	1.048	5.839	5.846	1.83E-06	2.44E-04	4.987
118	Chst2	1.095	5.458	5.835	1.89E-06	2.48E-04	4.977
119	Hnrnpll	0.863	5.934	5.834	1.89E-06	2.48E-04	4.946
120	Il18r1	-1.079	6.080	-5.823	1.96E-06	2.54E-04	4.899

2.7.11 Therapeutic DEGs CD8 (OTI) pGal-OVA vs OVA

	gene_name	logFC	AveExpr	t	P.Value	adj.P.Val	B
1	Fhl2	-1.292	4.209	-6.766	1.34E-07	1.07E-03	7.451
2	Itgax	-1.629	7.068	-6.550	2.47E-07	1.07E-03	6.961
3	Ifrd2	1.390	4.340	6.547	2.48E-07	1.07E-03	6.764
4	Plek	-1.160	7.417	-6.404	3.72E-07	1.07E-03	6.566
5	Chil5	-1.131	4.347	-6.270	5.45E-07	1.07E-03	6.145
6	Cd68	-1.043	4.030	-6.244	5.86E-07	1.07E-03	6.054
7	Prss12	1.396	4.479	6.227	6.15E-07	1.07E-03	5.977
8	Parp8	0.872	5.204	6.164	7.37E-07	1.07E-03	5.906
9	Smyd5	1.009	4.843	6.159	7.48E-07	1.07E-03	5.866

10	Itga4	-1.081	8.102	-6.157	7.52E-07	1.07E-03	5.889
11	Gzmk	-1.360	7.241	-6.155	7.55E-07	1.07E-03	5.887
12	Lta	1.174	4.143	5.944	1.38E-06	1.79E-03	5.230
13	Cd163l1	2.000	4.709	5.830	1.92E-06	2.22E-03	4.965
14	Rarg	1.252	3.331	5.816	1.99E-06	2.22E-03	4.663
15	Cd40lg	1.411	3.364	5.746	2.44E-06	2.53E-03	4.520
16	Serpinb6b	-0.822	6.193	-5.629	3.41E-06	3.28E-03	4.451
17	Matk	1.160	5.203	5.598	3.73E-06	3.28E-03	4.380
18	Lair1	-0.973	5.089	-5.592	3.80E-06	3.28E-03	4.365
19	Tspyl2	0.802	4.934	5.545	4.35E-06	3.39E-03	4.233
20	Lmna	1.623	5.502	5.525	4.60E-06	3.39E-03	4.183
21	Ube2h	-0.592	8.386	-5.513	4.77E-06	3.39E-03	4.113
22	Art2b	-1.117	5.304	-5.512	4.79E-06	3.39E-03	4.141
23	Il7r	1.048	8.420	5.491	5.09E-06	3.44E-03	4.054
24	Pycard	-0.641	7.444	-5.462	5.52E-06	3.57E-03	3.978
25	Gpatch4	0.835	4.736	5.449	5.73E-06	3.57E-03	3.971
26	Arhgap5	1.273	4.003	5.436	5.96E-06	3.57E-03	3.847
27	Mcu	-0.583	4.881	-5.409	6.43E-06	3.66E-03	3.869
28	Pfkp	-0.531	8.856	-5.401	6.58E-06	3.66E-03	3.802
29	2410002F23Rik	0.709	6.456	5.374	7.13E-06	3.70E-03	3.748
30	Ovca2	-0.595	4.637	-5.359	7.44E-06	3.70E-03	3.734
31	Filip1l	0.734	5.689	5.348	7.68E-06	3.70E-03	3.696
32	Prrt1	1.778	0.525	5.339	7.87E-06	3.70E-03	1.964
33	Treml2	1.436	1.876	5.327	8.16E-06	3.70E-03	2.799
34	BC005561	0.903	4.250	5.323	8.24E-06	3.70E-03	3.602
35	Nsmaf	-0.492	7.976	-5.320	8.31E-06	3.70E-03	3.582
36	Ms4a6d	-0.629	4.376	-5.300	8.82E-06	3.82E-03	3.573
37	Bcl2	0.960	7.017	5.287	9.14E-06	3.85E-03	3.507
38	Cxxc5	1.602	3.242	5.267	9.68E-06	3.97E-03	3.332
39	St6gal1	1.094	5.965	5.243	1.04E-05	4.04E-03	3.400
40	Spint2	0.605	6.012	5.235	1.06E-05	4.04E-03	3.377
41	9930021J03Rik	0.853	4.765	5.224	1.10E-05	4.04E-03	3.368
42	Gimap7	-0.774	8.683	-5.211	1.14E-05	4.04E-03	3.276
43	Prpf40b	1.841	2.214	5.206	1.16E-05	4.04E-03	2.595
44	Zscan26	1.075	3.576	5.205	1.16E-05	4.04E-03	3.199
45	Hmgn1	0.751	6.627	5.203	1.17E-05	4.04E-03	3.274
46	Bscl2	-0.378	7.053	-5.176	1.26E-05	4.11E-03	3.192
47	Wnt10a	2.491	3.379	5.176	1.26E-05	4.11E-03	3.080
48	Fyn	-0.427	10.189	-5.170	1.28E-05	4.11E-03	3.160
49	Zfp683	1.294	2.478	5.167	1.29E-05	4.11E-03	2.781
50	Izumo1r	1.381	5.528	5.160	1.32E-05	4.11E-03	3.182
51	Arl5c	-0.550	6.416	-5.133	1.43E-05	4.35E-03	3.082
52	Ccdc191	1.209	3.545	5.090	1.61E-05	4.56E-03	2.883
53	Synrg	-0.646	6.129	-5.090	1.62E-05	4.56E-03	2.967
54	Mettl1	1.255	3.330	5.089	1.62E-05	4.56E-03	2.821
55	Zc3h13	0.613	6.819	5.086	1.63E-05	4.56E-03	2.949
56	Havcr2	-1.219	4.836	-5.080	1.66E-05	4.56E-03	2.977
57	Cd83	1.352	4.977	5.078	1.67E-05	4.56E-03	2.978
58	Ikzf3	-0.696	8.113	-5.071	1.71E-05	4.58E-03	2.892
59	Xdh	-0.800	6.668	-5.054	1.79E-05	4.73E-03	2.859
60	Ctla2b	-0.615	6.136	-5.035	1.89E-05	4.84E-03	2.818
61	Dnajb2	0.851	4.661	5.034	1.90E-05	4.84E-03	2.862
62	Eomes	-0.516	7.250	-5.012	2.02E-05	5.08E-03	2.734
63	Ctrc	1.587	2.792	4.998	2.10E-05	5.18E-03	2.387
64	Fndc3a	0.815	4.942	4.994	2.13E-05	5.18E-03	2.754
65	Rev1	0.784	4.173	4.974	2.25E-05	5.38E-03	2.695

66	Fut7	1.180	4.468	4.970	2.28E-05	5.38E-03	2.691
67	Rom1	-0.866	4.903	-4.965	2.31E-05	5.38E-03	2.664
68	Tespa1	0.724	7.160	4.956	2.38E-05	5.39E-03	2.588
69	Rccd1	0.733	4.680	4.954	2.39E-05	5.39E-03	2.647
70	Rmnd1	0.515	5.321	4.947	2.44E-05	5.42E-03	2.609
71	Rtn4rl1	-1.047	4.894	-4.913	2.69E-05	5.89E-03	2.525
72	Ccdc107	0.713	5.059	4.904	2.76E-05	5.91E-03	2.507
73	Scfd2	-0.588	5.272	-4.903	2.77E-05	5.91E-03	2.488
74	Mapk11	0.679	5.656	4.893	2.85E-05	5.93E-03	2.454
75	Tnfsf8	0.911	5.142	4.892	2.85E-05	5.93E-03	2.467
76	Mapre2	-0.525	7.045	-4.880	2.95E-05	6.05E-03	2.376
77	Cpped1	-0.861	3.221	-4.866	3.07E-05	6.21E-03	2.369
78	Rhbdd2	0.668	4.240	4.854	3.18E-05	6.24E-03	2.382
79	Ccr5	-0.822	6.339	-4.852	3.20E-05	6.24E-03	2.308
80	Hist2h4	1.126	2.426	4.850	3.22E-05	6.24E-03	2.022
81	Itgae	2.224	4.138	4.842	3.30E-05	6.24E-03	2.338
82	Haus5	0.818	5.647	4.840	3.31E-05	6.24E-03	2.316
83	Kmt2c	0.889	7.076	4.839	3.33E-05	6.24E-03	2.267
84	Phf11c	-0.494	6.088	-4.830	3.41E-05	6.32E-03	2.259
85	Bbc3	0.779	5.138	4.821	3.50E-05	6.41E-03	2.281
86	Cirbp	0.625	5.491	4.814	3.58E-05	6.48E-03	2.244
87	Top1mt	0.995	3.014	4.801	3.71E-05	6.64E-03	2.103
88	Cbx7	0.515	6.617	4.786	3.87E-05	6.85E-03	2.129
89	Tmem163	-0.837	4.497	-4.771	4.05E-05	7.08E-03	2.154
90	Arhgef3	-0.625	8.491	-4.758	4.20E-05	7.26E-03	2.027
91	Trim12c	-0.660	5.546	-4.745	4.35E-05	7.44E-03	2.046
92	Rmdn1	0.765	3.583	4.740	4.42E-05	7.44E-03	2.035
93	Srm	0.728	5.508	4.738	4.44E-05	7.44E-03	2.038
94	Fam129b	0.832	4.727	4.734	4.50E-05	7.45E-03	2.055
95	Phf11a	-0.828	4.714	-4.727	4.59E-05	7.46E-03	2.036
96	Nrp2	-1.346	2.758	-4.722	4.65E-05	7.46E-03	1.965
97	Igflr1	0.737	5.901	4.719	4.69E-05	7.46E-03	1.966
98	Pdlim5	-0.640	5.897	-4.717	4.72E-05	7.46E-03	1.956
99	Prr18	-3.626	-3.252	-4.713	4.77E-05	7.46E-03	-1.245
100	Sft2d3	0.724	4.379	4.712	4.79E-05	7.46E-03	2.006
101	Ak3	-0.908	6.524	-4.692	5.07E-05	7.81E-03	1.865
102	Gtf2i	-0.499	8.643	-4.684	5.19E-05	7.93E-03	1.823
103	Pabpc4	0.980	4.440	4.674	5.34E-05	8.05E-03	1.907
104	Capg	0.884	7.510	4.672	5.37E-05	8.05E-03	1.801
105	Myo1f	-0.680	9.519	-4.654	5.66E-05	8.39E-03	1.737
106	Mtmr1	-0.824	6.280	-4.644	5.82E-05	8.45E-03	1.738
107	Egr3	1.433	1.678	4.641	5.87E-05	8.45E-03	1.394
108	Cnpy3	0.439	5.793	4.637	5.94E-05	8.45E-03	1.751
109	Aph1a	-0.599	5.426	-4.636	5.95E-05	8.45E-03	1.751
110	Pcm1	0.735	5.141	4.635	5.97E-05	8.45E-03	1.780
111	Gnl2	0.483	6.329	4.629	6.07E-05	8.52E-03	1.708
112	Larp1b	0.721	4.728	4.611	6.40E-05	8.83E-03	1.730
113	Hnrnph3	0.636	5.256	4.608	6.45E-05	8.83E-03	1.702
114	Kdm4a	-0.763	5.639	-4.606	6.48E-05	8.83E-03	1.665
115	Pacsin1	0.918	5.599	4.600	6.61E-05	8.83E-03	1.656
116	Tmprss13	-1.626	2.024	-4.597	6.66E-05	8.83E-03	1.440
117	Arl5a	-0.713	6.103	-4.596	6.68E-05	8.83E-03	1.612
118	Arhgef6	-0.553	7.336	-4.595	6.69E-05	8.83E-03	1.590
119	Golgb1	0.826	5.926	4.592	6.76E-05	8.83E-03	1.633
120	Bcl7c	0.659	4.775	4.589	6.80E-05	8.83E-03	1.669

2.7.12 Therapeutic DEGs CD8 (OTI) pGal-OVA vs Saline

	gene_name	logFC	AveExpr	t	P.Value	adj.P.Val	B
1	Rap1a	0.658	7.431	5.951	1.36E-06	0.021	5.309
2	Pprc1	-0.762	5.512	-5.335	7.97E-06	0.027	3.631
3	Tnfrsf13b	0.898	5.052	5.331	8.05E-06	0.027	3.657
4	Sh2d1a	0.553	6.881	5.309	8.59E-06	0.027	3.538
5	Tspan32	0.940	6.709	5.307	8.65E-06	0.027	3.532
6	Mmd	0.880	4.145	5.143	1.39E-05	0.029	3.146
7	Tstd3	0.739	4.812	5.141	1.40E-05	0.029	3.145
8	Ifitm3	-1.309	3.258	-5.120	1.48E-05	0.029	3.089
9	Chst2	0.972	5.458	5.076	1.68E-05	0.029	2.940
10	Ap3s1	0.708	6.166	4.997	2.11E-05	0.031	2.697
11	Oasl2	-1.407	3.151	-4.984	2.19E-05	0.031	2.722
12	Mospd3	0.545	5.960	4.832	3.39E-05	0.044	2.248
13	Eva1b	0.646	5.553	4.785	3.88E-05	0.046	2.145
14	Izumo1r	1.556	5.528	4.756	4.22E-05	0.047	2.067
15	Jakmip1	-0.433	7.330	-4.701	4.94E-05	0.048	1.840
16	Samd3	0.461	7.571	4.684	5.19E-05	0.048	1.795
17	Pecam1	0.536	6.153	4.683	5.21E-05	0.048	1.825
18	Lrrc61	0.775	4.434	4.646	5.79E-05	0.050	1.822
19	Myb	1.221	5.983	4.627	6.11E-05	0.050	1.692
20	Nab2	0.735	5.631	4.591	6.77E-05	0.053	1.600
21	Ftsj3	-0.525	6.705	-4.544	7.75E-05	0.055	1.416
22	Fxyd4	-1.584	0.279	-4.535	7.94E-05	0.055	1.097
23	Znrf3	-0.687	4.758	-4.529	8.08E-05	0.055	1.457
24	Zbtb32	1.080	6.241	4.410	1.13E-04	0.074	1.103
25	Ifitm2	-1.466	3.147	-4.360	1.31E-04	0.081	1.059
26	Lag3	0.942	4.139	4.335	1.40E-04	0.084	1.022
27	Bcl2	-0.883	7.017	-4.272	1.68E-04	0.097	0.669
28	Cbx6	0.790	4.861	4.244	1.81E-04	0.099	0.726
29	Ptger2	0.810	3.840	4.238	1.85E-04	0.099	0.771
30	Resf1	-0.642	7.482	-4.199	2.06E-04	0.107	0.470
31	Slamf6	0.597	8.666	4.182	2.16E-04	0.109	0.417
32	Il7r	-0.908	8.420	-4.083	2.85E-04	0.138	0.147
33	Aldh1l1	4.675	-1.149	4.074	2.93E-04	0.138	-1.452
34	Hmgcs2	3.538	-4.212	4.053	3.11E-04	0.139	-2.195
35	Psen2	0.433	6.675	4.037	3.24E-04	0.139	0.065
36	Sema4f	-0.696	5.129	-4.036	3.25E-04	0.139	0.098
37	Ndnf	1.573	2.731	4.032	3.29E-04	0.139	0.232
38	Mpp2	1.546	1.067	3.993	3.67E-04	0.151	-0.086
39	Cxadr	-2.026	-1.350	-3.981	3.80E-04	0.152	-0.671
40	Pacs2	-0.568	5.234	-3.967	3.95E-04	0.154	-0.073
41	Nacc2	-1.426	2.038	-3.955	4.09E-04	0.155	0.063
42	Wdr4	-0.518	4.891	-3.935	4.31E-04	0.160	-0.127
43	Mmp9	3.238	0.139	3.866	5.22E-04	0.182	-0.928
44	Spock2	1.560	1.901	3.863	5.27E-04	0.182	-0.244
45	Cstad	2.509	-0.599	3.843	5.57E-04	0.182	-1.206
46	Gdi2	0.489	8.189	3.841	5.59E-04	0.182	-0.484
47	Zcwpw1	-0.724	3.205	-3.832	5.74E-04	0.182	-0.257
48	Exo5	0.577	4.379	3.829	5.78E-04	0.182	-0.311
49	Ly6a	-0.522	7.947	-3.820	5.94E-04	0.182	-0.541
50	Neu3	0.780	3.357	3.810	6.10E-04	0.182	-0.290
51	Ipo4	-0.625	5.094	-3.809	6.12E-04	0.182	-0.478
52	Ifitm1	-1.548	4.945	-3.805	6.18E-04	0.182	-0.541
53	Prss16	-0.819	2.997	-3.804	6.20E-04	0.182	-0.326

54	Rab37	0.464	6.543	3.798	6.31E-04	0.182	-0.567
55	Tank	0.547	5.558	3.789	6.46E-04	0.182	-0.524
56	Litaf	0.563	4.890	3.774	6.74E-04	0.182	-0.515
57	Plcl1	1.731	1.582	3.761	6.99E-04	0.182	-0.623
58	Elk3	0.448	5.870	3.757	7.06E-04	0.182	-0.639
59	Unc13a	2.337	1.226	3.754	7.11E-04	0.182	-0.675
60	Trim30c	-0.942	2.143	-3.750	7.19E-04	0.182	-0.443
61	Sytl3	-0.442	6.888	-3.750	7.19E-04	0.182	-0.709
62	Lclat1	1.077	3.981	3.746	7.28E-04	0.182	-0.484
63	Rfx5	0.872	4.435	3.737	7.45E-04	0.182	-0.546
64	Ripor3	-1.867	-0.141	-3.729	7.61E-04	0.182	-0.803
65	Ctdnep1	0.449	5.062	3.724	7.72E-04	0.182	-0.654
66	Prr5l	1.057	3.444	3.720	7.82E-04	0.182	-0.508
67	Ramac	0.504	6.546	3.719	7.84E-04	0.182	-0.766
68	Rab39	3.276	-1.595	3.702	8.21E-04	0.184	-1.688
69	Rnf19a	0.468	6.356	3.699	8.28E-04	0.184	-0.814
70	1700061G19Rik	-2.085	-1.641	-3.699	8.28E-04	0.184	-1.256
71	Ddit4	0.681	5.178	3.689	8.50E-04	0.186	-0.759
72	Mpp1	0.640	5.818	3.664	9.10E-04	0.195	-0.865
73	Nrip3	-2.183	0.045	-3.656	9.31E-04	0.195	-0.963
74	Ift80	0.667	4.732	3.655	9.33E-04	0.195	-0.799
75	Gyg	0.638	5.387	3.652	9.40E-04	0.195	-0.855
76	Sit1	-0.482	6.914	-3.648	9.50E-04	0.195	-0.974
77	Macrod1	-0.781	2.438	-3.639	9.75E-04	0.197	-0.698
78	Dcxr	0.765	2.538	3.633	9.90E-04	0.198	-0.719
79	Gm12216	-0.596	3.989	-3.628	1.00E-03	0.198	-0.808
80	E2f3	1.013	2.516	3.596	1.10E-03	0.213	-0.811
81	Tmem221	-0.613	4.206	-3.585	1.13E-03	0.217	-0.961
82	Chic2	0.454	6.525	3.570	1.17E-03	0.218	-1.151
83	Mecr	-0.647	4.196	-3.568	1.18E-03	0.218	-1.005
84	Gpr146	-0.655	4.193	-3.565	1.19E-03	0.218	-1.021
85	Tmem126a	0.402	5.481	3.558	1.21E-03	0.218	-1.106
86	Abhd14a	-0.688	3.062	-3.554	1.23E-03	0.218	-0.933
87	Gm42420	-2.257	-2.892	-3.553	1.23E-03	0.218	-1.995
88	Oas2	-1.786	1.501	-3.551	1.24E-03	0.218	-0.909
89	T2	1.395	0.055	3.548	1.25E-03	0.218	-1.327
90	Slco3a1	-0.548	7.589	-3.535	1.29E-03	0.222	-1.273
91	Spef2	-0.843	2.555	-3.534	1.30E-03	0.222	-0.981
92	Selenop	0.553	6.256	3.530	1.31E-03	0.222	-1.235
93	Vsig10l	0.596	4.300	3.520	1.34E-03	0.223	-1.058
94	6330403K07Rik	0.858	2.911	3.519	1.35E-03	0.223	-0.979
95	Rasa4	-0.641	4.264	-3.515	1.36E-03	0.223	-1.158
96	Tm6sf1	0.446	7.814	3.508	1.39E-03	0.225	-1.339
97	Tgtp1	-0.805	5.475	-3.505	1.40E-03	0.225	-1.292
98	Prdm11	0.623	4.206	3.493	1.45E-03	0.228	-1.140
99	Cct3	-0.373	8.048	-3.492	1.45E-03	0.228	-1.385
100	Nrn1	1.860	3.197	3.489	1.46E-03	0.228	-1.052
101	Tmem154	0.485	6.249	3.482	1.49E-03	0.229	-1.356
102	Stx1a	-0.722	3.553	-3.472	1.53E-03	0.234	-1.185
103	Casp3	0.640	5.839	3.468	1.55E-03	0.234	-1.359
104	Myc	-0.604	7.006	-3.456	1.60E-03	0.237	-1.465
105	Ap1s2	0.537	5.443	3.454	1.61E-03	0.237	-1.353
106	Decr1	0.681	4.262	3.453	1.61E-03	0.237	-1.244
107	Zfp748	0.606	4.489	3.444	1.65E-03	0.238	-1.285
108	Ucp2	0.586	10.021	3.442	1.66E-03	0.238	-1.525
109	Limd2	0.423	10.065	3.439	1.67E-03	0.238	-1.531

110	Tox	0.653	6.067	3.436	1.69E-03	0.239	-1.462
111	Desi1	0.453	5.257	3.426	1.73E-03	0.241	-1.427
112	AW549877	0.534	4.892	3.425	1.74E-03	0.241	-1.368
113	Gpr174	0.494	6.179	3.422	1.75E-03	0.241	-1.508
114	Timeless	-0.440	4.661	-3.414	1.79E-03	0.242	-1.429
115	Itga4	0.716	8.102	3.401	1.85E-03	0.242	-1.606
116	Rab20	-0.724	2.768	-3.399	1.86E-03	0.242	-1.269
117	Pold1	-0.357	6.576	-3.396	1.88E-03	0.242	-1.607
118	Tbc1d4	0.857	5.170	3.395	1.88E-03	0.242	-1.489
119	Stap1	0.355	6.123	3.391	1.90E-03	0.242	-1.582
120	Man2c1	-0.559	5.634	-3.391	1.90E-03	0.242	-1.574

CHAPTER 3: TARGETING LACTADHERIN-MEDIATED EFFEROCYTOSIS FOR ANTIGEN IMMUNOTHERAPY

3.1 Abstract

Current treatment for autoimmunity, allergy, and drug hypersensitivity generate global immune suppression, resulting in an increased risk of infection and malignancy. For this reason, a therapy that leverages the body's inherent mechanisms for the induction of antigen-specific immune tolerance would represent a major step forward in the treatment of numerous diseases. One such mechanism is the steady state presentation of apoptotic cell debris that results in tolerogenic T cell education (i.e. deletion, anergy, and Treg induction). Mimicking this process, strategies based on the ex vivo coupling of antigens to apoptotic cells have been used to induce tolerance in various murine models of autoimmunity and are currently under clinical investigation. However, the ex vivo coupling and apoptotic induction of harvested cells is challenging in a clinical setting. Here, we present an injectable tolerance-inducing therapy that targets antigen to cells undergoing apoptosis, resulting in antigen-specific tolerance. In order to target antigen to apoptotic cells we coupled the model antigen ovalbumin (OVA) to lactadherin (MFGE8), which binds to both phosphatidylserine exposed on apoptotic bodies and endocytic-integrins on macrophages and dendritic cells, thereby acting as a bridge for the phagocytosis of apoptotic cells. When mice were treated prophylactically with MFGE8-OVA (prior to immunization with OVA protein), we observed a reduced response to secondary challenge. T cell tolerance was induced via deletion and induction of co-

inhibitory receptors. Using cellular and transcriptional data from in vivo and ex vivo experiments in mice, MFGE8-OVA fusion proteins are shown to induce highly efficient presentation of antigen and downstream tolerance in OVA-specific T cells.

3.2 Introduction

Clearance of apoptotic debris is associated with anti-inflammatory responses, such as those that fail in lupus.[82] Presentation of antigen in the context of efferocytosis (from *efferre*, Latin for "to take to the grave", "to bury") results in tolerance. MFGE8 binds to exposed PS on apoptotic cell membranes and bridges with integrins $\alpha_V\beta_{3/5}$ expressed on phagocytes. Work has been done showing recombinant Mfge8 treatment alone has anti-inflammatory effects, but conjugated antigen delivery has not been explored.[83] By fusing MFGE8 with a protein of interest (e.g., OVA), we reasoned that we may route antigen into the efferocytosis network and induce antigen-specific tolerance.

OVA was recombinantly expressed at the C-term of MFGE8, separated with an inert Gly4Ser linker, along with an 8xHis tag on the C-term for affinity purification. Protein constructs were designed and cloned into pSecTagA mammalian expression vectors, which were transfected into suspension human embryonic kidney (HEK) cells. Constructs were purified from culture supernatants using nickel-affinity and size exclusion columns, and finally confirmed to be endotoxin free. Constructs were confirmed to have proper affinity for their target ligands (data not shown). We then carried out in vitro and in vivo characterization of MFGE8-mediated antigen delivery in conjunction with OTI and OTII transgenic T cells.

3.3 Results

3.3.1 MFGE8 facilitates antigen uptake and presentation in vitro

Due to the systemic nature of MFGE8-mediated efferocytosis, and the ubiquitous expression of its receptors on phagocytes, we took the opportunity to gain an understanding for how MFGE8 could mediate antigen presentation in vitro. Using bone marrow-derived macrophages and dendritic cells (BMDM, BMDC), we cultured APCs for fifteen minutes with either OVA mixed with MFGE8, or with OVA fused to MFGE8 (MFGE8-OVA). **Figure 3.1 a** illustrates the uptake of OVA as measured by flow cytometry, with the top plot showing antigen mixed with MFGE8 and the bottom plot showing antigen fused to MFGE8. A greater amount and intensity of OVA uptake was seen in the fused group compared to mixed. Furthermore, we measured antigen uptake under these conditions via immunofluorescence and saw clear punctate nodules of OVA only in the fused condition (**Figure 3.1 b**).

We increased the incubation period to thirty minutes and found the predominance of phagocytosed antigen to be present in $CD86^-$ immature APCs across the spectrum of F4/80 expression (**Figure 3.1 c**). I was surprised upon first noticing there were no dead cells detected in the fused condition, but then realized this should have been expected – it was an excellent demonstration of the functionality of our antigen constructs to be directly involved in efferocytosis. This confirmed the ability of MFGE8 to shuttle our target antigen into our desired antigen processing pathway with great efficiency.

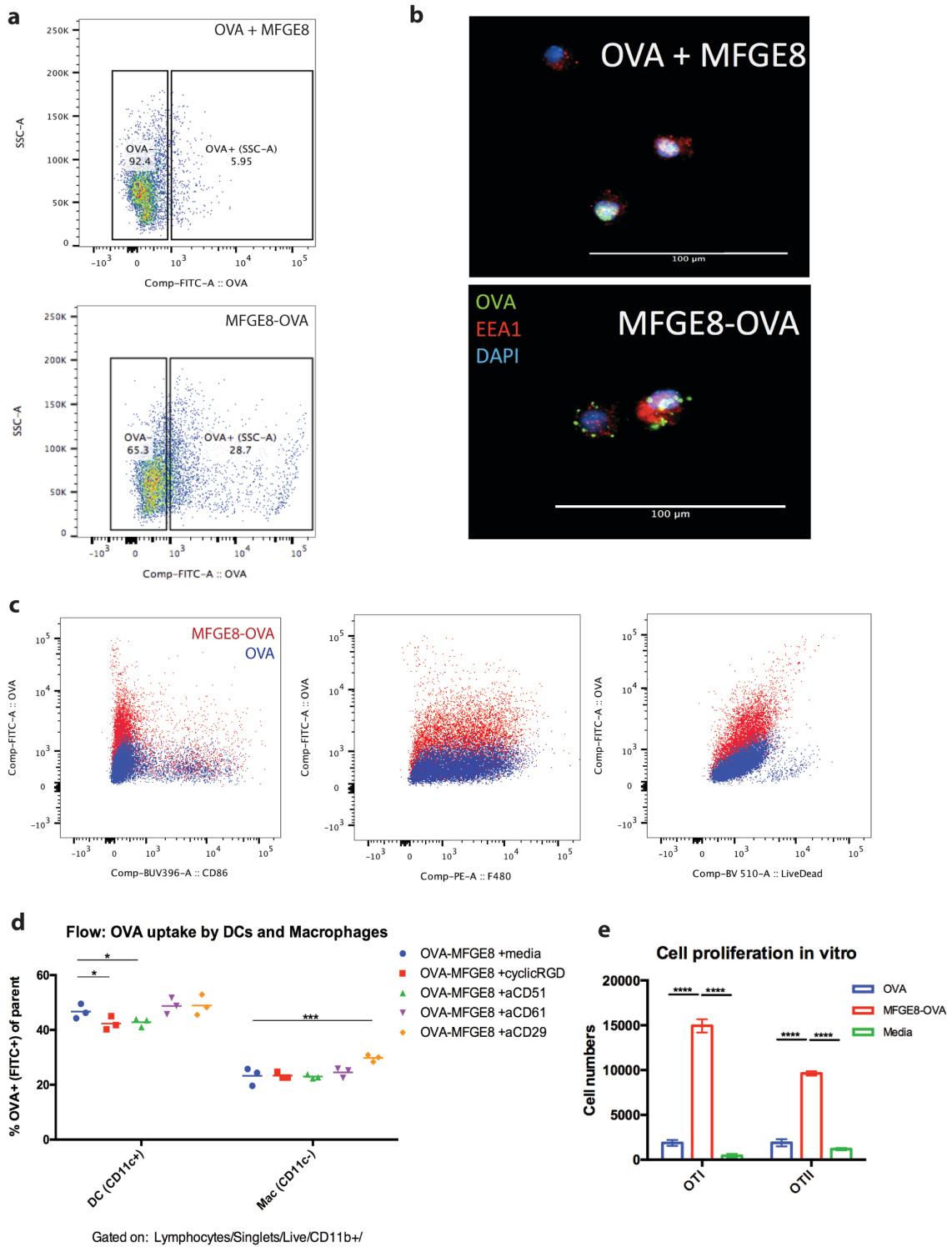

Figure 3.1 | MFGE8 facilitates antigen uptake and presentation in vitro. a) BMDCs were pulsed with antigen for 15 minutes and then assayed for OVA uptake by intracellular flow cytometry. **b)** As in (a), but cells were analyzed using immunofluorescence. **c)** As in (a) but with a 30-minute pulse. **d)** BMDC were pulsed as in (c) with the addition of indicated inhibitors and then analyzed by intracellular flow cytometry

(**Figure 3.1 continued)** for OVA uptake. **e)** BMDC were pulsed with antigen for one hour and then washed, followed by addition of isolated OTI or OTII cells. Cells were cocultured overnight and cell number was measured by flow cytometry the next day. All statistical comparisons were performed by one-way ANOVA.

In attempt to confirm the route of uptake for our fusion proteins, we repeated the previous MFGE8-OVA pulse in the presence of various inhibitors for integrins $\alpha_V\beta_{3/5}$ and measured OVA uptake by flow (**Figure 3.1 d**). We were able to detect an impairment in $CD11c^+$ cell uptake with cyclic RGD peptide or blocking antibody for integrin alpha V (αCD51), both which outcompete MFGE8 for binding. The $CD11c^-$ APC population showed an increase in uptake when blocking integrin beta I (αCD29), which does not bind MFGE8 but perhaps receptor recycling due to antibody binding would increase the surface levels of the other relevant integrins.

After gaining an appreciation for the dramatic increase in antigen uptake efficiency with MFGE8-fusion, we then wanted to determine if there was a corresponding increase in efficiency of antigen presentation to T cells in our in vitro system. We pulsed BMDCs with OVA alone or fused to MFGE8 for an hour, then washed the APCs and added purified OTI or OTII cells separately for overnight coculture. The resulting cell expansion is quantified in **Figure 3.1 e**, which depicts a massive increase in proliferation of both CD8 and CD4 T cells with MFGE8 fusion to OVA. Together, these in vitro data showed the significant potential for MFGE8 to mediate highly efficient antigen uptake and presentation to cognate T cells.

3.3.2 In vivo T cell tolerance induction with MFGE8-OVA conjugates

Preliminary in vivo experimentation performed by Alizée with MFGE8-OVA (data not shown) had demonstrated some success with prophylactic treatment; however, there were questions regarding dose response that prevented further progress. In vitro experiments had demonstrated the powerful efficiency of MFGE8 in antigen delivery, and this suggested a minimal dosing schedule may be best for tolerance induction without disrupting the vital endogenous efferocytosis machinery. We decided to compare MFGE8-OVA and plain OVA treatments using a minimal 1μg equimolar OVA dose, employing separately either one or three doses i.v.

Mice received adoptive transfer of ~225k OTI and OTII cells each. Treatment was initiated the next day, given once every three days. Ten days after the last treatment mice were immunized in the forelimbs with OVA plus LPS. Spleens and dLN were collected five days after challenge. **Figure 3.2 a** depicts the flow cytometric readout at endpoint, showing recovery of OTI cells in the dLN of mice that received one dose of either OVA or MFGE8-OVA treatment. The recovery frequencies are quantified in **Figure 3.2 b**. Although there were no visible differences in the OTII populations, antigen fusion with MFGE8 greatly facilitated prophylactic AIT suppression of cognate CD8 T cell expansion in response to challenge. We also detected an increase in the expression of PD-1 on splenic OTI with MFGE8-OVA treatment (**Figure 3.2 c**).

Lymphocytes were restimulated with antigen for three days. Analysis of cytokines in the supernatant revealed abolishment of IFNγ production with MFGE8-OVA treatment (**Figure 3.2 d**). IL-10 production was detectable in all restimulation cultures from mice

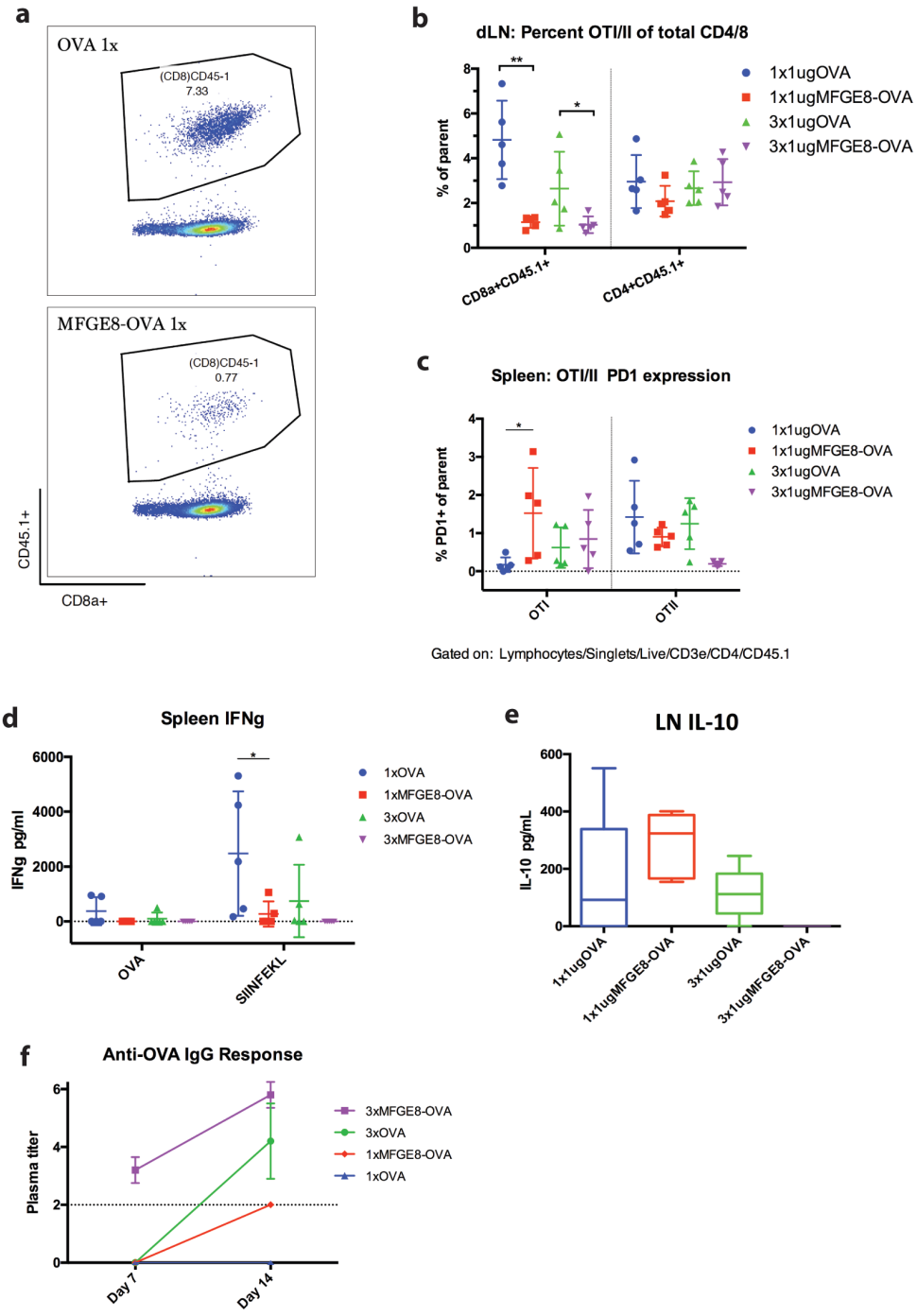

Figure 3.2 | In vivo T cell tolerance induction with MFGE8-OVA conjugates. Mice received adoptive transfer of OTI&II cells, followed by antigen dose, and ten days later LPS challenge. Mice were sacrificed five days after challenge. **a)** Representative flow cytometry plots of recovered OTI cells in the dLN of mice receiving one dose of OVA or MFGE8-OVA. **b)** Quantification of OTI&II cell recovery in the dLN as a percentage of parent population. **c)** Quantification of PD-1 expression frequency on OTI cells in the spleen. **d,e)** Three-day antigen restimulations were carried out with whole protein or class-I peptide, and the production of cytokines was measured by ELISA on **(Figure 3.3.2 continued)** culture supernatants. **f)** Plasma levels of anti-OVA IgG was measured by ELISA after antigen treatment and before challenge. All statistical comparisons were performed by one-way ANOVA.

treated with one dose of MFGE8-OVA (compared to OVA), but the triple dose group showed a loss of IL-10 (**Figure 3.2 e**). Furthermore, prior to LPS challenge we detected an induction of anti-OVA IgG in the serum of animals receiving the triple MFGE8-OVA dosing regimen, signifying undesirable induction of immunity with multiple doses (**Figure 3.2 f**). We concluded that a single dose approach would offer the greatest opportunity for tolerance induction going forward without risk of destabilizing any natural efferocytotic processes.

3.3.3 Non-canonical dominant tolerance induction with MFGE8-OVA

Our data suggested that MFGE8-mediated AIT could effectively prevent CD8 activation in a prophylactic tolerance model. While this was promising, induction of classical Tregs would provide a more robust level of tolerance. To interrogate Treg induction, we carried out the experiment shown in **Figure 3.3 a**. Mice were first treated i.v. with one 5μg dose of OVA or equimolar MFGE8-OVA to tolerize the endogenous compartment to OVA. Three weeks later, mice received adoptive transfer of naïve OTI and OTII cells, followed by s.c. challenge with OVA plus LPS one day later. This was designed to test the ability of the previously tolerized endogenous compartment to suppress the activation of naïve OTI&II cells in the same host.

Two additional treatment groups, receiving either MFGE8-OVA or pGal-OVA treatment, underwent prior Treg depletion via αCD25 seven days after initial antigen

dose. The reduction of bulk Tregs is quantified in **Figure 3.3 b**. Mice were euthanized five days after challenge to collect spleen and dLN.

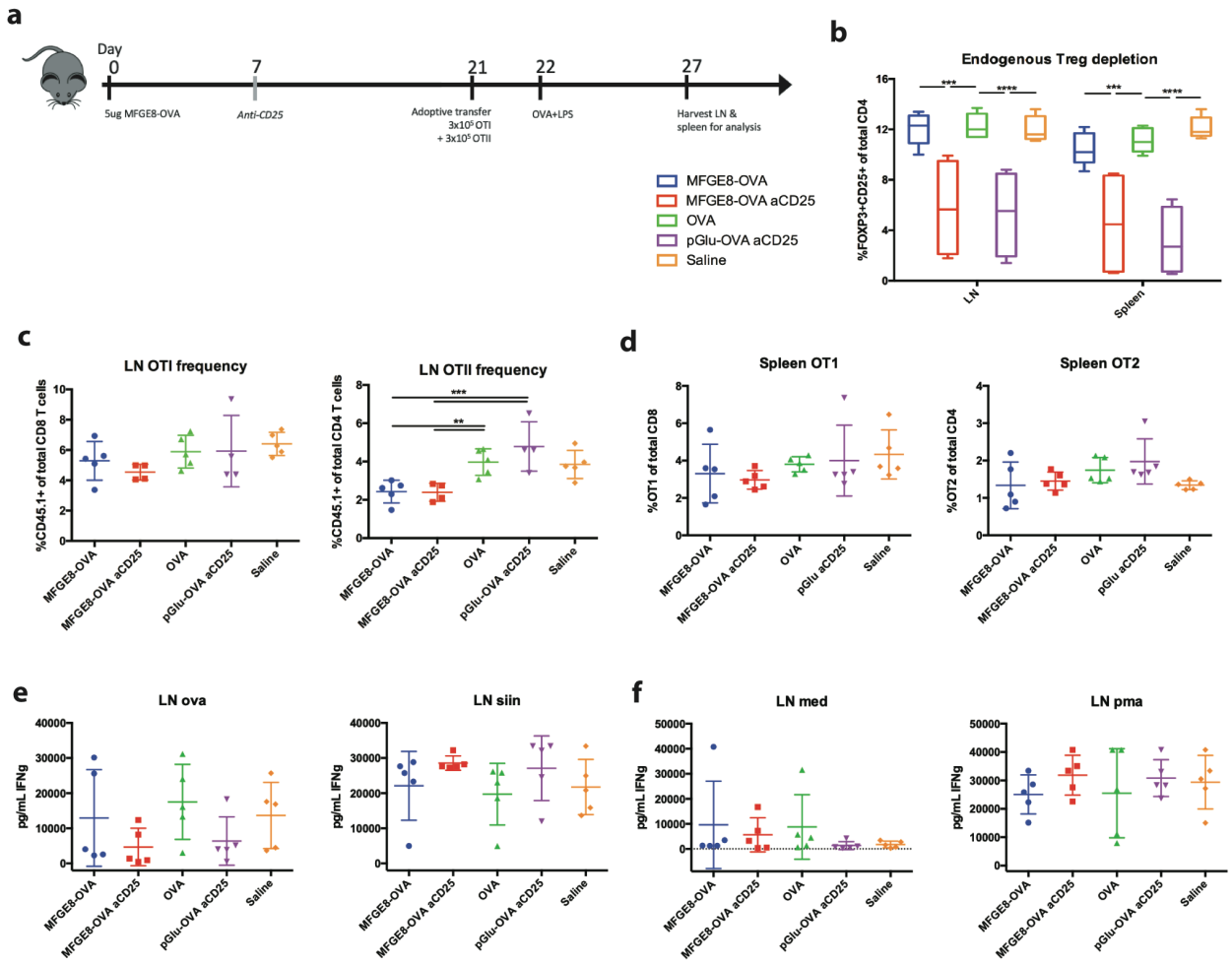

Figure 3.3 | Non-canonical dominant tolerance induction with MFGE8-OVA. a) Experimental design. Mice were first treated i.v. with antigen and 3 weeks later received adoptive transfer of ~225k OTI and OTII each, followed by s.c. challenge with OVA+LPS. SLOs were harvested five days after challenge. Indicated groups received aCD25 i.p. 7 days after initial antigen treatment. **b)** Successful depletion of endogenous Tregs was confirmed in groups receiving αCD25 antibody. **c,d)** Quantification of recovered OTI&II cells as a frequency of parent population in the dLN and spleen. **e)** Three-day antigen restimulations were performed and culture supernatants were analyzed for IFNγ by ELISA. **f)** Cells were cultured as in (e) but with plain media or PMA/ionomycin. All statistical comparisons were performed by one-way ANOVA.

The recovery of OTI and OTII cells as a percentage of parent population is shown in **Figure 3.3 c** and **d** for dLN and spleen. Intriguingly, we see a reduction in OTII

frequency in the dLN of mice treated with MFGE8-OVA, whether or not they received αCD25. Cytokine analysis after restimulation did not show any clear patterns besides a slight trend towards increased IFNγ in SIINFEKLL stimulations of lymphocytes isolated from dLN of MFGE8-OVA treatments with αCD25 (**Figure 3.3 e,f**).

Interpretation of these results taken together with the previous prophylactic experiment paints a picture of direct MFGE8-OVA inhibition of OTI cells, and a dominant CD25-independent inhibition of OTII cells. This type of dominant tolerance is perhaps mediated by Tr1 cells, which do not upregulate CD25 as Tregs do. Further investigation is required to confirm these preliminary findings.

3.3.4 MFGE8 as an antigen delivery platform for vaccination

Because we knew MFGE8 facilitated excellent antigen uptake and presentation, particularly cross presentation to CD8 T cells, we considered it's use as vaccine platform. To this end we immunized mice s.c. in the front forelimbs with 10μg OVA or MFGE8-OVA mixed with the adjuvants alum plus Monophosphoryl Lipid A (MPLA), a synthetic analogue to LPS that stimulates TLR4.

Mice first received adoptive transfer of OTI&II cells, then primary immunization followed by a boost two weeks later. Spleens and dLN were collected a week after the boost. Although not statistically significant, MFGE8-OVA trended towards the highest level of cell recovery at the experimental endpoint (**Figure 3.4 a**). Induction of anti-

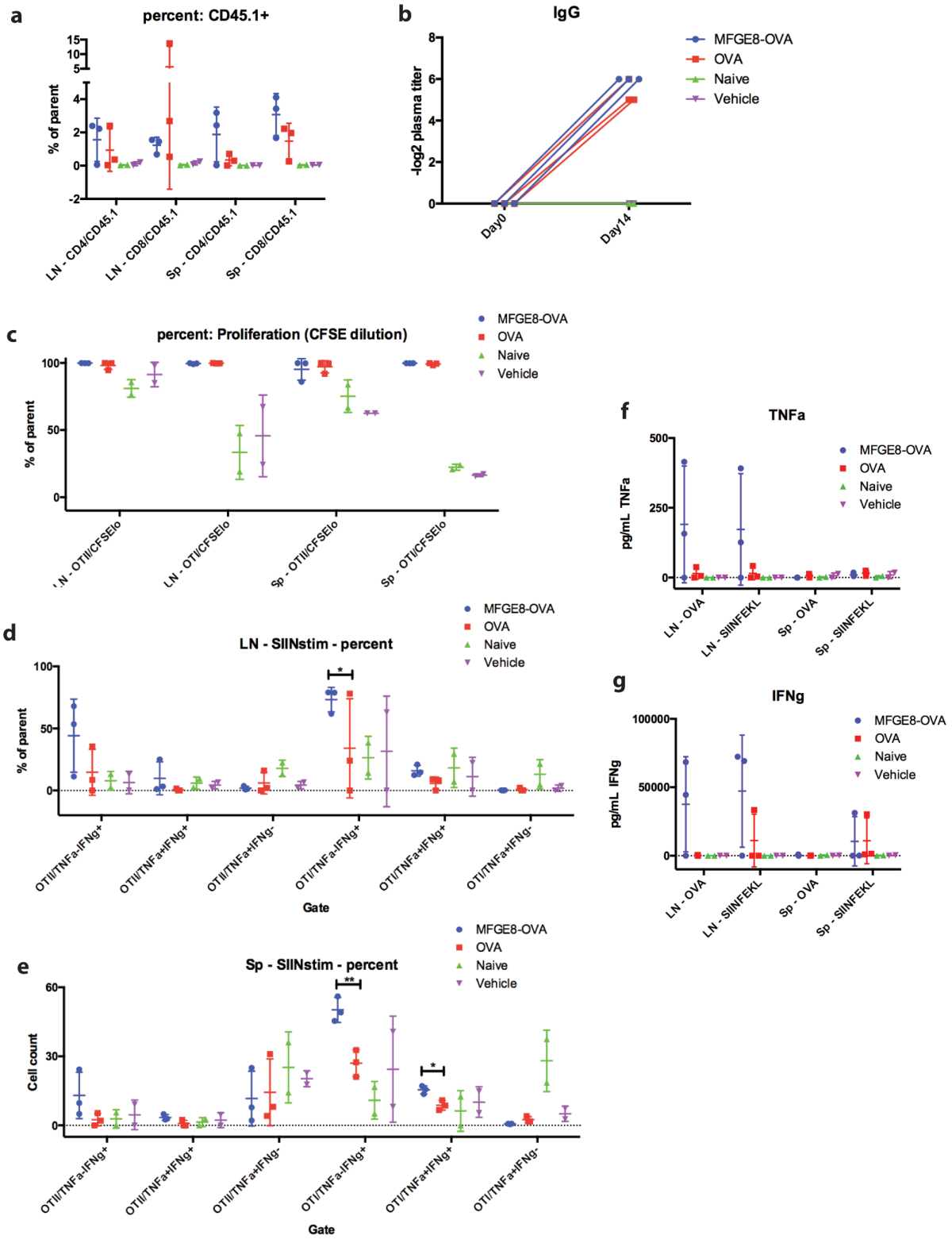
a
percent: CD45.1+
% of parent
LN - CD4/CD45.1
LN - CD8/CD45.1
Sp - CD4/CD45.1
Sp - CD8/CD45.1
b
IgG
-log2 plasma titer
Day0
Day14
MFGE8-OVA
OVA
Naive
Vehicle
c
percent: Proliferation (CFSE dilution)
% of parent
LN - OTII/CFSElo
LN - OTI/CFSElo
Sp - OTII/CFSElo
Sp - OTI/CFSElo
d
LN - SIINstim - percent
% of parent
OTII/TNFa+IFNg+
OTII/TNFa+IFNg+
OTII/TNFa+IFNg-
OTI/TNFa+IFNg+
OTI/TNFa+IFNg+
OTI/TNFa+IFNg-
Gate
e
Sp - SIINstim - percent
Cell count
Gate
f
TNFa
pg/mL TNFa
LN - OVA
LN - SIINFEKL
Sp - OVA
Sp - SIINFEKL
g
IFNg
pg/mL IFNg

Figure 3.4 | MFGE8 as an antigen delivery platform for vaccination (previous page). Mice received adoptive transfer of ~100k OTI and OTII each, followed by two s.c. immunizations two weeks apart using alum plus MPLA with either MFGE8-OVA, plain OVA, or saline. Eight days after the second challenge, mice were sacrificed for SLO collection. **a)** Quantification of recovered OTI&II cells as a frequency of parent population. **b)** Induction of anti-OVA IgG responses were measured before and after primary immunization. **c)** Quantification of CFSE-dilute cells as a percentage of OTI or OTII cells. **d,e)** Six-hour ex vivo antigen restimulations were performed and intracellular flow cytometry was used to detect production of the indicated cytokines in OTI&II cells. **f,g)** Three-day restimulations were carried out for ELISA-based analyses of cytokines in culture supernatants. All statistical comparisons were performed by one-way ANOVA.

OVA IgG after primary immunization was the same for the two immunization groups when measured before boost (**Figure 3.4 b**). Carboxyfluorescein succinimidyl ester (CFSE) was used to track cell proliferation, where dilution of signal indicates proliferation. CFSE-dilution was similar for OVA and MFGE8-OVA vaccination groups (**Figure 3.4 c**).

Short term restimulation with SIINFEKL peptide uncovered an increase in cytokine production of IFNγ in OTI cells as detected by flow cytometry (**Figure 3.4 d,e**). Analysis of multi-day restimulation by supernatant ELISA demonstrated a trend in MFGE8-OVA mice to produce more IFNγ and TNFα (**Figure 3.4 f,g**). These results provide evidence that efficient antigen delivery mediated by MFGE8 can also be used to drive cognate T cell expansion and proinflammatory cytokine production when mixed with a potent adjuvant.

3.4 Discussion

Prior literature, along with work done by Alizée in the conception, design, and initial testing of the antigen fusion proteins, suggested that MFGE8 has potential for

application to AIT. The experiments I carried out furthered this line of inquiry and mounted additional evidence in favor of efficient antigen delivery and presentation in a tolerogenic manner by MFGE8. Further work is required to determine its efficacy in a therapeutic setting as well as elucidate the associated underlying programs of tolerance.

Our in vitro investigation of MFGE8-antigen delivery with BMDC cultures provided a quantitative approach to the investigation of antigen uptake and presentation to T cells. We saw rapid and bountiful uptake of MFGE8-OVA compared to OVA alone, without any associated induction of APC activation markers. OTI&II coculture revealed a dramatic increase in cognate T cell expansion associated with MFGE8-OVA uptake. Together, these in vitro data confirmed MFGE8 as a powerful mediator of antigen delivery.

Previous in vivo trials of prophylactic tolerance induction had given mixed results concerning the dose responsiveness of MFGE8-OVA constructs. We evaluated a low dose approach for single or multiple treatments and found that a single treatment offered the best window for dynamic range against plain OVA. This strategy also avoided possible signs of a proinflammatory response, such as anti-OVA IgG after treatment and before challenge. Here, we observed clear suppression of OTI cells.

Investigation of CD4-mediateed tolerance led us to test for induction of dominant regulators. Treatment of the endogenous compartment followed a fresh transfer of OTI&II cells weeks later allowed us to measure the ability of the previous tolerization to suppress cell activation in vivo. Our results were surprising in that observed inhibition in the OTII compartment with MFGE8-OVA treatment but not the OTI compartment.

Furthermore, the inhibition was not affected with Treg depletion. This suggests a CD25-independent means of dominant regulation, perhaps Tr1 cells. Further evidence is required to confirm these results of non-canonical tolerance induction and explore the biological mechanisms involved.

Finally, we were interested to determine the translatability of MFGE8-antigen delivery to vaccination. Because we knew MFGE8-OVA could drive efficient T cell – p:MHC encounter, we figured the addition of adjuvant could drive robust T cell immunity. We chose alum and MPLA as a potent, clinically relevant adjuvant. Our results pointed toward an increase in cell recovery and activity with MFGE8-antigen coupling in this setting. The concept of directed antigen uptake for immunization was also explored by Scott using a mannose glycopolymer.[84]

Our investigations into MFGE8 as antigen delivery platform demonstrate the increased efficiency of T cell education via either inhibitory or activating contexts. This project is being taken on by a younger grad student in the lab, who will investigate an alternative soluble efferocytotic mediator, GAS6, alone and in combination with MFGE8. Investigation of therapeutic efficacy with these molecules for tolerance is underway.

3.5 Methods

3.5.1 Production of MFGE8 protein variants

MFGE8 and MFGE8-OVA vectors were ordered from GenScript. Recombinant MFGE8 and MFGE8-OVA fusion proteins were expressed in HEK293T suspension cells in

FreeStyle 293 Expression Medium (Thermo Fisher Scientific). At 1 million cells/mL in log-phase growth, cells were transfected with 1 μg of plasmid and 2 μg of polyethylenamine in 40 μl OptiPRO SFM (Gibco) per million cells. Transfected cells were cultured for 6 days in shake flasks. The cells were then pelleted by centrifugation, and the supernatant was filtered through a 0.22 um filter and pH-adjusted to 7.0 using 1 M Tris buffer, pH 9.0. The Fabs were then purified by affinity chromatography using a 5 mL HisTrap Excel column (GE Life Sciences) via fast protein liquid chromatography. The column was first equilibrated with 5 column volumes (CVs) of PBS at 5 mL/min. The crude protein solution was then flowed over the column at 5 mL/min and the column washed with 10 CVs of PBS at 2 mL/min. Protein was then eluted with 500mM imidazole and neutralized with1 M Tris buffer, pH 9.0. Elution peaks were pooled and dialyzed into PBS. Where necessary, proteins were concentrated (Amicon). For all studies, produced proteins were verified to contain <0.01 endotoxin units by HEK-TLR4 assay. Proteins were aliquoted and frozen at -80^{o}C.

3.5.2 BMDCs

Hematopoietic stem cells were obtained from mouse bone marrow and cultured in the presence of 200 U/mL GM-CSF, added at days 0, 3, and 6. BMDCs were ready to use at day 8. BMDCs were pulsed with 10 μl/mL antigen for 6 hours, washed, and CFSE-labeled OT-I or OT-II were added for 3 days.

3.5.3 Immunofluorescence

Cells were fixed with 4% paraformaldehyde (PFA). Cells were mounted on slides and blocked with 10% casein solution, then with 20% rat serum prior to incubation with primary antibodies: rabbit anti-OVA (Abcam), biotinylated mouse anti-mouse EEA1 (Sigma) for 2 hours at room temperature, followed by staining with Alexa Fluor 750-conjugated streptavidin (BioLegend), and goat anti-rabbit-647 (Abcam) (1:400 final concentration for all) for 1 hour. Slides were mounted with ProLong gold antifade medium with DAPI (Invitrogen) before imaging on Olympus confocal microscope. Images were taken with 20x oil lens, and composite images and scale bar overlays were made using ImageJ.

3.5.4 Transgenic T cell adoptive transfer

Spleens were isolated from TCR transgenic mice. OTI and OTII T cells were isolated by negative magnetic bead selection using a CD8 and CD4 (Stemcell) negative selection kit, respectively. Indicated numbers of OT-I and OT-II cells in DMEM were injected through the tail vein. In experiments assessing T cell proliferation, cells were labeled with 5 M CFSE for 7 minutes at room temp and quenched with PBS + 10% FBS.

3.5.5 Antibody depletion experiments

Mouse aCD25 (Clone C1.182, BioXCell) was used for Treg depletion studies. Depletion antibodies were administered once i.p. on day 7 after treatment. Cellular depletions were confirmed via flow cytometry analysis of spleen and dLN populations.

CHAPTER 4: CONCLUSIONS AND FUTURE DIRECTIONS

Through the efforts detailed above, my thesis research has aimed to improve our understanding of AIT using contemporary approaches in protein engineering. By targeting distinct networks of peripheral tolerance induction that mediate inhibitory immune surveillance, we may be able to improve the efficacy of AIT towards broader clinical application than currently employed. Targeting hepatic APCs with pGal led to clear patterns of therapeutic tolerance induction and ultimately suppression of established autoimmunity in a mouse model of multiple sclerosis. Our alternative approach of directly targeting apoptotic uptake machinery with soluble mediators of efferocytosis such as MFGE8 shows promise in vitro and in vivo experimental models. These are just two of the many emerging approaches being applied to control aberrant antigen-specific immunity. Collectively, the fields of immunology and biomedical engineering are approaching new horizons for the control of inflammatory disorders.

The many dogmas of immunology can often seem to conflict, as in the case of AIT. Re-encounter of a previously established foe should drive potent recall responses, but the more foundational rule of reliance upon innate cues for adaptive immunity takes precedent and offers a means by which to correct aberrant education. Inoculation with a purified protein antigen under conditions of homeostasis can lead to re-education and inhibition of previously established immune responses; however, the overlapping laws of immune system dynamics grant only a small theoretical window for redirecting established immunity. As demonstrated in the experiments above, plain antigen can only

induce a limited degree of tolerance. Conjugation of a targeting moiety to the antigen of interest can direct focused uptake into specific phagocytic pathways and networks of peripheral tolerance.

Initial forays into a therapeutic setting, where immunity was previously established, were hampered by a lack of confidence in the ability of pGal to drive tolerance in circulating memory T cells. After being pushed to screen a variety of adjuvants against pGal-OVA, we were elated to discover substantial evidence of recall inhibition (Supplemental Figure 2.3.1.2). We observed a consistent trend of improved recall suppression when antigen was conjugated to pGal across all therapeutic settings tested.

The various differences observed across adjuvants, CD4 or CD8 cell types, and local or systemic SLO reveal the complexity involved in peripheral tolerance dynamics. Besides a reduction in cell magnitude, we consistently observed induction of T cell co-inhibitory ligands such as PD-1 and association of suppressive transcription factors such as TOX. We also observed reduction of CTLA4 in Figure 2.1, which we interpret as a sign of reduced cell activation. Distinguishing between exhaustion or anergy is difficult because there is ambiguity and continuity between the two states, for example anergy is defined as a reduction in IL-2 production, but exhausted cells exhibit this behavior as well. Overall, we describe recovered cognate T cells as having a hyporesponsive phenotype. This is further supported by the reduction in proinflammatory cytokines detected after ex vivo antigen restimulations.

Transcriptional investigations and antibody interventions attempted to elucidate cellular programs and mechanisms at play in our CFA/IFA model of therapeutic tolerance induction. RNAseq results illustrated pGal-antigen modification to drive distinct cellular pathways associated with anti-inflammatory molecules; however, there were also counterintuitive pathways and proinflammatory molecules detected. Analyses of canonical pathways, upstream regulators, and causal networks paint a coherent picture of T cell suppression upon antigen encounter mediated by co-inhibitory ligands. PD-1 blockade during treatment supported these data, while IL-10 depletion showed no defect in tolerance.

The relapsing-remitting EAE model provided the opportunity for us to test pGal-antigen intervention in a murine model of autoimmunity. This model afforded a therapeutic window during the primary remission phase. After first titrating PTX in this model, we were able to observe a proper disease course (data not shown). We then tested pGal-PLP versus plain PLP therapy, compared to fingolimod, and were overjoyed to find the pGal group was the only group that did not relapse. The pGal treated mice retained motor function through the end of our 50-day study, with only slight tail drooping or minor foot wobbling on average. The other treatment groups had obvious motor defects in their hind limbs. The success of pGal-antigen therapy in this setting, using a self protein against an actively destructive endogenous repertoire, proved the ability of pGal-antigen therapy to mediate suppression of autoimmunity. Furthermore, these results validated our work done with OVA.

Our working model for pGal-mediated AIT is depicted below. After immune insult has been initiated (**Figure 4.1 a**), activated T cells circulate through the blood (**Figure 4.1 b**). pGal-antigen administration focuses presentation to the immunosuppressive environment of the liver (**Figure 4.1 c**). Encounter of circulating cognate T cells with p:MHC in this context drive apoptosis and hyporesponsiveness (**Figure 4.1 d**). Continued induction of T cell tolerance results in diminution of the local immune response and eventually provide the opportunity for tissue repair to occur (**Figure 4.1 e**).

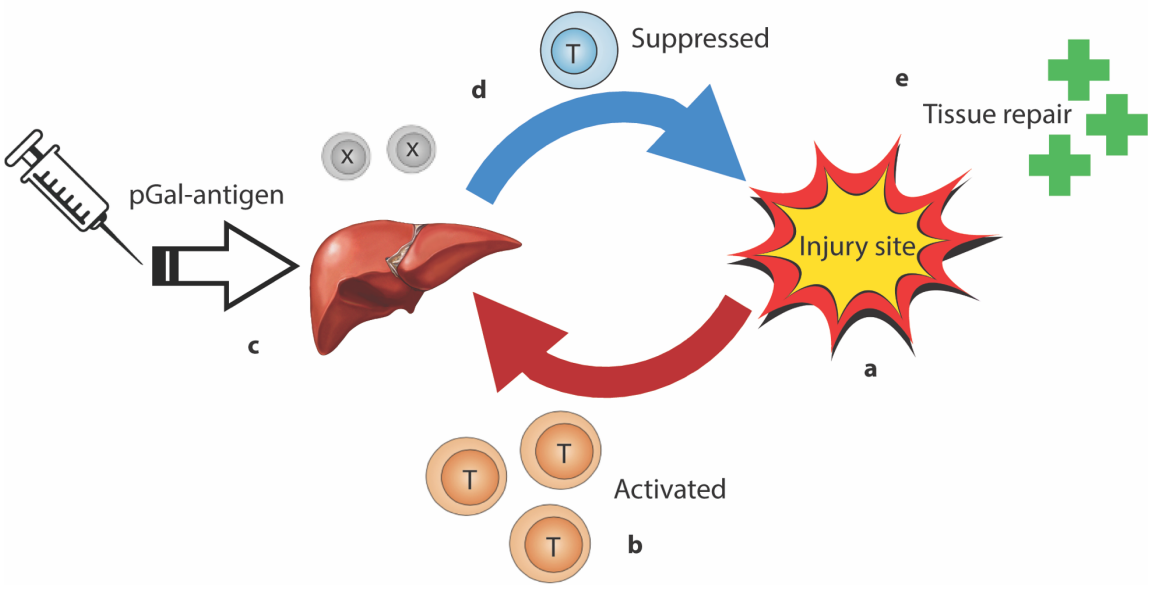

Figure 4.1 | Model for therapeutic tolerance induction via pGal-antigen therapy. a) Immunization or injury results in local activation of the innate and adaptive immune system at the site of insult and in the dLN. **b)** Activated T cells exit the dLN and circulate through the blood as they home back to the injured tissue. **c)** I.v. administration of pGal-antigen homes to hepatic APCs and presents the antigen in the immunosuppressive context of the liver, mediated by co-inhibitory ligands such as PD-1. **d)** Resulting T cell **(Figure 4.1 continued)** encounter with pGal-mediated p:MHC drives apoptosis and suppression of inflammatory programs. **e)** Continued pGal-antigen dosing and suppression of circulating pathogenic T cells can prevent further immune exacerbation at the injury site and theoretically allow the opportunity for tissue repair to occur.

Weaknesses to the pGal approach involve the reliance upon circulating cells, and the lack of solid evidence in favor of dominant tolerance induction such as Treg conversion. Diseases driven primarily by tissue-resident immunity may be difficult to suppress with pGal-antigen therapy because deletion and induction of hyporesponsiveness in the circulating population of T cells may not be sufficient to dampen ongoing pathology. In the case of our RR-EAE model, we did see resolution of immunity in the spinal columns, but other conditions may not be as amenable. In airway allergy, where pathogenic T cells do not circulate after the initial sensitization phase, there are no cells to be affected by hepatic APC presentation. Circumstances such as these will require localized induction of tolerance.

Efferocytosis is an omnipresent network of inhibitory immune surveillance machinery. The efforts detailed in this thesis demonstrate the potential for utilizing soluble efferocytotic molecules, otherwise known as "eat me" signals, for routing antigen into tolerogenic APCs. Delivery of MFGE8-antigen fusion proteins may provide a unique advantage of systemic uptake. Furthermore, MFGE8 itself has immunosuppressive signaling potential that can help downregulate a pro-inflammatory environment and any activated APCs that scavenge the antigen constructs. Experiments are currently underway in our lab to investigate the therapeutic potential of MFGE8 and GAS6 as individual molecules and as a co-therapy. Future studies may explore topical application as well, for example aspiration into the lung for airway allergy models.

Clinical evaluation of novel engineering approaches to AIT are ongoing. For pGal, our lab's collaboration with industry partner Anokion offers a unique opportunity to

engage with translational discovery from bench to bedside as part of my graduate education. Anokion has demonstrated efficacy of pGal-antigen therapy in mouse models of adoptive transfer-induced chronic EAE, as well as a non-human primate (NHP) model of immunity. In their EAE experiments, Anokion demonstrates that prophylactic and early-stage paralysis intervention can suppress disease and maintain motor function. The NHP experiment utilizes a DNA vaccine against human immunodeficiency virus (HIV) to induce cellular immunity against Gag and Nef proteins, followed by treatment with pGal-Nef that drives down the antigen-specific immune response faster over time than it naturally wanes in untreated animals. Both experiments, chronic EAE and NHP immunity, provide further evidence in support of pGal-mediated therapeutic tolerance induction. Their results show induction of co-inhibitory markers on T cells along with clearer indication of Treg induction in the therapeutic context, together which provide confirmation of our results and further clarification of my outstanding questions regarding dominant tolerance induction. We are submitting all our data together in a single publication, which will provide a rich diversity of studies outlining the clinical potential for its application to AIT. Furthermore, Anokion is beginning clinical trials for indications including celiac disease, MS, and T1D.

My efforts investigating soluble efferocytotic mediators for tolerance induction have continued from a previous graduate student's work and is being passed off to another student after me. This will allow for a richer interrogation and evaluation of this strategy's potential for therapeutic efficacy and clinical application. There are additional strategies are being developed in the lab for AIT that have built off the same foundational

work of previous lab members. For example, using antibody fragments to piggyback antigen on RBCs as a more translatable alternative to the original peptide-based strategy employed by ERY1. Other types of tolerance inducing strategies are also being studied, including engineered cytokine therapies such as IL-4 and IL-10.

Cumulatively, my graduate education has provided me first with a foundation in immunology through coursework and rotations in classical immunology labs, and second with hands on research using a novel bioengineered approach currently in clinical trials with the hope of curative potential for multiple autoimmune diseases. The various efforts of my lab and research community towards the understanding and intervention of inflammatory disorders shows promise for a healthier future.

REFERENCES

1. Davis, M. M. & Bjorkman, P. J. T-cell antigen receptor genes and T-cell recognition. *Nature* **334**, (1988).
2. Jenkins, M. K., Chu, H. H., McLachlan, J. B. & Moon, J. J. On the composition of the preimmune repertoire of T cells specific for peptide-major histocompatibility complex ligands. *Annual Review of Immunology* **28**, (2010).
3. Frank Macfarlane Burnet. *Cellular Immunology: Self and Not-self*. (Melbourne University Press, 1969).
4. Janeway, C. A. Approaching the asymptote? Evolution and revolution in immunology. Cold spring harb symp quant biol. 1989. 54: 1-13. *Cold Spring Harb. Symp Quant Biol* **54**, (1989).
5. Feldmann, M. Development of anti-TNF therapy for rheumatoid arthritis. *Nature Reviews Immunology* **2**, (2002).
6. De Blay De Gaix, F. *et al.* A Single-Dose of REGN1908-1909 Reduced Bronchoconstriction in Cat-Allergic Subjects with Mild Asthma for up to 3 months following a controlled cat allergen challenge: A Phase 2, Randomized, Double-Blind, Placebo-Controlled Study. in *American Academy of Allergy Asthma & Immunology Virtual Annual Meeting* AB158-Abstract 504 (Journal of Allergy and Clinical Immunology, 2021).
7. Herold, K. C. *et al.* An Anti-CD3 Antibody, Teplizumab, in Relatives at Risk for Type 1 Diabetes. *N. Engl. J. Med.* **381**, (2019).

8. Marek-Trzonkowska, N. *et al.* Therapy of type 1 diabetes with CD4(+) CD25(high)CD127-regulatory T cells prolongssurvival of pancreatic islets-results of one year follow-up. *Diabetes Technology and Therapeutics* **17**, (2015).
9. Lutterotti, A. *et al.* Antigen-specific tolerance by autologous myelin peptide-coupled cells: A phase 1 trial in multiple sclerosis. *Sci. Transl. Med.* **5**, (2013).
10. The College of Physicians of Philadelphia. Royal Support of Inoculation. *The History of Vaccines*
11. Germain, R. N. t-cell development and the CD4-CD8 lineage decision. *Nature Reviews Immunology* **2**, (2002).
12. Liston, A., Lesage, S., Wilson, J., Peltonen, L. & Goodnow, C. C. Aire regulates negative selection of organ-specific T cells. *Nat. Immunol.* **4**, (2003).
13. Takaba, H. *et al.* Fezf2 Orchestrates a Thymic Program of Self-Antigen Expression for Immune Tolerance. *Cell* **163**, 975–987 (2015).
14. Steinman, R. M. *et al.* Dendritic cell function in Vivo during the steady state: A role in peripheral tolerance. in *Annals of the New York Academy of Sciences* **987**, (2003).
15. Medzhitov, R. & Janeway, C. A. Decoding the patterns of self and nonself by the innate immune system. *Science* **296**, (2002).
16. Gallucci, S., Lolkema, M. & Matzinger, P. Natural adjuvants: Endogenous activators of dendritic cells. *Nat. Med.* **5**, (1999).
17. Bonifaz, L. *et al.* Efficient Targeting of Protein Antigen to the Dendritic Cell Receptor DEC-205 in the Steady State Leads to Antigen Presentation on Major Histocompatibility Complex Class I Products and Peripheral CD8 $^{+}$ T Cell

Tolerance. *J. Exp. Med.* **196**, 1627–1638 (2002).

18. Griffith, T. S., Yu, X., Herndon, J. M., Green, D. R. & Ferguson, T. A. CD95-induced apoptosis of lymphocytes in an immune privileged site induces immunological tolerance. *Immunity* **5**, (1996).

19. Limmer, A. *et al.* Efficient presentation of exogenous antigen by liver endothelial cells to CD8+ T cells results in antigen-specific T-cell tolerance. *Nat. Med.* **6**, (2000).

20. Esterházy, D. *et al.* Compartmentalized gut lymph node drainage dictates adaptive immune responses. *Nature* **569**, (2019).

21. Sharma, P., Wagner, K., Wolchok, J. D. & Allison, J. P. Novel cancer immunotherapy agents with survival benefit: Recent successes and next steps. *Nature Reviews Cancer* **11**, (2011).

22. Nossal, G. J. V. A purgative mastery. *Nature* **412**, (2001).

23. Walker, L. S. K. & Abbas, A. K. The enemy within: Keeping self-reactive T cells at bay in the periphery. *Nature Reviews Immunology* **2**, (2002).

24. Yadav, M., Stephan, S. & Bluestone, J. A. Peripherally induced Tregs-role in immune homeostasis and autoimmunity. *Front. Immunol.* **4**, (2013).

25. Müller, Y., Wolf, H., Wierenga, E. & Jung, G. Induction of abortive and productive proliferation in resting human T lymphocytes via CD3 and CD28. *Immunology* **97**, (1999).

26. Macian, F. NFAT proteins: Key regulators of T-cell development and function. *Nature Reviews Immunology* **5**, (2005).

27. Martinez, G. J. *et al.* The Transcription Factor NFAT Promotes Exhaustion of

Activated CD8+ T Cells. *Immunity* **42**, (2015).

28. Kim, J. M., Rasmussen, J. P. & Rudensky, A. Y. Regulatory T cells prevent catastrophic autoimmunity throughout the lifespan of mice. *Nat. Immunol.* **8**, (2007).

29. Nutsch, K. *et al.* Rapid and Efficient Generation of Regulatory T Cells to Commensal Antigens in the Periphery. *Cell Rep.* **17**, (2016).

30. Groux, H. *et al.* A CD4+ T-cell subset inhibits antigen-specific T-cell responses and prevents colitis. *Nature* **389**, (1997).

31. Zhao, F. *et al.* Opposing T cell responses in experimental autoimmune encephalomyelitis. doi:10.1038/s41586-019-1467-x

32. Yanaba, K. *et al.* A Regulatory B Cell Subset with a Unique CD1dhiCD5+ Phenotype Controls T Cell-Dependent Inflammatory Responses. *Immunity* **28**, (2008).

33. US Department of Health and Human Services. Progress in Autoimmune Diseases Research. *Natl. Institutes Heal.* **05–5140**, (2005).

34. Pawankar, R., Canonica, G. W., Lockey, R. F. & Holgate, S. T. (Editors). White Book on Allergy 2011-2012: Executive Summary. *World Allergy Organ. J.* (2011).

35. The Finnish-German, A. C. An autoimmune disease, APECED, caused by mutations in a novel gene featuring two PHD-type zinc-finger domains. The Finnish-German APECED Consortium. Autoimmune Polyendocrinopathy-Candidiasis-Ectodermal Dystrophy. *Nat.Genet.* **17**, (1997).

36. Simmonds, M. & Gough, S. The HLA Region and Autoimmune Disease: Associations and Mechanisms of Action. *Curr. Genomics* **8**, (2009).

37. Rewers, M. *et al.* The Environmental Determinants of Diabetes in the Young (TEDDY) Study: 2018 Update. *Current Diabetes Reports* **18**, (2018).

38. Todd, J. A. Etiology of Type 1 Diabetes. *Immunity* **32**, (2010).

39. Vreugdenhil, G. R. *et al.* Molecular mimicry in diabetes mellitus: The homologous domain in coxsackie B virus protein 2C and islet autoantigen GAD65 is highly conserved in the coxsackie B-like enteroviruses and binds to the diabetes associated HLA-DR3 molecule. *Diabetologia* **41**, (1998).

40. Wen, L. *et al.* Innate immunity and intestinal microbiota in the development of Type 1 diabetes. *Nature* **455**, (2008).

41. Willis, S. N. *et al.* Investigating the antigen specificity of multiple sclerosis central nervous system-derived immunoglobulins. *Front. Immunol.* **6**, (2015).

42. Molberg, Ø. *et al.* Tissue transglutaminase selectively modifies gliadin peptides that are recognized by gut-derived T cells in celiac disease. *Nat. Med.* **4**, (1998).

43. Averbeck, M., Gebhardt, C., Emmrich, F., Treudler, R. & Simon, J. C. Immunologic principles of allergic disease. *JDDG - Journal of the German Society of Dermatology* **5**, (2007).

44. Noon, L. PROPHYLACTIC INOCULATION AGAINST HAY FEVER. *Lancet* **177**, (1911).

45. Flicker, S. & Valenta, R. Renaissance of the blocking antibody concept in type I allergy. *International Archives of Allergy and Immunology* **132**, (2003).

46. Feng, M. *et al.* Functional and Immunoreactive Levels of IgG4 Correlate with Clinical Responses during the Maintenance Phase of House Dust Mite

Immunotherapy. *J. Immunol.* **200**, (2018).

47. Sabatos-Peyton, C. A., Verhagen, J. & Wraith, D. C. Antigen-specific immunotherapy of autoimmune and allergic diseases. *Current Opinion in Immunology* **22**, (2010).

48. Seddon, B., Tomlinson, P. & Zamoyska, R. Interleukin 7 and T cell receptor signals regulate homeostasis of CD4 memory cells. *Nat. Immunol.* **4**, (2003).

49. Stanley, J. S. *et al.* Identification and mutational analysis of the immunodominant IgE binding epitopes of the major peanut allergen Ara h 2. *Arch. Biochem. Biophys.* **342**, (1997).

50. Ebner, C. *et al.* Common epitopes of birch pollen and apples-Studies by western and northern blot. *J. Allergy Clin. Immunol.* **88**, (1991).

51. Ohman, J. L., Lorusso, J. R. & Lewis, S. Cat allergen content of commercial house dust extracts: Comparison with dust extracts from cat-containing environment. *J. Allergy Clin. Immunol.* **79**, (1987).

52. Chapman, M. D. & Platts-Mills, T. Purification and characterization of the major allergen from Dermatophagoides pteronyssinus-antigen P1. *J. Immunol.* **123**, 587–592 (1980).

53. Koffeman, E. C. *et al.* Epitope-specific immunotherapy of rheumatoid arthritis: Clinical responsiveness occurs with immune deviation and relies on the expression of a cluster of molecules associated with T cell tolerance in a double-blind, placebo-controlled, pilot phase II trial. *Arthritis Rheum.* **60**, (2009).

54. Muller, S. *et al.* Spliceosomal peptide P140 for immunotherapy of systemic lupus

erythematosus: Results of an early phase II clinical trial. *Arthritis Rheum.* **58**, (2008).

55. Fischer, B., Elias, D., Bretzel, R. G. & Linn, T. Immunomodulation with heat shock protein DiaPep277 to preserve beta cell function in type 1 diabetes an update. *Expert Opinion on Biological Therapy* **10**, (2010).

56. Warren, K. G., Catz, I., Ferenczi, L. Z. & Krantz, M. J. Intravenous synthetic peptide MBP8298 delayed disease progression in an HLA Class II-defined cohort of patients with progressive multiple sclerosis: Results of a 24-month double-blind placebo-controlled clinical trial and 5 years of follow-up treatment. *Eur. J. Neurol.* **13**, (2006).

57. Golebski, K. *et al.* Induction of IL-10-producing type 2 innate lymphoid cells by allergen immunotherapy is associated with clinical response. *Immunity* **54**, (2021).

58. Huurman, V. A. L. *et al.* Immunological efficacy of heat shock protein 60 peptide DiaPep277^{TM} therapy in clinical type I diabetes. *Clin. Exp. Immunol.* **152**, (2008).

59. Roncarolo, M. G., Gregori, S., Lucarelli, B., Ciceri, F. & Bacchetta, R. Clinical tolerance in allogeneic hematopoietic stem cell transplantation. *Immunological Reviews* **241**, (2011).

60. Satitsuksanoa, P., Jansen, K., Głobińska, A., van de Veen, W. & Akdis, M. Regulatory immune mechanisms in tolerance to food allergy. *Front. Immunol.* **9**, (2018).

61. Umeshappa, C. S. *et al.* Suppression of a broad spectrum of liver autoimmune pathologies by single peptide-MHC-based nanomedicines. *Nat. Commun.* **10**, (2019).

62. Maldonado, R. A. *et al.* Polymeric synthetic nanoparticles for the induction of

antigen-specific immunological tolerance. *Proc. Natl. Acad. Sci.* **112**, E156–E165 (2015).

63. Kontos, S., Kourtis, I. C., Dane, K. Y. & Hubbell, J. A. Engineering antigens for in situ erythrocyte binding induces T-cell deletion. *Proc. Natl. Acad. Sci.* **110**, E60–E68 (2012).

64. Lorentz, K. M., Kontos, S., Diaceri, G., Henry, H. & Hubbell, J. A. Engineered binding to erythrocytes induces immunological tolerance to E. coli asparaginase. *Sci. Adv.* **1**, (2015).

65. Wilson, D. S. *et al.* Synthetically glycosylated antigens induce antigen-specific tolerance and prevent the onset of diabetes. *Nat. Biomed. Eng.* **3**, (2019).

66. Stockert, R. J. The asialoglycoprotein receptor: Relationships between structure, function, and expression. *Physiological Reviews* **75**, (1995).

67. Kenneth Hoober, J. Asgr1 and its enigmatic relative, CLEC10A. *International Journal of Molecular Sciences* **21**, (2020).

68. Kreuwel, H. T. C., Aung, S., Silao, C. & Sherman, L. A. Memory CD8+T cells undergo peripheral tolerance. *Immunity* **17**, 73–81 (2002).

69. Stoop, J. N., Tibbitt, C. A., van Eden, W., Robinson, J. H. & Hilkens, C. M. U. The choice of adjuvant determines the cytokine profile of T cells in proteoglycan-induced arthritis but does not influence disease severity. *Immunology* **138**, (2013).

70. Khan, O. *et al.* TOX transcriptionally and epigenetically programs CD8+ T cell exhaustion. *Nature* **571**, 211–218 (2019).

71. Kalekar, L. A. *et al.* CD4+T cell anergy prevents autoimmunity and generates

regulatory T cell precursors. *Nat. Immunol.* **17**, 304–314 (2016).

72. Carlin, L. M. *et al.* Secretion of IFN-γ and not IL-2 by anergic human T cells correlates with assembly of an immature immune synapse. *Blood* **106**, (2005).

73. Rumpret, M. *et al.* Functional categories of immune inhibitory receptors. *Nature Reviews Immunology* (2020). doi:10.1038/s41577-020-0352-z

74. Wang, X. *et al.* TOX promotes the exhaustion of antitumor CD8+ T cells by preventing PD1 degradation in hepatocellular carcinoma. *J. Hepatol.* **71**, (2019).

75. Gagliani, N. *et al.* TH17 cells transdifferentiate into regulatory T cells uring resolution of inflammation. *Nature* **523**, (2015).

76. Llorente, L. *et al.* Clinical and biologic effects of anti-interleukin-10 monoclonal antibody administration in systemic Lupus erythematosus. *Arthritis Rheum.* **43**, (2000).

77. Dobin, A. *et al.* STAR: Ultrafast universal RNA-seq aligner. *Bioinformatics* **29**, (2013).

78. Tarasov, A., Vilella, A. J., Cuppen, E., Nijman, I. J. & Prins, P. Sambamba: Fast processing of NGS alignment formats. *Bioinformatics* **31**, (2015).

79. Liao, Y., Smyth, G. K. & Shi, W. The Subread aligner: Fast, accurate and scalable read mapping by seed-and-vote. *Nucleic Acids Res.* **41**, (2013).

80. Bray, N. L., Pimentel, H., Melsted, P. & Pachter, L. Near-optimal probabilistic RNA-seq quantification. *Nat. Biotechnol.* **34**, (2016).

81. Robinson, M. D., McCarthy, D. J. & Smyth, G. K. edgeR: A Bioconductor package for differential expression analysis of digital gene expression data. *Bioinformatics* **26**,

(2009).

82. Hanayama, R. *et al.* Autoimmune disease and impaired uptake of apoptotic cells in MFG-E8-deficient mice. *Science (80-.).* **304**, (2004).

83. Cheyuo, C. *et al.* Recombinant human MFG-E8 attenuates cerebral ischemic injury: Its role in anti-inflammation and anti-apoptosis. *Neuropharmacology* **62**, (2012).

84. Wilson, D. S. *et al.* Antigens reversibly conjugated to a polymeric glyco-adjuvant induce protective humoral and cellular immunity. *Nat. Mater.* **18**, 175–185 (2019).